Gas Turbine Combustor Exit Temperature Measurement

John E. Sullivan and John E. Kendall
Astron Research and Engineering
130 Kifer Court
Sunnyvale, CA 94086

August 1991

Final Report for Period January 13, 1987 — May 31, 1989

TECHNICAL REPORTS
FILE COPY

**ARNOLD ENGINEERING DEVELOPMENT CENTER
ARNOLD AIR FORCE BASE, TENNESSEE
AIR FORCE SYSTEMS COMMAND
UNITED STATES AIR FORCE**

NOTICES

When U. S. Government drawings, specifications, or other data are used for any purpose other than a definitely related Government procurement operation, the Government thereby incurs no responsibility nor any obligation whatsoever, and the fact that the Government may have formulated, furnished, or in any way supplied the said drawings, specifications, or other data, is not to be regarded by implication or otherwise, or in any manner licensing the holder or any other person or corporation, or conveying any rights or permission to manufacture, use, or sell any patented invention that may in any way be related thereto.

Qualified users may obtain copies of this report from the Defense Technical Information Center.
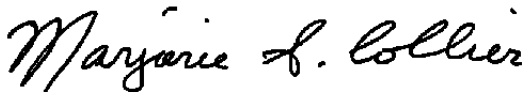
References to named commercial products in this report are not to be considered in any sense as an endorsement of the product by the United States Air Force or the Government.

This report has been reviewed by the Office of Public Affairs (PA) and is releasable to the National Technical Information Service (NTIS). At NTIS, it will be available to the general public, including foreign nations.

The reproducibles used in publishing this Small Business Innovative Research (SBIR) report were supplied by the authors. AEDC has not edited nor altered this manuscript.

APPROVAL STATEMENT

This report has been reviewed and approved.

Marjorie S. Collier

MARJORIE S. COLLIER
Directorate of Technology
Deputy for Operations

Approved for publication:

FOR THE COMMANDER

Keith L. Kushman

KEITH L. KUSHMAN
Director of Technology
Deputy for Operations

REPORT DOCUMENTATION PAGE

1 AGENCY USE ONLY (Leave blank)	2. REPORT DATE **August 1991**	3. REPORT TYPE AND DATES COVERED **Final, January 13, 1987 -- May 31, 1989**	
4 TITLE AND SUBTITLE **Gas Turbine Combustor Exit Temperature Measurement**		5. FUNDING NUMBERS **F40600-87-C-0002**	
6. AUTHOR(S) **Sullivan, John D. and Kendall, John E., Astron Research and Engineering**			
7 PERFORMING ORGANIZATION NAME(S) AND ADDRESS(ES) **Astron Research and Engineering 130 Kifer Court Sunnyvale, CA 94086**		8. PERFORMING ORGANIZATION REPORT NUMBER **AEDC-TR-91-11**	
9. SPONSORING/MONITORING AGENCY NAMES(S) AND ADDRESS(ES) **Arnold Engineering Development Center/DO Air Force Systems Command Arnold AFB, TN 37389-5000**		10. SPONSORING/MONITORING AGENCY REPORT NUMBER	

11 SUPPLEMENTARY NOTES

Available in Defense Technical Information Center (DTIC).

12a DISTRIBUTION/AVAILABILITY STATEMENT **Approved for public release; distribution is unlimited.**	12b. DISTRIBUTION CODE

13. ABSTRACT (Maximum 200 words)

A new gas temperature measurement technique is presented that has the capability to eliminate radiation errors typically observed in high-temperature environments. The technique should allow high measurement accuracy and high spatial resolution and can be implemented in rugged probe designs capable of surviving in a gas turbine combustor exit environment. The theoretical operation of the probe is described, and sources of measurement uncertainty are investigated. Probes fabricated for demonstration purposes are capable of surviving prolonged operation at temperatures up to 3,000°F. Tests were run in two facilities, the Astron High-Temperature Furnace and the NASA Lewis Combustor Rig, and results are presented in this report. The test results are favorable; however, further analysis should be performed and a method of qualifying probe accuracy should be defined. Currently the probe does not operate satisfactorily in a real-time mode, but algorithms developed for posttest data reduction should be suitable for implementation in a microprocessor-based controller allowing real-time operation.

14. SUBJECT TERMS temperature probe radiation-compensated thermocouples radiation-compensated transient effect probe temperature probe radiation-corrected local gas temp. probe			15. NUMBER OF PAGES **112**
			16. PRICE CODE
17 SECURITY CLASSIFICATION OF REPORT **UNCLASSIFIED**	18. SECURITY CLASSIFICATION OF THIS PAGE **UNCLASSIFIED**	19 SECURITY CLASSIFICATION OF ABSTRACT **UNCLASSIFIED**	20. LIMITATION OF ABSTRACT **SAME AS REPORT**

Contract No. F40600-87-C0002

Contractor: Astron Research & Engineering

For a period of two (2) years after delivery and acceptance of the last deliverable item under the above contract, the technical data identified on pages 3-1 through 3-33 and 5-1 through 5-24 of this document shall be subject to the restrictions contained in the definition of "Limited Rights" in DFARS clause at 252.227-7013. After the two-year period, the data shall be subject to the restrictions contained in the definition of "Government Purpose License Rights" in DFARS clause at 252.227-7013. The Government assumes no liability for unauthorized use or disclosure by others. This legend, together with the indications of the portions of the data which are subject to such limitations shall be included on any reproduction hereof which contains any portions subject to such limitations and shall be honored only so long as the data continues to meet the definition of Government purpose rights.

ABSTRACT

A new gas temperature measurement technique is presented that has the capability to eliminate radiation errors typically observed in high-temperature environments. The technique should allow high measurement accuracy and high spatial resolution and can be implemented in rugged probe designs capable of surviving in a gas turbine combustor exit environment. The theoretical operation of the probe is described, and sources of measurement uncertainty are investigated. Probes fabricated for demonstration purposes are capable of surviving prolonged operation at temperatures up to 3000°F. Tests were run in two facilities, the Astron High-Temperature Furnace and the NASA Lewis Combustor Rig, and results are presented in this report. The test results are favorable, however further analysis should be performed and a method of qualifying probe accuracy should be defined. Currently the probe does not operate satisfactorily in a real-time mode, but algorithms developed for posttest data reduction should be suitable for implementation in a microprocessor-based controller allowing real-time operation.

Contents

List of Figures

List Of Tables

Table

List Of Symbols

English Letter Symbols

A = surface area
Bi = Biot number (hs/k)
C = circumference
c = specific heat
D = diameter
E = modulus of elasticity
F = angle factor for radiation heat transfer
h = convective heat transfer coefficient
I = moment of inertia
K = ratio of m_1c_1/m_2c_2 ; factor in normal-mode equation (6-1)
k = thermal conductivity
L = thermocouple lead length
m = mass
Nu = Nusselt number (hD/k)
Pr = Prandtl number
Q = rate of energy transfer
Re = Reynolds number
s = radius (when using Biot number definition)
T = temperature
w = mass per unit length

Greek Letter Symbols

ε = emissivity
Λ = generalized thermal conductivity term (Btu/hr-$^{\circ}$F)
σ = Stefan-Boltzmann constant
τ = characteristic response time of first-order instrument

Subscripts

c = combined energy transfer (conduction+convection+radiation)
cond. = conduction effects
f = properties evaluated at film conditions
g = freestream gas properties
h = properties influenced by convection effects only
m = wall properties (Menshikov)
p = probe thermocouple junction properties
r = properties influenced by radiation only
s = surface or wall properties
w = wall properties

SECTION 1 - INTRODUCTION

This report describes a technique being developed by Astron Research and Engineering to measure gas temperatures in the combustor exit section of a jet engine. The method provides high measurement accuracy and high spatial resolution and can be implemented using rugged probe designs capable of surviving in a typical gas turbine environment at temperatures up to 3200°F. Radiation-induced errors are eliminated, which should allow the calculation of true gas temperatures to within 0.5 percent of the actual temperature over the range of interest.

This work is performed as Phase II of a Small Business Innovative Research (SBIR) Program funded through AEDC, and the work described in this Final Report represents the current status of the program. The temperature measurement concept has evolved over the course of the 3 years of our involvement with AEDC, and it is intended that the changes that have been made have improved the usefulness of this probe in the gas turbine environment. The probe demonstrated in the Phase I program was capable of accurately measuring gas temperatures above the melting point of the thermocouple junction and could also provide approximately an order of magnitude improvement in time response when compared to a conventional thermocouple with a junction of the same size. While the Phase I program was successful, and should find other applications, it did not address some of the principal concerns expressed by AEDC.

In particular, AEDC and Sverdrup personnel expressed the need to design a probe that could accurately compensate for the measurement errors caused by thermal radiation. To meet this objective, the Phase I technique was adapted to this use at the cost of reducing the time response of the probe. The current design operates at near the equilibrium temperature of the probe, and by exposing the thermocouple junction to perturbations in the thermal environment, the true gas temperature can be determined. We have demonstrated·experimentally that the Astron probe does behave as expected in a well-behaved furnace environment, and the test results presented in this report substantiate this. Test results in the NASA Lewis Combustor Rig were disappointing due to the high level of turbulent mixing in that facility in the vicinity of our probe, but useful data were recorded and analyzed. Providing real-time gas temperature calculations has proven to be a difficult challenge.

Section 2 of this report provides a review of the fundamentals of thermocouple use in the measurement of gas temperatures, and this is followed by a brief survey of previously demonstrated measurement techniques that are related to the Astron method. Section 3 describes the Astron concept in detail. Deviations from ideal probe behavior are identified and

quantified in this section, and a rigorous error analysis is presented. Section 4 presents descriptions of the Astron Furnace Facility and the NASA Lewis Combustor Rig, including discussions of instrumentation and data acquisition systems. Temperature measurement test results from both facilities are discussed in Section 5. Section 6 describes the structural integrity tests performed at Astron. Section 7 presents a summary of our accomplishments to date, an evaluation of the current status of our probe development effort, and recommendations for future work.

During the course of this program we have received assistance from many Government personnel and contractors, and we would like to express our thanks. In particular, we want to acknowledge the contributions of our Technical Monitor, Marjorie Collier, in organizing our design review at AEDC and in helping to obtain permission to test at NASA Lewis. Don Davidson of the Sverdrup Corporation AEDC Group attended a demonstration of our probe at the Astron facility along with Ms. Collier and provided comments and suggestions that were greatly appreciated. Also, thanks are due to Lewis Research Center personnel, particularly Gus Fralick, for the time and energy required to provide test time in their combustor facility.

SECTION 2 - REVIEW OF RELATED WORK

The accurate measurement of gas temperatures in high-velocity flows is a common requirement in many engineering and scientific applications. Because of this need, and due to the many advantages associated with the use of thermocouples in gas temperature measurement, a large body of literature has been devoted to this subject. A review of this work during the course of a new probe development effort is beneficial for several reasons. First, an examination of the limitations inherent in conventional thermocouple usage provides an appreciation for the areas in which measurement accuracy can be improved. Secondly, a description of several existing techniques to improve measurement accuracy will provide a better understanding of the operating principles, the necessary tradeoffs, and the design goals of the Astron probe. This section provides background information that will prove useful during the discussion of the operation of the Astron probe in Section 3.

Section 2.1 examines the conventional use of thermocouples to measure gas temperatures, including a discussion of accuracy limitations associated with thermocouple response time, probe recovery factors, radiation-induced errors, and conduction losses. A review of four advanced temperature measurement methods demonstrated during the last 30 years is presented in Section 2.2. The design goals of the Astron probe and the relationship of this probe to previous work are presented in Section 2.3.

2.1 CONVENTIONAL TECHNIQUES

Due to their relatively low cost and ease of use, thermocouples are the instrument of choice in most temperature measurement applications. A great deal of versatility is provided by the ability to vary wire and junction dimensions, to use either sheathed or bare wire probes, and to shield junctions if necessary to minimize radiation errors. These variations in probe design can be combined to allow the use of fairly basic thermocouple techniques over a broad range of measurement conditions. In almost all applications, the thermocouple can be tailored to the specific use to the extent that the only signal conditioning required is signal amplification and filtering of high frequency noise.

In a typical application, the thermocouple junction is inserted into the moving gas stream and allowed to come to a steady or quasi-steady temperature. The thermoelectric voltage generated by this junction provides a fairly accurate estimate of

the true gas temperature in the vicinity of the thermocouple. In effect, the user is solving one equation for one unknown:

$$T_{gas} = T_{probe} \qquad\qquad (2-1)$$

In this equation, T_{gas} is the gas temperature in the vicinity of the thermocouple junction and T_{probe} is the temperature of the junction at the time of the measurement. The assumptions implied by the use of this equation are that the thermocouple and the moving gas are in fact at the same temperature and that the voltage generated by the thermocouple junction can be accurately correlated to the actual junction temperature.

In reality, the temperature measured when using a thermocouple can differ significantly from the true temperature of the gas in contact with the probe. Differences between actual and measured temperatures can be attributed to the following principal phenomena.

- The temperature of a thermocouple junction represents an equilibrium value based on all forms of energy transfer between the probe and its surroundings. Energy can be transferred between the probe and its environment by means of convection, conduction, and radiation. If convection is the predominant method of transfer, then the thermocouple will appear to come to equilibrium with the gas stream.

- A thermocouple junction has a finite response time due to its inherent mass and heat capacitance. No thermocouple can respond instantaneously to changes in the thermal environment. If the mass and specific heat of a junction are small compared to the convective heat transfer rate, then the thermocouple will respond quickly to gas temperature changes.

- In a high-velocity gas stream, compressible flow effects can significantly impact measurement accuracy. These effects are the result of boundary layer friction losses and flow stagnation at points on the probe surface, so this aerodynamic heating is not necessarily uniform over the surface of a probe. In practice, empirical recovery ratios and recovery factors are defined as a function of probe geometry and Mach number to correct for these effects.

- The thermoelectric voltage generated by a junction is subject to small variations due to the presence of impurities in the thermocouple alloys. Contamination occurring during the fabrication process can be calibrated out prior to use, but contamination occurring during operation can lead to large unknown errors. Signal conditioning electronics can also be a source of inaccuracy, but it will be assumed for the purposes of this analysis

that signal conditioning errors are well controlled and that errors in the output signal are due solely to thermoelectric phenomena.

The impact that these known sources of error have on the accurate measurement of gas temperatures will be evaluated on the following pages. A sketch of a typical bare-wire thermocouple is presented as Figure 2-1. Included with this sketch are typical probe dimensions and a summary of flow conditions that approximate the gas turbine combustor environment. These values will be used to quantify the relative magnitudes of the various sources of error in the combustor exit. This knowledge can then be used to design a probe that is optimized for this particular environment.

2.1.1 Errors Due to Combined Heat Transfer Mechanisms

If local gas temperature is the desired parameter to be measured, then energy exchange between the thermocouple junction and the surroundings by any means other than convection will most likely introduce an error to the measurement. The junction tends toward an equilibrium heat transfer balance such that the net transfer of energy to the probe by conduction, convection, and radiation is zero. If convective heat transfer was the only energy transfer mechanism present, then the equilibrium temperature of the thermocouple would equal the local gas temperature.

V

Flow Properties:

T_{gas} = 2800°F
Velocity = 280 ft/s
Mach Number = 0.1
Static Pressure = 5 atm
T_{wall} = 2000°F

Probe Dimensions:

Wire Diam = 0.030 in (20 gage)
Bead Diam = 0.050 in
Exposed Lead Length = 0.25 in

446-89
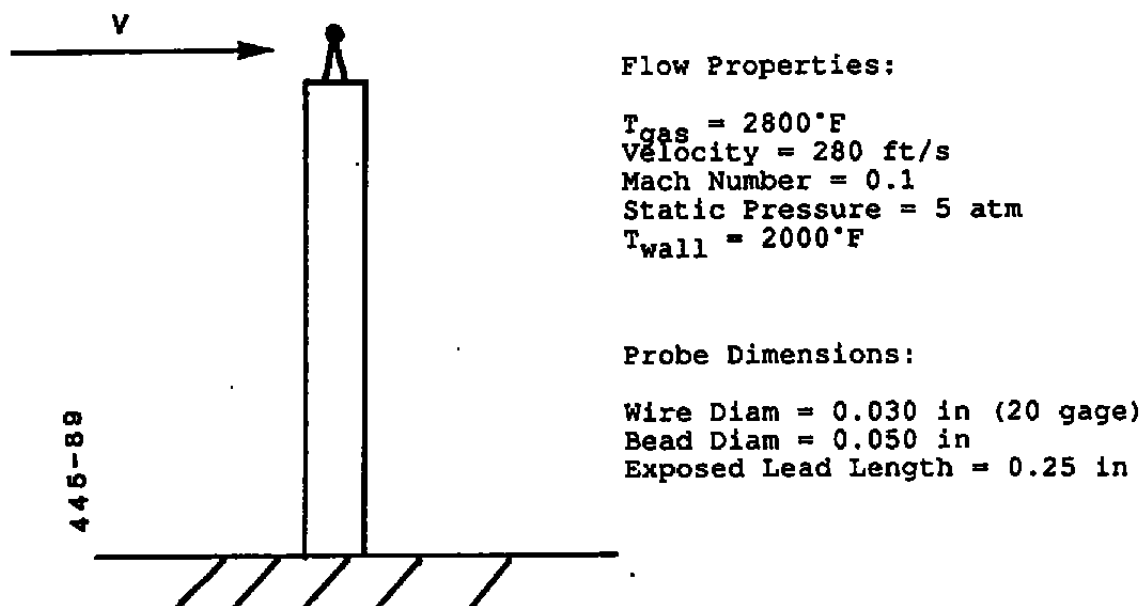
Figure 2-1. Typical Flow Properties and Thermocouple Dimensions

Conduction errors are introduced by the conduction of heat from the junction through the thermocouple wires to a hotter or colder probe base. The probe base itself is at a temperature that is near the freestream gas temperature due to the high ratio of probe length to probe diameter. We will assume for the sake of simplicity that the probe base temperature is 20°F to 50°F lower than the gas temperature. Based on typical assumptions of one-dimensional heat transfer in the thermocouple legs (i.e., wire temperature is a function of axial displacement only, temperature differences across a wire cross-section are negligible), constant gas temperature, and constant base temperature, the following equation can be used to solve for the measurement error due to conduction effects[1]:

$$T_p - T_{gas} = (T_b - T_{gas})/(\cosh mL) \qquad (2-2)$$

where: $\qquad m = (hC/kA)^{1/2}$

In Equation 2-2, $T_p - T_{gas}$ is the difference in temperature between the probe and the gas, so in effect this difference represents the conduction error. This error is linearly proportional to the difference between the gas temperature and the probe base temperature, so the advantage to having a probe base temperature that is nearly equal to that of the gas is obvious. The variable h is the convective heat transfer coefficient, C is the circumference of the extended surface (in this case the thermocouple wire), k is the conductivity of the wire, and A is the cross-sectional area. A value will be calculated for the convective heat transfer coefficient based on the Reynolds number of the flow. Since platinum-rhodium thermocouples will be used in our applications, we will use the conductivity of platinum in our calculations.

Assuming that the wire can be modeled as a cylinder in crossflow, an empirical correlation is used to calculate a value for h. A heat transfer coefficient of 404 Btu/hr-ft^2-°F is found for a Reynolds number based on wire diameter of 0.050-in. Using this value of h, the conductivity of platinum, and the dimensions and gas properties specified in Figure 2-1, a plot of the conduction error as a function of exposed wire length for different values of $T_b - T_{gas}$ is shown as Figure 2-2. It is shown that in a high-velocity gas stream, convection dominates the energy balance between convection and conduction. Depending on the base temperature, an exposed wire length of 0.25 to 0.375 inches can be chosen to reduce the conduction error to about 5°F, which is about 0.2 percent of the actual gas temperature. An error of this magnitude is negligible in almost all cases, and we will therefore choose to ignore conduction errors in most of our analyses.

Errors introduced by radiation effects will be evaluated in a manner similar to the technique used in quantifying the conduction error. Representative flow conditions have been identified, but we will need to define two additional properties.
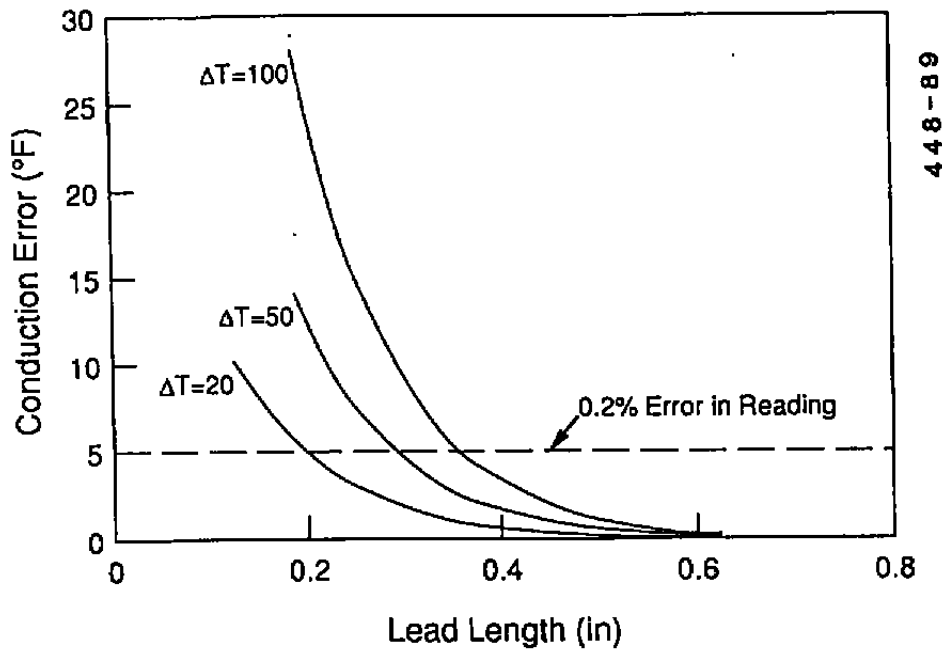
Figure 2-2. Measurement Error Caused By Conduction Losses

We will assume that the probe surroundings have a uniform temperature of 2000°F and that the thermocouple has an emissivity of 0.5. These two additional properties will allow the calculation of the temperature measurement error using the following equations. The transfer of energy due to radiation is modeled as:

$$Q_r = \varepsilon \sigma A (T_w^4 - T_p^4) \qquad (2\text{-}3)$$

where Q_r is the energy transfer rate, ε is the emissivity, σ is the Stefan-Boltzmann constant, A is the surface area of the probe, T_w is the wall temperature defined in the previous paragraph, and T_p is the unknown to be solved.

We can now set up an energy balance equation where the combined energy transfer due to convection and radiation must equal zero for the thermocouple to be in thermal equilibrium.

$$h(T_{gas} - T_{probe}) + \varepsilon \sigma (T_{wall}^4 - T_{probe}^4) = 0 \qquad (2\text{-}4)$$

The value used for h is 374 Btu/hr-ft^2-°F, which is slightly smaller than the value defined in the conduction error

calculation. The probe junction may be more accurately modeled as a sphere rather than a cylinder, and the diameter of the sphere is assumed to be larger than the diameter of the cylinder by about 67 percent. These differences result in the 8 percent drop in h. Solving Equation 2-4 iteratively for the probe temperature we find that at the conditions specified, the probe equilibrium temperature would be 2665°F, which is 135°F below the true gas temperature. This error is substantial, but it could likely be reduced by a factor of 3 to 4 using proper shielding techniques. As we would anticipate using a shielded probe in this environment, an error on the order of 30°F to 40°F is anticipated. This error is still substantially larger than the conduction error previously calculated and cannot be ignored.

2.1.2 Time Response Errors

Another source of measurement error identified in this section is related to the time response of the probe. In a flow where the gas temperature is changing, a finite time is required for the thermocouple junction to accurately respond. This time lag is a function of the mass of the junction, the heat transfer area, the heat capacity, and the convective heat transfer coefficient of the probe in the moving stream. The following equation applies:

$$T_{gas} = T_p + \tau \dot{T}_p \qquad (2\text{-}5)$$

where: $\qquad \tau = mc/hA$

$\dot{T}_p$ is the first derivative of probe temperature with respect to time, and τ is the characteristic response time of the probe. From this equation it is apparent that the time response error could be eliminated entirely from the measurement if the change in probe temperature with respect to time and the time constant, τ, could be determined. While it is fairly straightforward, at least in theory, to differentiate the probe temperature, it is extremely difficult to obtain an accurate value of τ. This time constant can be determined empirically to provide an estimate of the steady-state temperature, and this method has been demonstrated. A fairly recent and well-documented example of this technique is provided by Vonada[2].

In estimating the error in a measurement due to response time, it is instructive to assume that a thermocouple behaves as an ideal first-order instrument. Basically this requires that Equation 2-5 apply and that τ be constant. If these restrictions are accurate then the following observations can be made. A time lag of approximately 5.3 time constants is required for a probe to make a temperature change of 99.5 percent of the total value of a step change in gas temperature. If exposed to a constant temperature ramp, the junction temperature will always lag the true gas temperature by a value equal to the probe time constant multiplied by the ramp rate.

In the combustor application, we are interested in determining time-averaged steady-state gas temperatures. High-frequency temperature fluctuations of several hundred Hz may exist even at steady engine conditions, but the time-averaged temperature over periods of several seconds should be constant. Due to our interest in measuring steady-state temperatures, the response time contribution to measurement error should be zero in the combustor application.

Continuing in our effort to quantify measurement errors in the combustor environment, a time constant will be evaluated for the conditions described by Figure 2-1. The time constant, τ, will have a value of approximately 0.28 sec under these conditions. A step change in temperature of 1000°F would settle to within 5°F of the equilibrium value in less than 2 sec. Under conditions in which the gas temperature is increasing at a constant rate, a temperature rise of 100°F/min would result in a constant measurement error of 0.5°F.

2.1.3 Probe Recovery Factor

An additional source of error can occur if one is attempting to measure either a true static or true stagnation temperature in a high-velocity flow. The aerothermal heating effects that result during deceleration of the gas stream around the thermocouple cause errors that must typically be dealt with empirically. This problem is most severe when attempting to measure the true static temperature of a flow with a Mach number above approximately 0.5.

In measuring the gas temperature in a gas turbine combustor, two factors work in our favor. First, the temperature of the gas is highest in this section of the engine, so the sound speed is high and Mach numbers tend to be low. At a typical combustor temperature of 2800°F, a gas velocity of 500 ft/s corresponds to a Mach number of approximately 0.2. The gas velocity could easily be decreased to a Mach number of 0.1 using a shielded probe, and the corresponding difference between static and stagnation temperature at this Mach number would be about 6°F at 2800°F.

The second factor reducing the static/stagnation uncertainty in our application is that we are interested in stagnation conditions in the gas turbine environment. While we cannot measure stagnation conditions exactly, the error involved in measuring a stagnation temperature with a thermocouple is much less than the error in a static measurement. Even if the stagnation temperature measurement has a 10 percent recovery error associated with it, that error would be 10 percent of a total difference between static and stagnation conditions of about 6°F in a representative combustor environment. That would translate to a total measurement error of about 0.6°F. This calculation shows that deceleration of flow past the thermocouple

to about 250 ft/s in the hot combustor environment will reduce the recovery error to practically zero.

As an example of why probe recovery factors can be a concern, consider the case of a 2800°F gas stream flowing at a Mach number of 0.5 past a probe. In this case, the difference between static and stagnation temperatures is 160°F, and a recovery factor of 0.90 indicates that the true stagnation temperature differs from the measured value by 16°F. In many regions in a gas turbine engine, recovery factor errors can be significant. As these examples have shown, the high temperature and relatively low velocity between the combustor and the turbine inlet in a typical engine minimize the effects of this problem in our application.

2.1.4 Calibration Errors and Contamination

All thermocouple alloy pairs exibit some nonuniformity in the voltage generated at a given temperature. This is due to impurities and inhomogeneity present in the thermocouple alloys, and is unavoidable. Fortunately, this error resulting from impurities in the fabrication process is typically small. In particular, the noble metal thermocouples (Types R, S, and B) are the most stable and can be fabricated to exacting standards. The Type S thermocouple (platinum vs. platinum - 10 percent rhodium) is so stable that it is specified as the standard for temperature calibration betweeen the antimony point (630.74°C) and the gold point (1064.43°C). Type B thermocouples are almost as stable in a well-behaved environment and can be specified to be accurate to within approximately 0.1 percent of the reading between 1500°F and 3100°F.

Unfortunately, while the noble metal thermocouples are stable in a protected environment, they are all subject to metallic vapor diffusion at high temperatures, which can readily change the platinum wire calibration. Because of this, the noble metal thermocouples are typically protected in high-purity alumina sheaths. A platinum sheath would serve the same purpose, but at a much higher cost. In typical combustor test rig applications, bare wire platinum thermocouples are frequently used. Due to the short duration of typical engine tests (less than 8 hours), it is possible that metallic vapor contamination is not a problem. This source of error should be examined in greater detail.

2.1.5 Minimizing Errors in the Combustor Environment

Having investigated sources of temperature measurement uncertainty (other than signal conditioning sources) for the gas turbine combustor environment, it should be apparent that the primary source of error will almost certainly be due to radiant exchange. It is also clear that by careful design, radiation should present the only error large enough to be significant under constant temperature conditions. Probe recovery errors will not be a factor, and conduction errors should be reduced to an acceptable level during the design process. We are, for the

present, assuming that wire contamination due to the harsh combustor environment will not be significant over the course of a several-hour test period. We have defined the principal sources of error for a combustor probe, and in doing so we have reached a conclusion consistent with earlier input from AEDC technical personnel. Before proceeding with a discussion of the Astron probe, advanced measurement techniques related to the Astron method will be presented.

2.2 ADVANCED METHODS

The remainder of the measurement techniques presented in this report use the conventional thermocouple materials previously described, but the methods combine information from two junctions or information from one junction at more than one time during a transient to solve for two unknowns. These unknowns are typically the gas temperature and either the probe response time or the convective heat transfer coefficient. The four techniques are presented in the approximate order that they were developed.

2.2.1 General Electric Pulse Technique

Work performed by A. F. Wormser and R. A. Pfuntner for General Electric in 1964[3] resulted in a temperature pulsing technique claimed to be capable of extending the temperature range of Chromel-Alumel thermocouples to 7000°F. Results were reported for tests in an oxy-hydrogen laboratory blast burner flame at 5260°F. The measured results agreed to within 1 percent with the theoretical gas temperature, and no deterioration of the thermocouple was observed.

The principle of operation was based on the assumption that a bare thermocouple wire will respond as a constant property isothermal mass when exposed to a high velocity gas stream. If this assumption is valid, then the temperature response of the probe follows an exponential curve. If the time constant for the probe is known, then the instantaneous gas temperature can be calculated using Equation 2-5 from Section 2.1.

It follows that the gas temperature can be calculated without the thermocouple ever reaching the final gas temperature if the time constant of the probe is known. Unfortunately, as discussed in Section 2.1, the time constant of a thermal probe is difficult to calculate. The convective heat transfer coefficient, h, which has a linearly proportional impact on the value of τ, is a function of variables such as fluid density and viscosity that are difficult to measure under typical test facility conditions. The measurement of these properties is so difficult that it is usually not feasible to calculate a time constant directly.

Wormser and Pfuntner circumvented this problem with a unique circuit design and the assumption of constant gas properties over the duration of a temperature cycle. The temperature probe was

intermittently cooled with air and then allowed to respond to a partial thermal transient when the cooling air was shut off. Using analog circuitry, the thermocouple signal during a temperature transient was amplified and added to the output from a circuit differentiating the temperature signal. The gain on the differentiator was varied with a motor-driven potentiometer. Assuming a constant gas temperature over the duration of the transient, a constant output from the summed temperature and derivative circuits indicated that the proper value for the time constant was being used.

Feedback control on the analog circuitry was provided by monitoring the output signal from the summation of the temperature and temperature derivative signals. A decrease in the output voltage with time indicated that the electrical network time constant(RC) was greater than the thermocouple time constant, while an increase in the output voltage indicated that the electrical network time constant was less than the thermocouple time constant. By monitoring the slope of this output signal, a feedback voltage was generated to adjust the motor-driven potentiometer. In this way, the system converged on the real gas temperature. A graphical representation of the solution employed is presented as Figure 2-3.
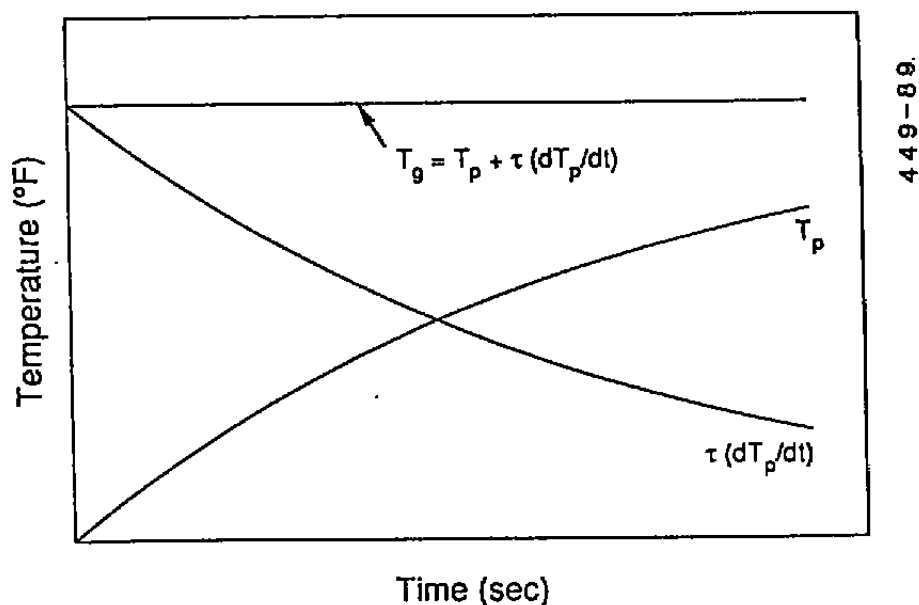
Figure 2-3.   Graphical Solution of the Transient Thermocouple Equation Using the General Electric Method

Reference 3 stated that the pulse thermocouple technique compared favorably with conventional thermocouples at high temperatures because it required no radiation correction. It is clear that this assumption is not always correct, although there appear to be several instances when this would be true.

- If the sources of radiation error are less than the gas temperature (e.g., cooled engine walls) and the probe is cycled at a temperature close to the radiant source temperature, then it is clear that heat transfer due to radiation would be negligible compared to the rate of convective transfer. In fact, in any case in which the radiant energy transfer is negligible when compared to convective transfer, then no radiation correction is required.

- If the radiant source temperature is approximately equal to the local gas temperature, then an equivalent radiant heat transfer coefficient can be determined. The radiation coefficient can be combined with the more conventional convective heat transfer coefficient to form a combined heat transfer coefficient that is a function of temperature. If the method discussed here is used over a narrow temperature range, and if the probe temperature is significantly lower than the gas temperature, then the combined heat transfer coefficient will be nearly constant. The tradeoff is that by decreasing the temperature range of the probe transient and by keeping the probe temperature low, the need for a radiation correction is eliminated, but this is done at the expense of significantly reducing the sensitivity of the instrument.

This method could be improved somewhat using modern digital signal processing techniques. Rather than using a motor-driven pot, temperature derivatives and the correct time constant could be derived more accurately using digital electronics and software. Spectral analysis could provide information on the time-averaged temperature as well as fluctuations with frequency. Two problems remain with this concept. First, it would give incorrect answers in cases where the mean temperature or gas velocity is changing with time. Secondly, probe sensitivity may not be adequate to meet accuracy requirements if radiation effects are not accounted for in a more direct manner.

2.2.2 NASA Lewis Radiation-Compensated Probe

A pulsed thermocouple technique that compensated for radiation errors was also designed and demonstrated by Herbert Will of the NASA Lewis Research Center[4]. This work was based on an earlier program to develop a pulsed probe that would measure gas temperatures above the melt temperature of the thermocouple material. The earlier work has not been studied, but it is apparently a digital implementation of the earlier work by Wormser and Pfuntner. By assuming constant gas conditions over

the duration of a thermocouple pulse, and by also assuming that the thermocouple behaves as an ideal first-order instrument, a large number of simultaneous equations can be solved for two unknowns, the final probe temperature and the time constant of the thermocouple. Wormser and Pfuntner realized that they were solving for two unknowns, but their solution to this problem was to vary one of the unknowns, the time constant, until the other unknown, the gas temperature, had a constant value over the duration of the pulse.

In Will's later work[4], the method was improved by adding the ability to numerically compensate for radiation-induced errors. Given a wall temperature and probe properties including emissivity, a computer program was developed to find the best fit to the probe data collected during a transient. The best fit correlation technique assumes that the probe is acted on by both radiation and convection. Compensation for radiation errors using this technique does require accurate knowledge of probe emissivity and the wall temperature. The probe is not intended to accurately respond to temperature fluctuations that are faster than a typical pulse length. Experimental results from tests performed at the Air Force Wright Aeronautical Laboratory (AFWAL) showed a maximum deviation between measured and extrapolated temperatures of 3 percent.

2.2.3 Two-Probe Steady-State Technique

A method for determining the radiation-corrected local gas temperature using two thermocouples with different emissivities was proposed by V. I. Menshikov and published in the Journal of Engineering Physics in 1975[5]. The original article is in Russian and has been translated. This method requires the assumption that thermocouple junctions behave as lumped thermal masses, and the size of the two probes and the spacing between them must be small compared to variations in flow conditions.

The two probes have different, but known emissivities, so when the two probes come to thermal equilibrium they will have different temperatures in an environment with a strong radiation component. Menshikov calculated conductivity losses and radiation losses, and by knowing the probe temperatures and the wall temperature, he was able to eliminate the convective heat transfer coefficient from the gas temperature calculation.

The derivation of this method proceeds as follows. Knowing that the two temperature probes are in thermal equilibrium, it can be demonstrated that the sum of the energy inputs into the probe due to convection, conduction, and radiation are equal to zero. The radiant exchange is modeled as:

$$Q_r = \varepsilon \sigma A (T_1^4 - T_m^4) \qquad (2-6)$$

This is essentially the same equation as Equation 2-3, where the temperature T_1 is the temperature of Probe 1, and T_m is

assumed to be the temperature of the surrounding environment. The probe temperatures will be differentiated by the numbers 1 and 2 in this derivation. It is assumed that values for all of the parameters in this equation are known. The equation for the conductive energy loss is:

$$Q_{cond.} = \Lambda(T_1 - T_m) \tag{2-7}$$

The variable Λ is a generalized thermal conductivity term for the thermocouple lead wire, taking into account heat loss by convection from the wire leads, and the temperature T_m from above is also the temperature of the probe base. Basically, the point of using this form of the conduction equation is to allow the calculation of a constant, in this case Λ, that defines the conduction loss as a function of temperature difference. As expected, convective heat transfer is modeled as a function of a convective heat transfer coefficient and the temperature difference between the probe and the freestream gas. Writing an energy balance for Probe 1 in thermal equilibrium and solving for the gas temperature yields the following equation.

$$T_{gas} = T_1 + \frac{\varepsilon_1\sigma}{h}(T_1^4 - T_m^4) + \frac{\Lambda}{hA}(T_1 - T_m) \tag{2-8}$$

Writing a similar equation for Probe 2 yields the following:

$$T_{gas} = T_2 + \frac{\varepsilon_2\sigma}{h}(T_2^4 - T_m^4) + \frac{\Lambda}{hA}(T_2 - T_m) \tag{2-9}$$

Subtracting Equation 9 from Equation 8 and solving for the convective heat transfer coefficient results in:

$$h = \frac{[\varepsilon_2\sigma(T_2^4-T_m^4) - \varepsilon_1\sigma(T_1^4-T_m^4) + (\Lambda/A)(T_2-T_1)]}{(T_2 - T_1)} \tag{2-10}$$

Knowing this coefficient, one can now solve for the gas temperature based on the two probe temperatures using Equation 2-8 or Equation 2-9 and substituting in the heat transfer coefficient determined in Equation 2-10.

This method was verified experimentally by performing the measurements necessary to calculate the temperature of a propane-air flame. Temperatures were measured using platinum-rhodium thermocouples. One junction was a polished thermocouple wire. The other bead was fabricated from chromium-nickle stainless steel. The thermal emissivity of the platinum bead was taken to be 0.21, and the thermal emissivity of the stainless bead was 0.70. The results yield a calculated temperature of 2065°K

(3717°R). For the stoichiometric conditions tested a predicted temperature of 2080°K (3744°R) was cited: The method was reportedly accurate to 0.75 percent.

It is evident that this method could provide accurate gas temperature measurements in a well-controlled environment, but there are several problems involved in using the method for measuring combustor temperatures. First, the propane-air mixture provided a very clean flame that would not participate in radiant exchange with the probe, and this would not be true in a combustor where it must be assumed that radiant emission from combustion gases is significant. Secondly, in the laboratory experiment discussed here, the temperature of the surroundings was controlled to the degree that a constant temperature radiation source could be assumed and this temperature was measured. The constant temperature of the surroundings will not be a valid assumption in the gas turbine. Therefore, in the test conditions of interest, namely the gas turbine combustor exit, the method as proposed by Menshikov would be inappropriate.

2.2.4 Astron Phase I Probe

In the Astron Phase I SBIR program[6], a probe was demonstrated that operated in a manner similar to that of the GE probe and the early NASA-Lewis probe. No compensation was made for radiation errors, but the use of two junctions instead of one allowed for the nearly instantaneous solution of two equations for the two unknowns, the gas temperature and the probe response time. This fast response time and an ability to operate at below the true gas temperature were the two main benefits of the Phase I Astron probe.

It can be observed from Equation 2-5 in Section 2.1 that the gas temperature, T_{gas}, can be determined exactly at any given time if the other parameters in the equation are known. The temperature T_{probe} is simply the measured instrument temperature. The determination of T_{probe} can be made by taking the first derivative of the probe temperature with respect to time. As demonstrated in two earlier methods, this can be done either digitally, with finite difference equations, or by using analog circuitry.

For a given probe, the mass, surface area, and heat capacity can be determined independently of testing with a great deal of accuracy. Unfortunately, the heat transfer coefficient is a variable that depends on flow conditions and probe geometry, and the heat transfer coefficient is often more difficult to determine than the gas temperature. The uncertainty involved in using empirical values of the heat transfer coefficient is severe enough to make this method of solution undesirable.

Assume that two probes (identified as Probe 1 and Probe 2) are placed in a flowstream. The probes are close enough to each other to be exposed to the same flowfield, yet far enough apart

so as not to interfere with the flowfield of the adjacent probe. This probe separation distance should be on the order of several probe diameters. The equations governing the transient thermal response of the two probes are given below. Again, heat losses between the probes and the environment due to radiation and conduction are neglected, and the probes are assumed to be isothermal.

$$T_{gas} = T_1 + \tau_1 \dot{T}_1 \qquad (2\text{-}11)$$

$$T_{gas} = T_2 + \tau_2 \dot{T}_2 \qquad (2\text{-}12)$$

where $\tau_1 = (mc/hA)_1$ and $\tau_2 = (mc/hA)_2$.

Now, assume that the convective heat transfer coefficient is a function only of flow conditions in the vicinity of the probes and the external geometry of the probes. If the two probes are exposed to the same flow conditions, and if the probes are designed to have identical external dimensions, then it follows that $h_1 A_1 = h_2 A_2$. Using this information, hA can be eliminated from Equations 2-11 and 2-12 and the resulting solution in terms of gas temperature is:

$$T_{gas} = (T_1 \cdot \dot{T}_2 - K \cdot T_2 \cdot \dot{T}_1)/(\dot{T}_2 - K \cdot \dot{T}_1) \qquad (2\text{-}13)$$

where $K = m_1 c_1 / m_2 c_2$

This equation is valid at any instant in time provided that T_1 is not equal to T_2. If T_1 is equal to T_2, then the two equations are no longer independent and the equations cannot be solved. Written in matrix form the two equations become:

$$\begin{bmatrix} 1 & -\dot{T}_1 \\ 1 & -\dot{T}_2/K \end{bmatrix} \begin{bmatrix} T_{gas} \\ \tau_1 \end{bmatrix} = \begin{bmatrix} T_1 \\ T_2 \end{bmatrix} \qquad (2\text{-}14)$$

It is evident in this form that simultaneous solution is provided for the two unknowns, the gas temperature and the probe response time. By increasing the difference in temperature between Probe 1 and Probe 2, the sensitivity of the temperature measurement is increased, but errors introduced by radiation effects also become more significant. This same behavior was observed in the operation of the Wormser and Pfuntner probe. An optimum choice of probe temperatures can likely be determined for different operating conditions. Results from the Phase I program are shown in Figure 2-4. In Figure 2-4a, the temperature traces of the two probes are plotted with the calculated gas temperature. As the theory predicts, when T_1 is equal to T_2 at the start of a test, the matrix of Equation 2-14 becomes singular
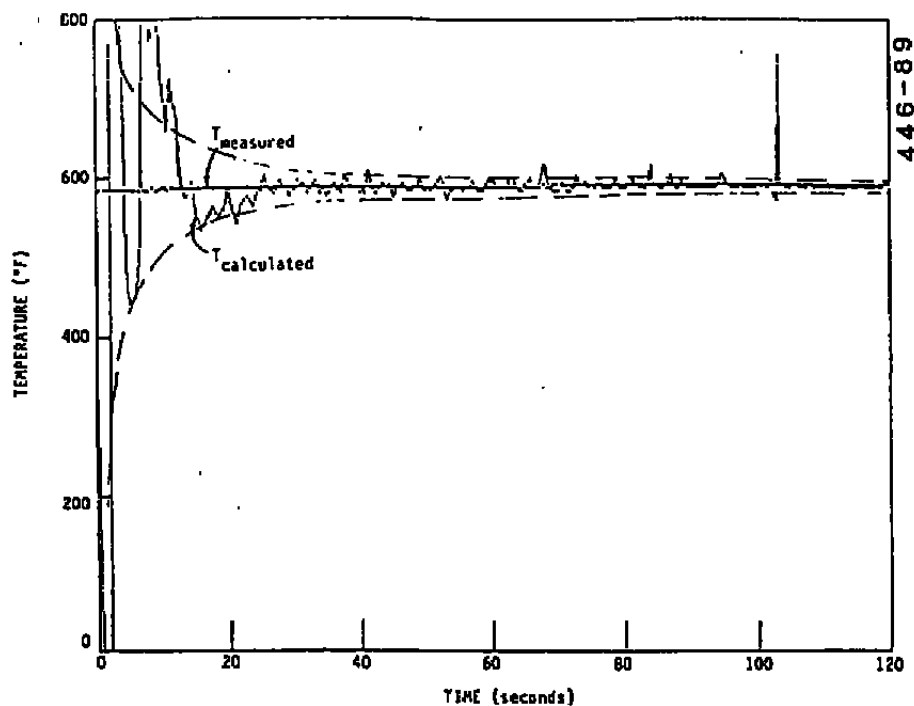
a. Calculated and Measured Gas Temperatures
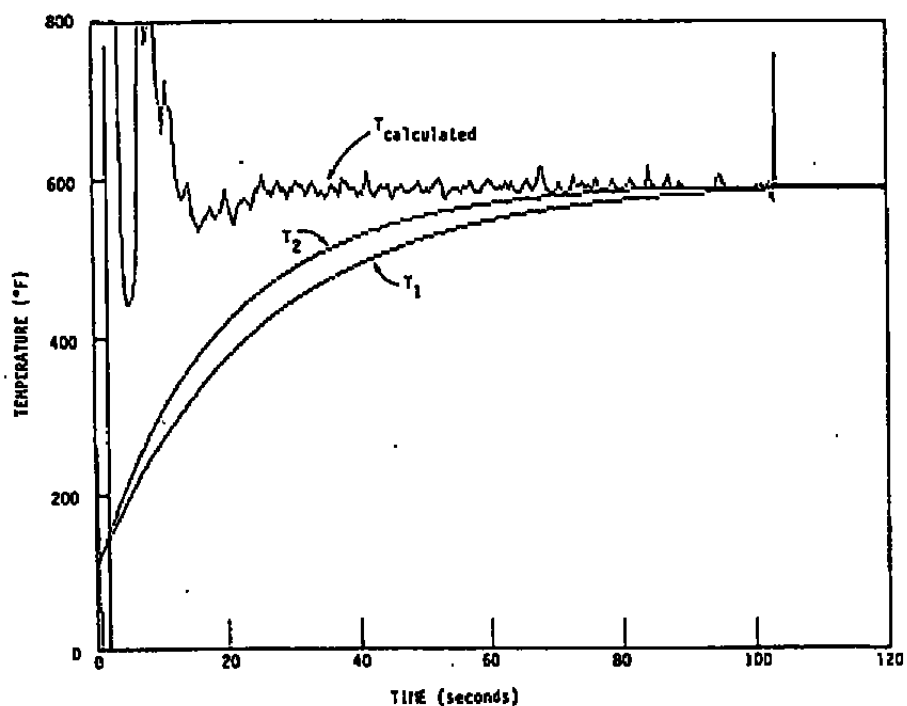
b. Calculated Gas Temperature and Measured Probe Temperatures

Figure 2-4. Comparison of Calculated and Measured Probe and Gas Temperatures Using Astron Phase I Probe

2-16

and the calculated gas temperature oscillates wildly. As shown in Figure 2-4b, the calculated temperature quickly settles to the value of the gas temperature as measured by another thermocouple.

The principal advantage of this method over the method demonstrated by Wormser and Pfuntner is that the method works equally well for both steady and unsteady flow conditions. It should be noted that if steady flow conditions are assumed, and if only one thermal probe is used, then the values of T_1 and T_2 to provide the two independent equations to solve for the two unknowns can come from any two points on the transient temperature curve where T_1 is not equal to T_2. This is essentially the digital counterpart to the General Electric method. Using more than two points from the response curve provides redundant data that can be analyzed statistically to improve measurement accuracy, making the probe concept very similar to the early Lewis Research Center work that did not compensate for radiation errors.

2.3 DESIGN GOALS OF THE ASTRON COMBUSTOR EXIT PROBE

A need was expressed by AEDC personnel for a probe capable of accurately measuring gas temperatures immediately downstream of gas turbine combustors. Desirable properties would include that the probe be:

- Optimized for accuracy, particularly with respect to errors introduced by radiation

- Small enough to minimize flow blockage and provide high spatial resolution

- Capable of surviving the gas turbine environment

The purpose of the probe was to measure steady-state or time-averaged gas temperatures, so rapid probe response time was not an important design criterion.

The probes presented so far compare several pieces of information to obtain an estimate of the true gas temperature that is more accurate than could be obtained by using a single reading from a single probe. The probes designed by Wormser and Pfuntner and by Herbert Will were designed to operate at below the temperature of the gas due to materials limitations of the thermocouple junctions. The Phase I Astron probe could operate in this manner, but could also provide an improved response time. Only the steady-state probe designed by Menshikov was designed with the sole intention of maximizing accuracy.

To meet the design goals set by AEDC, Astron has chosen to pursue the design of a probe that operates in a near steady-state mode, and allows the user to measure the contribution of radiant energy transfer to the probe in a temperature range that is near

2-17

the equilibrium probe temperature. Due to the requirements of the probe, it was optimized for accuracy and survivability. This accuracy requirement, by default, requires that the temperature measured be the stagnation temperature in most compressible flow applications. As discussed in Section 2.1, due to the relatively low Mach numbers encountered in the combustor environment, there is probably only a 10°F to 40°F difference between static and stagnation temperatures in this section of the engine. The one additional tradeoff that was allowed is that the probe has a response time of approximately 10 sec, but this should not reduce the usefulness of the probe in testing at near steady-state conditions.

SECTION 3 - PROBE ANALYSIS AND DESIGN

The operating principles of the Astron temperature probe can be most easily explained and understood under ideal or nearly ideal operating conditions. Following a brief discussion of probe concepts in Section 3.1, the presentation in Section 3.2 will present a list of assumptions concerning probe properties and the flow environment and will then proceed to a description of the theoretical operation of the probe. A thorough analysis of the consequences of deviations from ideal behavior will require quantification of these errors, and this requires that a hardware design exist. Section 3.3 presents the design of the probe used in both the Astron Test Furnace and the NASA Lewis Combustor Rig. This probe is nearly identical in appearance to the probe that would be used in a gas turbine combustor exit. Section 3.4 presents the quantification of measurement errors introduced by nonideal probe behavior. Having performed this exercise, it is possible in Section 3.5 to proceed with an analysis of the effects that these errors have on the actual gas temperature calculation. Section 3.6 presents a brief description of signal processing requirements. Since gas temperature must be calculated based on the measured thermocouple perturbations, signal processing plays a critical role in proper probe operation.

3.1 PROBE CONCEPT SELECTION

The design of the radiation-compensated probe has evolved over the course of the Phase II program, and there have been essentially three different probe concepts. In all cases the basic operating principles have remained unchanged. The Astron probe uses measured valves of total heat flux and radiation heat flux to determine a true gas temperature. The three principal probe concepts evaluated during this program (in chronological order) were:

- Dual probe concept with separate thermocouple junctions for total heat flux and radiation heat flux.

- Sapphire window concept with movable window to change the heat flux conditions to a single thermocouple junction.

- Suction probe concept where gas was drawn past the thermocouple junction and down a suction tube in convective mode and flow was stagnated around the junction in radiation mode.

The dual probe concept was first presented in the Phase II proposal and was similar in many respects to the Phase I probe described in Section 2. Early in the Phase II program probes were designed based on the assumption that one thermocouple was

required for each heat flux environment to be monitored (i.e., two junctions were required to meet our needs, one for the total heat flux environment and one for the radiation environment).

Theoretically the dual probe design was sound. However several restrictions imposed by "real world" behavior led to the single junction design. These restrictions were:

- Size. Due to durability requirements we are limited in our ability to use small thermocouple wires and thin radiation shields. AEDC desired a very compact probe, and as expected, the dual probe design was roughly twice the size of a single probe design.

- Environmental degradation. Proper probe operation requires that the two thermocouple junctions have identical emissivities. Oxidation of the exposed thermocouple is unavoidable over time, and the resulting emissivity mismatch between the two thermocouples would lead to significant errors. While different techniques of cancelling these emissivity-induced errors were studied, no satisfactory solution was found.

- The perturbations of the probe environment necessary for proper operation involve heating and cooling of the thermocouple junctions. The single probe designs simplify this requirement.

Early in the Phase II program a new probe design was introduced that addressed most of the shortcomings of the dual probe. A single thermocouple junction was housed inside of a platinum shield and a movable sapphire window was used to alternate between total heat flux and radiation heat flux conditions. Advantages over the earlier design were:

- Possible reduction in probe size due to the use of a single thermocouple.

- Elimination of the environmental degradation problem. Using a single junction, changes in emissivity will be self-compensating.

- Perturbations in the probe environment are self-induced. The probe cools itself in one mode and heats itself in the other with no need for external energy inputs.

This probe design was presented at our design review at AEDC in September 1987. Structural integrity concerns, coupled with the difficulty of ensuring that the sapphire window would remain clean, made this design undesirable. However, the many advantages of a single probe design were obvious.

The need to improve structural integrity led to the design of the suction probe that was built and demonstrated in this

Data on this page shall be subject to the restriction appearing on page ii of this document.

program. The theory of operation of this probe and details of hardware design are presented in the following sections.

3.2 THEORY OF OPERATION

The Astron temperature probe has been designed to accurately compensate for radiation-induced measurement errors in a high-temperature gas stream. The technique can be viewed as an extension of more traditional gas temperature measurement techniques. The design of the radiation-compensating probe requires nearly all of the design considerations that a conventional probe would require in the gas turbine environment. Because of this, it is logical to start our discussion with the description of a fairly conventional aspirated probe and then proceed with a discussion of deliberate perturbations of the probe environment. The following assumptions will be made in this section:

- The thermocouple junction has constant material properties and responds in an isothermal manner to changes in temperature.

- The radiation and conduction heat transfer environments are not affected by a change in gas velocity past the thermocouple.

- The convective heat transfer coefficient is constant (i.e., is not a function of temperature) over a 100°F temperature range.

- There is no difference between the static and stagnation gas temperatures.

- Gas flow past the thermocouple can be instantaneously started and stopped.

- The thermocouple does not act as a catalyst to further combustion reactions in the vicinity of the probe.

A sketch of a conventional aspirated probe is shown as Figure 3-1. The thermocouple junction is housed inside of a shield to reduce radiation errors, and care is taken to orient the probe so that gas coming in contact with the junction has not been cooled or heated during prior contact with the probe body. To achieve this second objective, the probe is oriented with the gas flow port facing upstream. Gas is drawn past the junction by suction through a tube on the downstream side of the probe.

To obtain an accurate gas temperature measurement, gas is drawn past the probe at a fairly high velocity in order to achieve a large convective heat transfer coefficient. For the purposes of this discussion, assume that radiation heat transfer
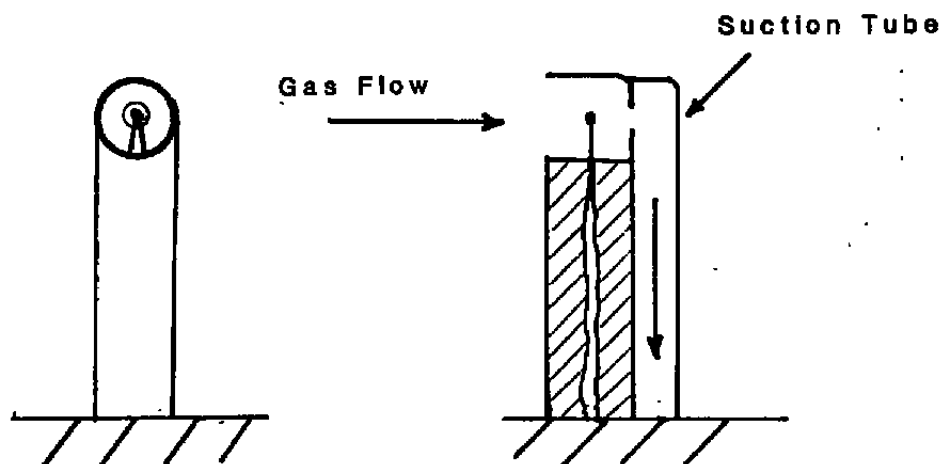
Figure 3-1. Conventional Aspirated Probe

has a net cooling effect on the junction. This would be typical in a gas turbine environment, where metal engine hardware is actively cooled. The probe would work equally well in cases in which the thermocouple junction is at a higher temperature than the gas due to radiant heating of the junction.

Assuming that the probe shown in Figure 3-1 is exposed to steady-state conditions and is in thermal equilibrium, the temperature of the junction can be determined by measuring the thermoelectric voltage of the thermocouple. Since the probe is assumed to be in equilibrium, the following energy balance equation applies:

$$Q_h + Q_r + Q_{cond.} = 0 \qquad\qquad (3-1)$$

where Q_h is the transfer of energy to the thermocouple junction due to convection, Q_r is the radiation heat transfer, and $Q_{cond.}$ is the conduction heat transfer. The net transfer of energy to the thermocouple junction is zero since a state of equilibrium exists. To simplify our discussion, we will assume that the magnitude of the conduction heat transfer term is significantly less than the heat transfer due to convection or radiation, and that the conduction term in Equation 3-1 can be omitted with

little or no loss in accuracy. This equation is rewritten without the conduction term as:

$$Q_h + Q_r = 0 \qquad (3\text{-}2)$$

The Q_h term can be expanded as:

$$Q_h = hA(T_g - T_p) \qquad (3\text{-}3)$$

where h is the area averaged convective heat transfer coefficient over the surface of the junction, A is the surface area of the junction, and T_g and T_p are the gas temperature and probe temperature, respectively.

The Q_r term cannot be so easily expanded without further information concerning temperatures of surfaces and form factors between these surfaces and the junction. The independent variables necessary to calculate the radiation heat flux can be grouped to show the functional dependency:

$$Q_r = f(\varepsilon, \sigma, A, T_p^4, T_{s1}^4, F_{p-s1}, T_{s2}^4, F_{1-s2}, \text{ etc.}) \qquad (3\text{-}4)$$

The T_s terms are temperatures of surfaces exchanging radiation with the probe and the F terms are form factors. In the simple textbook radiation case, the probe exchanges energy with one source and the familiar equation shown as Equation 3-5 can be used.

$$Q_r = \varepsilon\sigma A(T_s^4 - T_p^4) \qquad (3\text{-}5)$$

Since our probe will exchange radiation with many sources including an emitting flame, the formulation of an equation to model Q_r is difficult if not impossible. We will accept Q_r as a value that must be measured rather than calculated, and we will use this value in determining T_g.

Substituting Equation 3-3 into Equation 3-2:

$$hA(T_g - T_p) + Q_r = 0 \qquad (3\text{-}6)$$

Rearranging to solve for T_g:

$$T_g = T_p - Q_r/hA \qquad (3\text{-}7)$$

3-5

The probe temperature is equal to the gas temperature only if Q_r is equal to zero (or if h is infinitely large). In our case, in which the net transfer of radiant energy is away from the probe, Q_r is less than zero, and T_p will be less than the actual gas temperature by the amount Q_r/hA as shown in Figure 3-2. We will call the equilibrium temperature reached under the combined effects of convection and radiation T_c (for T combined). This should not be confused with variables using the subscript h for convection or variables using the subscript cond. for conduction.

By definition, when:

$$T_p = T_c \tag{3-8}$$

Then:

$$Q_c = Q_h + Q_r = 0 \tag{3-9}$$

Another equilibrium probe temperature that is of interest will exist when the convective heat transfer is reduced to zero. This can be accomplished in theory by stopping the suction of gas past the probe junction and allowing the gas to stagnate inside of the probe shield. At zero gas velocity the convective heat transfer coefficient drops to nearly zero, although a small amount of natural convection may immediately commence. In our example with the cool engine walls, this new equilibrium condition where Q_r is equal to zero will occur at a lower probe temperature than exists when Q_c is equal to zero.

Presenting a new set of equations, when:

$$Q_r = 0 \tag{3-10}$$

Then:

$$T_p = T_r \tag{3-11}$$

The drop in probe temperature to the new equilibrium value is shown as Figure 3-3. We have now defined the upper and lower limits of operation of the Astron probe. Transient operation of the probe between these two temperatures will provide the information necessary to calculate the true gas temperature.

When the thermocouple is not in thermal equilibrium, the net transfer of energy to the probe can be modeled using the following equation:

$$Q = mc\dot{T} \tag{3-12}$$

3-6
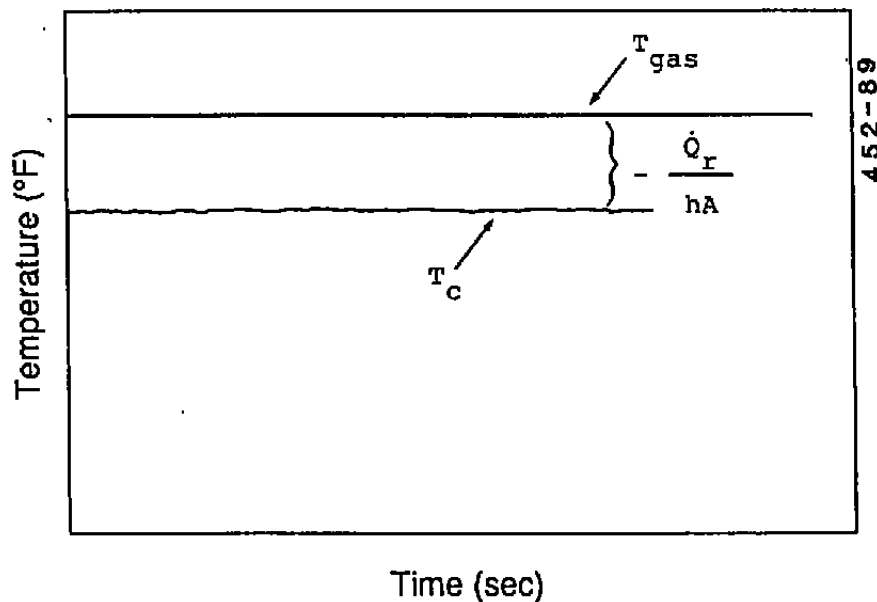
Figure 3-2. Definition of Combined Energy Transfer Equilibrium
Temperature
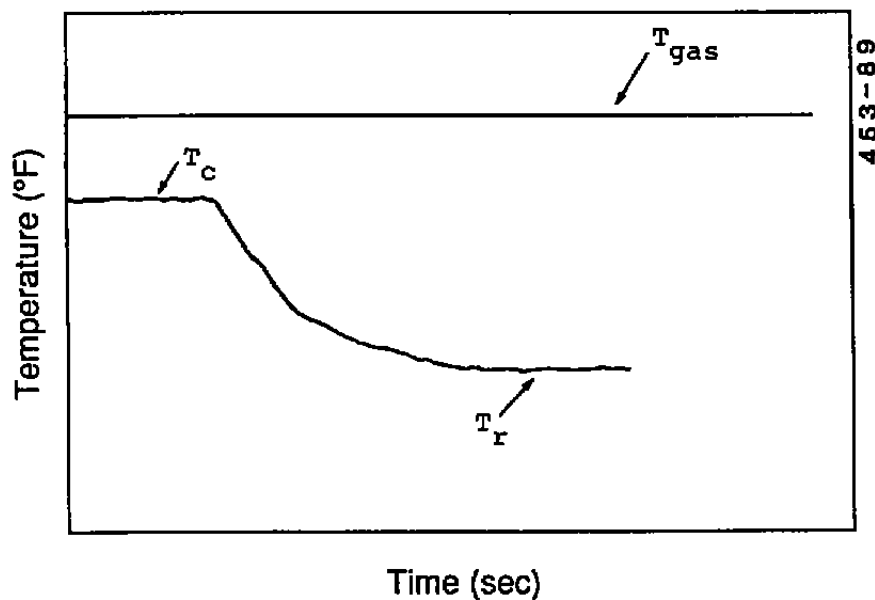
Figure 3-3. Definition of Radiation Energy Transfer Equilibrium
Temperature

Referring to Figure 3-4, if the probe is at the radiation equilibrium temperature T_r and probe gas suction is instantaneously initiated, then the thermocouple temperature will rise to the equilibrium combined energy transfer temperature, T_c. At the instant that probe aspiration begins, the thermocouple is at the temperature T_r and the net flux of radiation to the probe at that temperature is by definition zero. It follows that heat transfer to the probe at the temperature T_r is due solely to convection. Because of this, the following equations apply:

$$Q_h = mc\dot{T}_c \text{ at } T_p = T_r \qquad (3\text{-}13)$$

$$Q_h = hA(T_g - T_p) \text{ at } T_p = T_r \qquad (3\text{-}14)$$

Combining these two equations and evaluating at T_r:

$$hA(T_g - T_r) = mc\dot{T}_c \qquad (3\text{-}15)$$

Rearranging to solve for T_g gives:

$$T_g = T_r + \tau\dot{T}_c \quad . \qquad (3\text{-}16)$$

where:
$$\tau = mc/hA$$

In this equation both T_g and τ are unknowns. One additional equation is required to obtain a solution for T_g. Referring back to Figure 3-4, after approximately five time constants the thermocouple will reach the previously defined combined mode equilibrium temperature, T_c. By definition, Q_h is equal to $-Q_r$ at the temperature T_c (because $Q_h + Q_r = 0$ at T_c). If the probe aspiration is instantaneously stopped after the thermocouple reaches the temperature T_c, the thermocouple temperature will drop and will eventually reach the radiation equilibrium temperature, T_r. Referring now to Figure 3-5, at the instant that flow past the thermocouple junction stops, the sole means of energy transfer to the probe is by radiation, and the following equations apply.

$$Q_r = mc\dot{T}_r \text{ at } T_p = T_c \qquad (3\text{-}17)$$

$$Q_h = -Q_r \text{ at } T_p = T_c \qquad (3\text{-}18)$$

$$Q_h = hA(T_g - T_p) \text{ at } T_p = T_c \qquad (3\text{-}19)$$
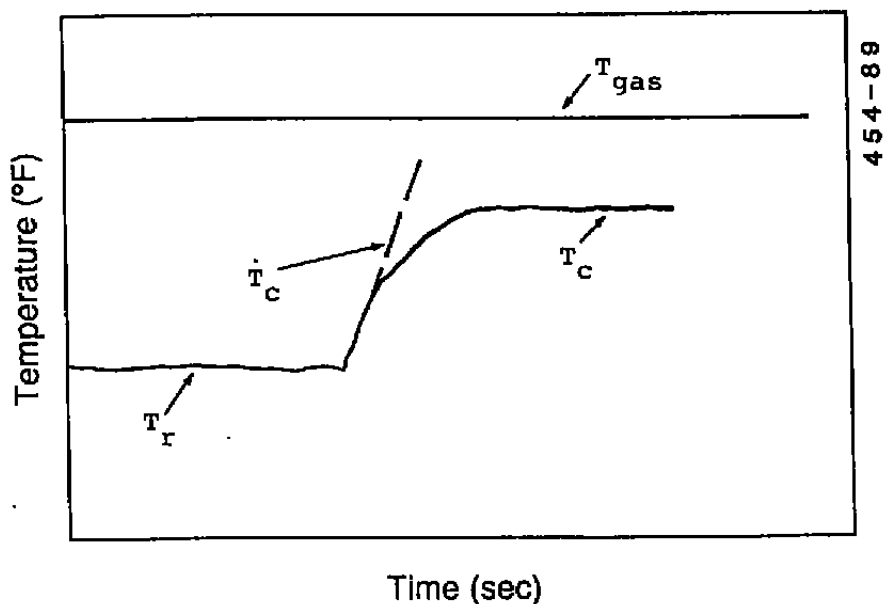
Figure 3-4. Transient Energy Transfer Due To Convection and Radiation
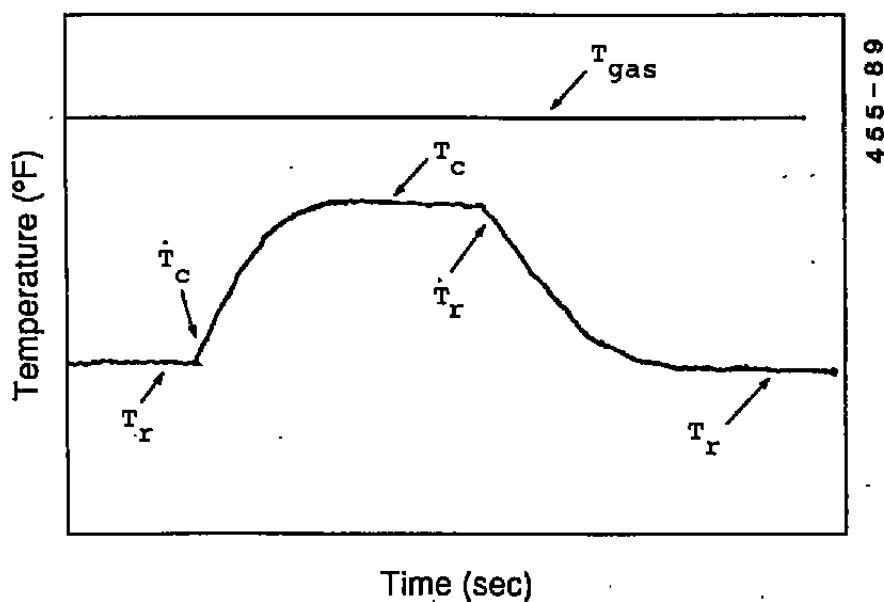
Figure 3-5. Transient Energy Transfer Due To Radiation

3-9

Combining these three equations and evaluating at T_c results in the following:

$$hA(T_g - T_c) = -mc\dot{T}_r \qquad (3\text{-}20)$$

Rearranging to solve for T_g gives:

$$T_g = T_c - \tau\dot{T}_r \qquad (3\text{-}21)$$

where:

$$\tau = mc/hA$$

It is important to note that the τ defined in Equation 3-16 is the same τ that is defined in Equation 3-21. In both cases m, c, and A are properties of the thermocouple junction, and h is the convective heat transfer coefficient. The h used in these two equations is not an "equivalent" h based on combined convective and radiative heat transfer. By careful choice of the temperatures at which the temperature derivatives are evaluated, the component of the energy transfer due solely to convection has been isolated. Only by isolating the transfer due to convection can this method be used. Combining Equations 3-16 and 3-21 to solve for T_g gives the following result:

$$T_g = (T_r\dot{T}_r + T_c\dot{T}_c)/(\dot{T}_r + \dot{T}_c) \qquad (3\text{-}22)$$

One of the two unknowns, T_g, is of interest to us, while the other unknown, τ, is of little interest in this exercise. (Although there may be instances where τ is of interest, and T_g is of secondary importance.) The equation can be evaluated at two probe temperatures, providing two equations for the two unknowns.

Equation 3-22 is undefined if $\dot{T}_c + \dot{T}_r$ is equal to zero. However, it can be shown that when this occurs, T_c must equal T_r, and that this can only happen when T_c and T_r are equal to the true gas temperature T_g. So in fact, the occurrence of the 0 in the denominator in Equation 3-22 can be used to our advantage if this condition is monitored. The true gas temperature can be actually measured, rather than calculated, in this case.

The technique for calculating the gas temperature that has just been described requires that the temperatures T_c and T_r be known along with the derivatives of temperature with respect to time at those two temperatures. A more general method of calculating the gas temperature using the temperatures and temperature derivatives of Figure 3-5 is now presented. During the temperature rise segment of a perturbation cycle, heat flux

to the probe is caused by the combined effects of radiation and convection except at the one probe temperature T_r where Q_r is equal to zero. The combined heat transfer Q_c can be determined as a function of probe temperature.

When suction is turned on:

$$Q_c = mc\dot{T}_c \qquad\qquad (3-23)$$

$$Q_c = Q_h + Q_r = f(T_p) \qquad\qquad (3-24)$$

so:

$$\dot{T}_c = f(T_p) \qquad\qquad (3-25)$$

In a similar manner, during the temperature decay shown in Figure 3-5, the heat flux between the probe and the environment is due solely to radiation. When suction is off:

$$Q_r = mc\dot{T}_r \qquad\qquad (3-26)$$

$$\dot{T}_r = f(T_p) \qquad\qquad (3-27)$$

Since:

$$Q_h = Q_c - Q_r, \qquad\qquad (3-28)$$

it follows that:

$$\dot{T}_h = \dot{T}_c - \dot{T}_r \qquad\qquad (3-29)$$

Since $\dot{T}_c$ and $\dot{T}_r$ are known as functions of temperature for every temperature between T_r and T_c, we can isolate the convective heat transfer to the probe by subtracting the radiation transfer deduced from the temperature decay section of a probe cycle from the combined convective and radiative transfer deduced during the temperature rise segment of a probe cycle.

Having isolated Q_h it follows that the following equation is valid at any temperature between T_r and T_c:

$$T_g = T_p + \tau(\dot{T}_c - \dot{T}_r) \qquad\qquad (3-30)$$

$\dot{T}_c$ and $\dot{T}_r$ are evaluated at the temperature T_p. Equation 3-30 is more general than the earlier Equations 3-16 and 3-21 because the two equations necessary to solve for T_g and τ can be evaluated at any two temperatures between T_r and T_c. We are not restricted to evaluating the temperature derivatives at the discontinuities that exist at the endpoint temperatures.

Setting:

$$\dot{T}_h = \dot{T}_c - \dot{T}_r \qquad (3\text{-}31)$$

and substituting into Equation 3-30, we can substitute two probe temperatures, T_1 and T_2, and the derivatives $\dot{T}_h$, at those two temperatures to get the following equation for T_g.

$$T_g = (T_1\dot{T}_{h2} - T_2\dot{T}_{h1})/(\dot{T}_{h2} - \dot{T}_{h1}) \qquad (3\text{-}32)$$

By using this general equation, we can now choose more than two equations to solve for our two unknowns, taking advantage of the redundancy of our calculations to eliminate errors introduced by noise in our signals. This solution using multiple equations is performed graphically using two different techniques. First in Figure 3-6a, T and $\dot{T}_h$ are plotted at equally spaced increments between T_r and T_c, inclusive. All lines defined by this slope and intercept should cross at a value of τ on the time axis and T_{gas} on the temperature axis. This reinforces the concept that at least two equations are necessary to solve for T_g and τ, and that additional equations provide redundancy in our calculations.

Another means of graphically demonstrating the solution to our equations for T_g is to transfer from a temperature versus time plot to a temperature derivative versus temperature plot. As shown in Figure 3-6b, at every temperature between T_r and T_c there exists a $\dot{T}_r$ and a $\dot{T}_c$ as a function of T_p. Neither of these temperature derivative functions must be linear with respect to the dependent variable T. However, if $\dot{T}_c$ and $-\dot{T}_r$ are added together, the sum, which is $\dot{T}_h$, must be linear. This is true if our assumptions regarding ideal probe behavior are accurate. The extrapolation of the $\dot{T}_h$ line to the temperature axis will cross that axis at T_g. This is always the case because the true convective heat transfer, and hence $\dot{T}_h$, would go to zero when T_p is equal to T_g.

Either of the graphical methods shown in Figure 3-6 could be implemented mathematically to use redundant equations to solve for T_{gas}. Also, Equation 3-22 using the derivatives at T_r and T_c could be solved for T_g. These different methods of calculating the gas temperature will be demonstrated using experimental results in Section 5.

3.3 HARDWARE DESIGN

Having discussed the operating principles of the Astron probe in the previous section, a probe design consistent with the Phase II program objectives will be presented. These objectives include a definition of the combustor environment which is
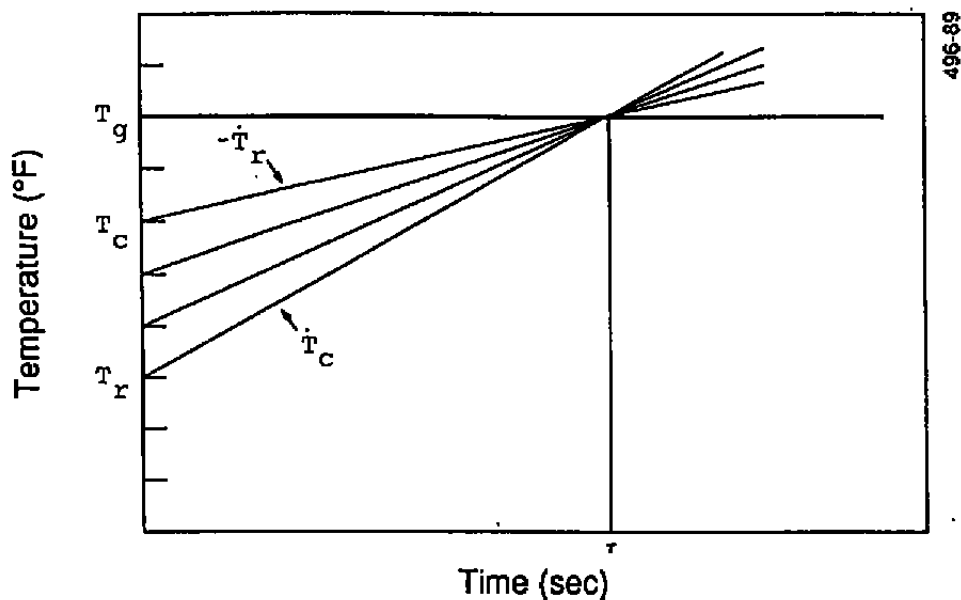
a. Plot in Temperature vs. Time Coordinates
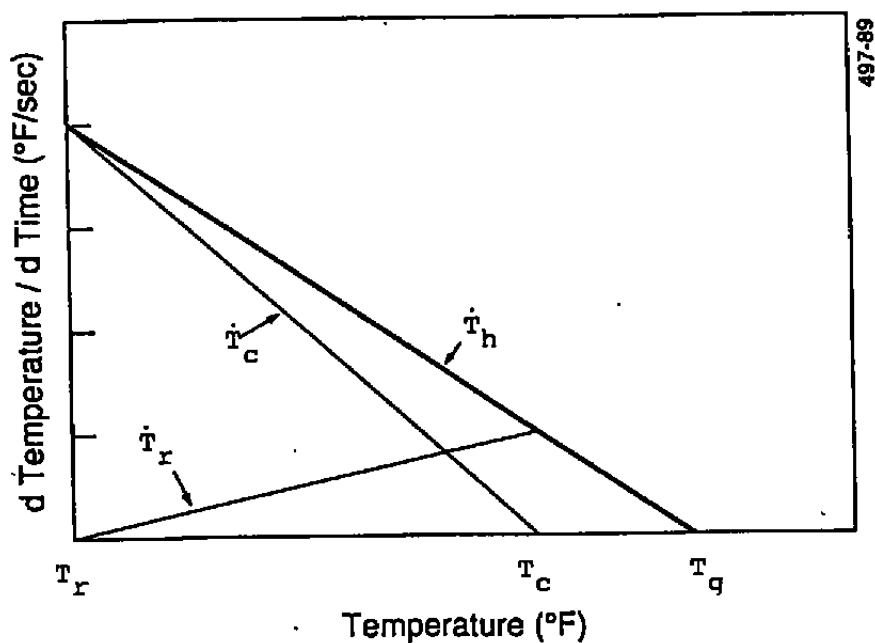
b. Temperature Derivative vs. Temperature Plot

Figure 3-6. Graphical Solution for Gas Temperature Using Astron Phase II Method

independent of the presence of our temperature probe, and also a definition of the operating requirements of a probe needed to survive in this severe environment. The presentation of this information is followed by a discussion of the process that led to our final probe design.

A considerable amount of effort was devoted to determining a suitable worst-case environment for the Astron probe in a gas turbine. This work was done early in the Phase II program, and the intent was to define an environment that was more severe than current combustor environments. The reason for this was to set the design goal at a level that would provide probe operability at a state consistent with future engines as they become operational. The design environment for the Astron probe, consistent with gas turbine combustor exit conditions anticipated over the next 5 years, is presented in Table 3-1.

In addition to the combustor exit environment definition, restrictions are placed on the probe such as maximum allowable size, required measurement accuracy, and durability. These restrictions were determined based on discussions with AEDC personnel. In all cases, these probe requirements appear to be reasonable goals, both from the standpoint of usefulness of the final product as well as being realistically attainable. These probe design conditions are presented as Table 3-2.

The information from Tables 3-1 and 3-2, along with data accessible from earlier contracts awarded by the Air Force to design engine probes, led to the probe design shown in Figures A-1 and A-2 of Appendix A. A platinum-rhodium alloy was chosen as the probe body material based on our peak temperature requirement. This is a fairly standard choice, although the platinum will degrade in a fuel-rich environment. We do anticipate that the degradation of our probe in the reducing environment would occur at a rate slow enough to allow us to meet the structural life requirement of 30 hours, although we do not have data to support this claim.

Another probe option evaluated was the use of tungsten protected by an oxidation-resistant coating. Tungsten would rapidly oxidize in the combustor environment, so the use of this material is feasible only when used in conjunction with a coating. This type of probe would actually survive to higher temperatures than the platinum probe (3500°F), but a crack in the protective coating would lead to a catastrophic probe failure. Since platinum does meet the 3200°F requirement for this probe and is cheaper than the coated tungsten, this material was chosen. A ceramic probe body and shield of fired alumina would survive the required temperatures, but like the tungsten, would be susceptible to catastrophic failure. Fired alumina was used as the thermocouple insulator in a non-load-bearing position.

Table 3-1. Gas Turbine Combustor Exit Environment

Gas Temperature	2000°F – 3200°F
Static Pressure	4 – 20 atmospheres
Gas Velocity	350 – 650 ft/s
Gas Composition	Fuel (nominal Jet A) and air (possible excess fuel or air)
Wall Temperatures	1800°F – 2400°F
Vibrational Load	10g nominal, 20 to 200 Hz 0.003 to 0.005 inch max. displacement (double amplitude)
Transient Conditions	
1) Idle-to-Intermediate Power	Temperature rise from 1300°F to 2600°F, pressure rise from 4 atm to 20 atm, in 5 sec
2) Intermediate-to-Idle Power	Temperature drop from 2600°F to 1300°F, pressure drop from 20 atm to 4 atm, in 5 sec

Table 3-2. Probe Design Requirements

Accuracy	+0.5% of Reading (2000°F – 3200°F)
Dimensions	Probe diameter of 0.15 inches max.
Operational Life	5 hours minimum
Structural Life	30 hours minimum
Response Time	Undefined (steady-state operation)

The thermocouple wire chosen was Type B, a platinum-6% rhodium versus platinum-30% rhodium wire pair. This is the only readily available thermocouple that will survive the peak temperature requirement of 3200°F. Type R and Type S thermocouples will survive to approximately 3000°F, but one leg of each of these thermocouple types is pure platinum, and the melting point of the platinum leg dictates the peak temperature. Tungsten-rhenium junctions will survive to even higher temperatures than the Type B junctions, but they must be protected in an inert environment. Our design dictates that the thermocouple junction be exposed directly to the gas flow.

While our material choices appear to be conventional, this is to be expected. Our measurement technique is unique in that perturbations of the probe environment are used to calculate the gas temperature. No new materials technology is required. At the same time, new technology that would aid other probe designers in the conventional use of thermocouples in the gas turbine environment would also be useful for the Astron probe.

In our Phase II program, we had allowed about .4 months for probe fabrication. This dictated that ease of fabrication and durability would dictate probe design. Photographs of the probes tested at Astron and at NASA Lewis are presented in Figures 3-7a through 3-7d. As seen in the photographs of Figure 3-7a and 3-7b, the hot end of the probe consists of three tubes of different diameters. One tube holds the fired alumina insulator and thermocouple. The upstream facing side of this tube has a "window" which allows hot gas to come in contact with the thermocouple. On the downstream side of this tube three bleed holes are concentrically located about the junction. (See the enlargement in Figure 3-7c, where the bleed holes should be directly behind the thermocouple bead.) These bleed holes connect the front tube holding the thermocouple to the back tube, which is the suction tube. This tube is connected to a vacuum line and can be isolated from the vacuum by a fast-acting solenoid valve. Figure 3-7d presents a photograph of the entire probe including interface connectors for thermocouples and airflow.

The three bleed holes were sized to provide flow past the thermocouple junction at Mach 0.1 when the flow was choked. Choked flow at this location was guaranteed by the large pressure drop between the hot gas environment and the vacuum line. It is not critical that the velocity at the junction have a particular value; however, it is important that this velocity be constant and repeatable over a several-second timeframe. Choking the flow at bleed holes of a fixed size appears to be the most expedient way to accomplish this.

We had intended to use a 0.010-inch-diameter Type B wire for our thermocouple junction. Due to the large number of temperature fluctuations that our probe would experience in normal operation, ARi Industries, our probe fabricator, suggested that we use a multistrand wire. This was done, and we had no problem with the durability of our junctions. However, possible detrimental side effects on performance, such as a possible loss of isothermality, should be investigated further. Also the stranded wires were more flexible, which causes the support legs of the probes above the ceramic insulator to be shorter, possibly leading to larger conduction losses. Again, this should be investigated further.

Suction is controlled approximately 3 feet from the probe tip by a fast-acting solenoid valve. This valve was AC powered and
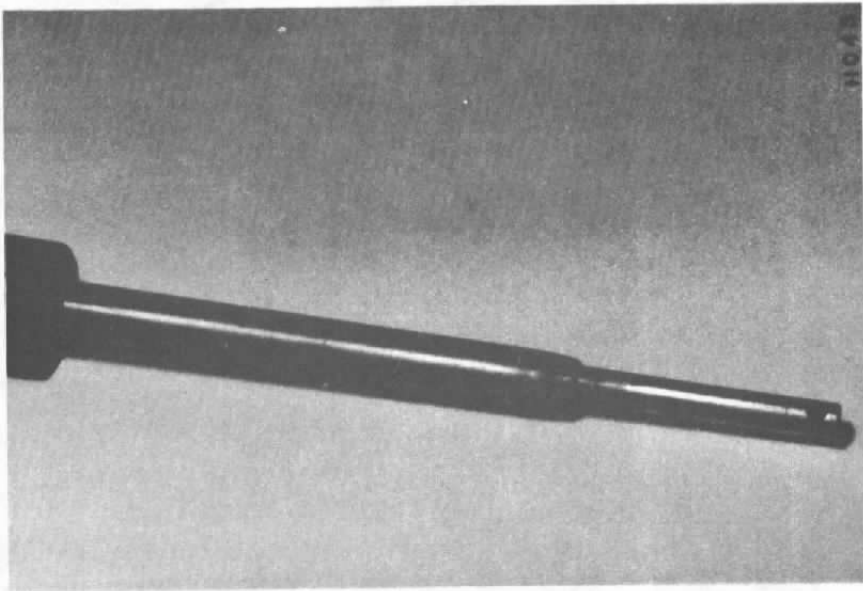
a. Front View, High-Temperature End
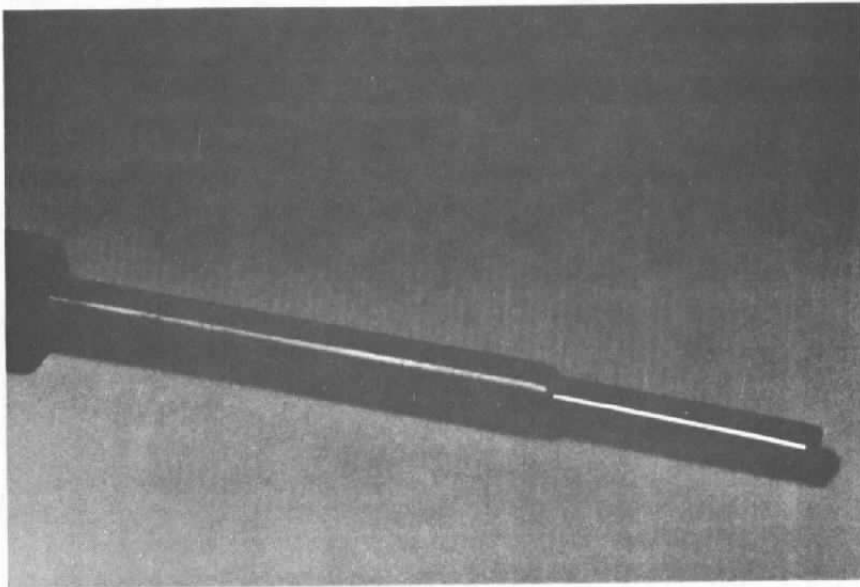
b. Back View, High-Temperature End

Figure 3-7. Astron High-Temperature Platinum Probe

3-17
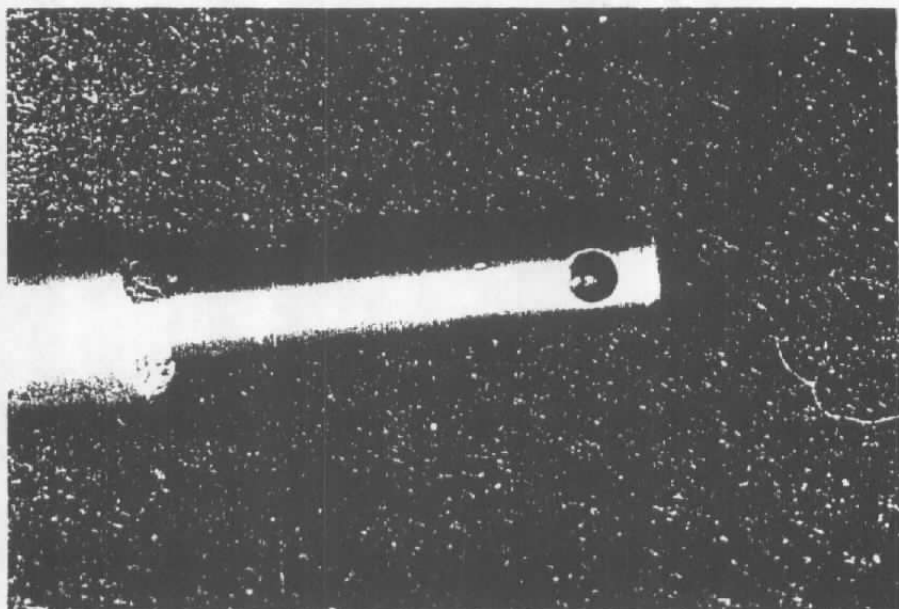
467-89

c. Closeup View of Flow Port
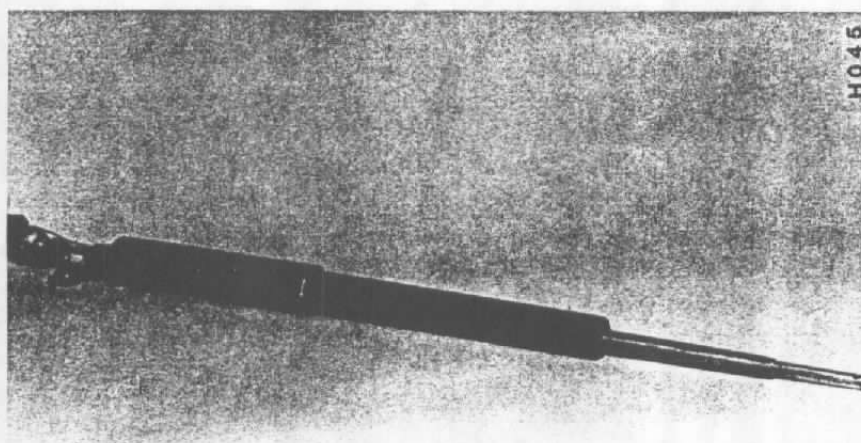
H046

d. Probe Body and Interface Connections

Figure 3-7. Astron High-Temperature Platinum Probe

isolated electrically from the low-level thermocouple signal. Valve opening and closing times are on the order of 10 ms, which is fast compared to the probe time constant of roughly 0.4 sec. The effects of the valve opening and closing time on probe behavior are discussed further in Section 3.3. The millivolt-level thermocouple signal was amplified to a 0V to 10V signal using a simple op-amp network with associated signal conditioning. The amplifier board was built to provide filtering of frequencies above 50 kHz. At the time the board was built our sampling frequency for our data acquisition system had not been determined. Additional low-pass filtering to meet Nyquist sampling requirements was dependent on the final sampling rate chosen so was not included with the probe amplifier.

Identical probes were fabricated for demonstration at Astron and at NASA Lewis. It is intended that the platinum "hot" end of these probes be used without modification in a gas turbine. The Inconel body of the probe will have to be modified to meet engine mounting requirements. These mounting requirements are at this time undefined, but flexibility has been provided by Astron.

As discussed in this section, a type B platinum-rhodium thermocouple was chosen for use in the probe. A schematic of the signal conditioning and amplification circuitry used during this program is presented on page A-5 of Appendix A. The basic design concept was to minimize the number of required circuit components, and to use components of very high accuracy and low thermal drift in order to optimize performance. As seen in the circuit schematic, the resulting design consists of three basic components; a voltage regulator, an operational amplifier, and a number of 0.01 percent tolerance resistors. No potentiometers are included in the design to adjust for offset and gain. These adjustments were made using software generated corrections based on zero and full-scale voltage inputs to the circuit prior to testing.

System errors due to thermal drift occurring after a circuit calibration were investigated. Drift of the op amp will result in a voltage offset error from the zero point. The ICL7652 is specified to have a "typical" drift of 0.1 $\mu V/°C$ and a maximum "typical" drift of 10 μV over the operating range of the amplifier (approximately 0°C to 65°C). At 2500°F, an input drift of 10 μV corresponds to a temperature measurement error of roughly 1°F. Gain drift will be caused primarily by thermal drift of the precision resistors. This drift is specified to be 5 ppm/°C by the manufacturer (General Resistance). Over the 10°C (18°F) temperature range anticipated during a typical test, the gain error should be negligible. Temperature gradients across dissimilar metal junctions that are formed during circuit fabrication will most likely be the major source of circuit error. These errors should be cancelled during the software calibration sequence if reasonable care is taken to maintain isothermal conditions on the circuit board during testing.

The low-pass filter inherent in the design of this circuit has a cutoff frequency of approximately 20 ms. This frequency was chosen prior to the determination of our A/D sampling rate. Provision is made for further filtering on the analog input board to the A/D converter to meet Nyquist sampling criteria. Our baseline digitization rate of 50 samples per second did require a slightly lower cutoff frequency (25 Hz).

3.4 DEVIATIONS FROM IDEAL BEHAVIOR

Many assumptions are required for the Astron probe to operate as described in Section 3.1. The validity of 8 of these assumptions is investigated in this section. In most, if not all cases, it can be shown that these assumptions are sufficiently accurate to allow the Astron probe to behave as described. Assumptions of isothermal probe behavior and a constant convective heat transfer coefficient are common to all transient measurement techniques. Other assumptions such as instantaneous velocity control past the junction are particular to this probe.

3.4.1 Constant Convective Heat Transfer Coefficient

Implicit in the assumption that the characteristic probe response time, τ, is constant over the temperature range between T_r and T_c is the assumption that the convective heat transfer coefficient is also constant over that temperature range. Mass, surface area, and heat capacity of the probe could also cause a nonconstant response time, but it is likely that the only parameter that can vary significantly enough over a 100°F temperature range to affect τ is h. To evaluate the effect of probe temperature on the heat transfer coefficient, we will assume that the junction approximates a sphere in a moving gas stream. The following formulas will be used to calculate a heat transfer coefficient based on fluid properties. These equations were taken from Reference 7.

$$Nu = 2.0 + 0.6(Re)^{1/2}(Pr)^{1/3} \tag{3-33}$$

where:

$$Nu = hD /k_f \tag{3-34}$$

The velocity used in the Reynolds number is the freestream velocity, and the diameter is the diameter of the spherical junction. All other fluid properties are evaluated at the film temperature, the average temperature of the freestream gas and the thermocouple junction.

These equations will be used to determine the effect of temperature changes on h. Use of these equations does not assume that we are correctly calculating an exact value of the heat transfer coefficient at a given temperature, but that trends in the variation of this coefficient with temperature can be correctly evaluated. Because of this we will be concerned with

the percentage change of h with temperature rather than with the actual values. Equation 3-33 can be used to correlate data in the Reynolds number range of 1 to 70,000.

The results of this evaluation are shown in Figure 3-8. For $T_c - T_r$ equal to approximately 60°F, the heat transfer coefficient will vary by 0.4 to 0.5 percent over the course of a temperature traverse. This trend is consistent in that h increases with increasing film temperature for all cases. The heat transfer coefficient will be underpredicted at the high end of the temperature range (near T_c) leading to an overprediction of τ, and hence a calculation of the gas temperature that is higher than the true value. The magnitude of the gas temperature error introduced by this uncertainty in the heat transfer coefficient is quantified in Section 3.5.

3.4.2 Isothermal Thermocouple Junction

In order to directly relate heat flux to the temperature rise of a thermocouple, it is necessary that the thermocouple temperature be uniform. If temperature transients exist across a thermocouple wire, then the determination of the amount of thermal energy stored in the junction as the function of a single temperature is meaningless. For a junction to respond isothermally, it is necessary that heat be conducted internally at a rate that is much higher than the external transfer of energy to the probe by means of convection, conduction, and radiation. This allows the probe to come to thermal equilibrium with itself over a time scale that is short compared with the rate at which additional energy is added to the junction.

To evaluate the ratio of internal conduction to external convection, the Biot number is used:

$$Bi = hs/k \qquad\qquad (3-35)$$

The variable s is the radius of the thermocouple junction. Under the conditions defined in Figure 2-1, a representative heat transfer coefficient of 374 Btu/hr-ft^2-°F was found for a junction under typical combustor conditions. For a junction radius of 0.025 inch, and a thermal conductivity of platinum of 42 Btu/hr-ft-°F, the Biot number is 0.018. In Figure 3-9, the variation of internal temperature of a sphere with respect to 1/Bi is plotted. For an inverse Biot number of 54, the difference between edge and centerline temperatures is less than 1 percent in terms of Θ and Θ_0. The variable Θ_0 is defined as $T_g - T_{centerline}$. For a value of $T_g - T_{centerline}$ of 100°F, the surface and centerline temperatures of a junction would differ by approximately 1°F.

The actual error in the Q_c measurement would be a fraction of the 1°F temperature error, because the error in the junction temperature would be less than 1°F everywhere except at the edge
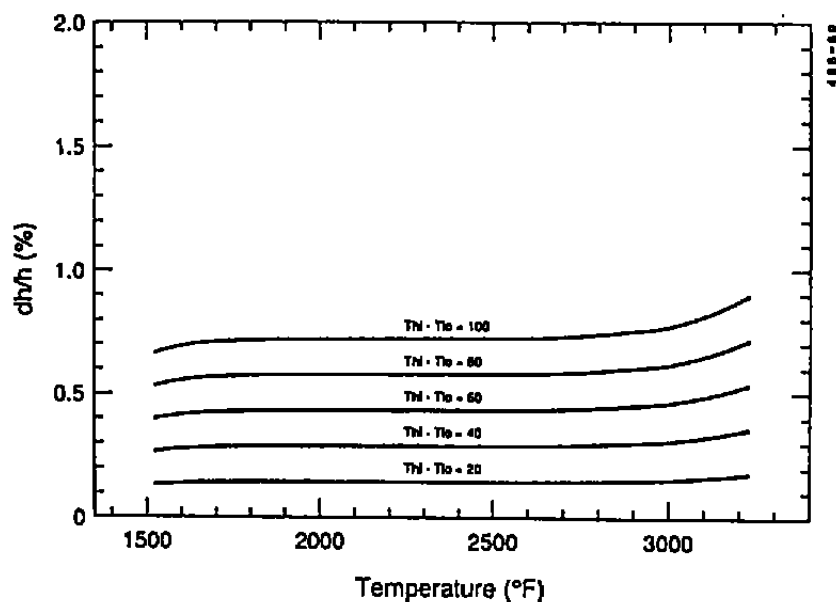
Figure 3-8. Sensitivity of Heat Transfer Coefficient to
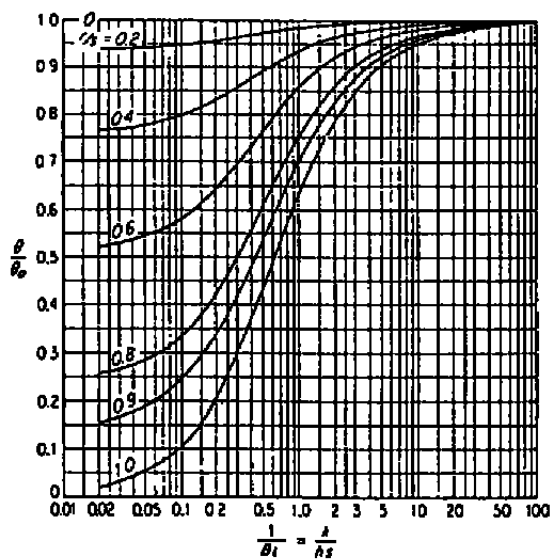Temperature

Figure 3-9. Temperature Distribution vs. Inverse Biot Number
(Ref. 7)

of the junction. The error due to the nonisothermal junction behavior will be even smaller during a temperature decay. The transfer of radiation to the probe is a slower process than the convective transfer by a factor of about 3, so the Biot number also decreases by the same factor. Although the heat flux error is small, the bias in the measurement would always tend to cause an underprediction of the heat flux. Since heat flux during the rise and decay are both underpredicted, and since the difference of the two values is used in calculating gas temperature, the errors do cancel each other to a large extent. However, the nonisothermal effects are always greater during the temperature rise. Since the T_c measured is always less than the ideal T_c, we will underpredict the true gas temperature.

3.4.3 Change in Conduction Environment

Conduction losses down the legs of a thermocouple junction are typically small due to the high gas velocity around the legs and the fact that the legs can be modeled as extended surfaces. This was demonstrated in Section 2.1. However, when the gas velocity decreases or is stagnated, the conduction errors will increase. Due to differences in the convective environment during different stages of probe operation, the conduction losses are also changed. The trend is that the magnitude of the conduction loss is greater when the probe is operated in the stagnated mode. This tends to increase the measured magnitude of radiant transfer.

To quantify this error, the probe geometry of Section 2.1, and more specifically Figure 2-1, will be used. As presented in Figure 2-2, in a high-velocity environment conduction losses will cause an error of about 3°F for a lead length of 0.25 inches and a temperature difference of 20°F between the freestream gas and the probe base. This was based on a convective heat transfer coefficient of roughly 400 Btu/hr-ft²-°F, calculated based on Reynolds number and Nusselt number correlations. When flow is stagnated, the rate of energy transfer to the probe leads from the gas will drop dramatically.

To compare conduction losses between the high-flow and zero-flow environments it is desirable to reuse Equation 2-2, leaving all parameters unchanged except the heat transfer coefficient. It is possible to define an equivalent radiation heat transfer coefficient, analogous to the convective coefficient, based on the following equations.

$$q_r = \varepsilon\sigma(T_w^4 - T_p^4) \qquad (3\text{-}36)$$

$$q_r = \varepsilon\sigma(T_w^2 + T_p^2)(T_w + T_p)(T_w - T_p) \qquad (3\text{-}37)$$

$$h_r = \varepsilon\sigma(T_w^2 + T_p^2)(T_w + T_p) \qquad (3\text{-}38)$$

$$q_r = h_r (T_w - T_p) \qquad (3\text{-}39)$$

3-23

Based on a wall temperature of 2000°F, a probe temperature of 2800°F, and an emissivity of 0.5, the value of h_r is 80 Btu/hr-ft^2-°F. Experimental results have shown that h_r is approximately one-third of the convective coefficient, or roughly 130 Btu/hr-ft^2-°F. Assuming that this experimental value is correct, we can use this h_r in Equation 2-2 to determine the error in thermocouple temperature due to conduction losses in the zero-flow condition. The result of this calculation is that the measurement error caused by conduction is increased by a factor of 2.5 in the zero-flow condition. This puts the magnitude of the error in the 6°F to 8°F range, where it cannot be considered to be negligible. Based on the fluctuating temperatures of the thermocouple junction and the probe base during operation, a more detailed analysis based on transient conditions is warranted.

3.4.4 Change in Radiation Environment

The radiation environment can also change during probe cycling even in the presence of a constant radiation environment external to the probe. This is due to the possibility that the probe shield temperature will change during operation due to the variation in the convection environment that the probe shield is exposed to. During the temperature decay segment of a cycle, the gas flow is stagnated inside of the shield and high convective transfer to the shield occurs only on the external surface. During the temperature rise segment of the probe cycle, high convective transfer is occurring on both the inside and outside surfaces of the shield.

The effect of the change in the radiation environment on probe behavior will be controlled by two criteria. The first is the magnitude of the change in the equilibrium temperature between the flowing and stagnating conditions, and the second is the response time of the shield to changes in the probe environment. A large temperature difference between the high and low flow conditions will cause the radiation environment to change substantially unless the shield response time is slow compared to the probe cycle time.

The section of the probe that acts as the shield is a platinum tube with an outside diameter of 0.25 inch and a 0.028-inch wall. Treating the shield as a cylinder in crossflow and evaluating the Reynolds number at a gas temperature of 2800°F, we calculate a Reynolds number of 20,000 and a convective heat transfer coefficient of 215 Btu/hr-ft^2-°F. Based on this coefficient and the dimensions of the shield, the time response of the shield is on the same time scale as the response time of the thermocouple. It is difficult to calculate the heat transfer on the inside of the shield, so further analysis is not presented at this time. The estimate of a time constant for the shield that is nearly equivalent to the thermocouple time constant does indicate that further study is required. The effect of a decrease in shield temperature during the decay segment of a cycle will be to overpredict the gas temperature.

3.4.5 Difference Between Static and Stagnation Temperatures

We are interested in measuring the true stagnation temperature of the combustor gas. Proper operation of the Astron probe requires that temperature measurements be made at zero velocity, corresponding to the stagnation condition, and also at some nonzero velocity. The amplitude of the perturbation signal generated during proper operation of the probe is directly related to the velocity of the flow past the thermocouple during the suction cycle. As demonstrated in Section 2.1, the high gas temperature in the combustor environment allows us to draw high-velocity (but low Mach number) gas through our probe. Adequate probe sensitivity has been demonstrated experimentally using a peak gas velocity of Mach 0.1. The difference between the static and stagnation temperatures at this temperature is 6°F, which is measurable by our present instrumentation but is only about twice the amplitude of our signal noise. If this potential error source proves to be significant, the gas flow past the thermocouple could be reduced to 120 ft/s (M = 0.05). This would clearly eliminate the problem.

3.4.6 Conductive Transport Through Stagnant Gas

In the zero-velocity operating mode, heat transfer to the thermocouple is assumed to be caused solely by radiation. Some conduction through the stagnant gas could also occur, and the magnitude of this energy transfer will be evaluated. Equations 3-33 and 3-34 can be used at zero velocity to calculate this effect. Equation 3-33 becomes:

$$Nu = 2 \qquad\qquad (3\text{-}40)$$

Based on the probe geometry and gas conditions of previous examples (2800°F gas, 0.050-inch diameter probe junction), the heat transfer coefficient due to gas conduction is 30 Btu/hr-ft^2-°F. This is 8 percent of the forced convection coefficient, and roughly 24 percent of the energy transfer during the radiant transfer segment of a probe cycle (based on experimental observations of the ratio of convective to radiant heat flux). Although this number seems to be too large to allow proper probe operation, it will be shown in Section 3.4 that fairly large uncertainties can be tolerated in the calculation of the heat flux in the radiation mode. In any event, the presence of this mode of energy transfer will decrease the apparent radiant heat flux. This will act to cause an underprediction of the true gas temperature.

3.4.7 Flow Control Time Lag Effects

The solenoid valve used to control gas flow past the thermocouple was chosen because of its relatively fast valve action of 10 to 20 ms. This is fast compared to the probe

response time of 0.3 to 0.4 sec. The solenoid valve is separated from the choking holes in the probe by about 2 ft, but even if the gas between these holes and the valve cooled to 70°F, the time required for the pressure drop at the solenoid to reach the choking holes would be on the order of 2 ms. The time delay between valve actuation and full flow or zero flow is believed to be less than 25 ms. This time lag would have no effect on probe performance.

3.4.8 Catalytic Effects

The potential for catalytic action by the platinum thermocouple wire to cause combustion to occur, or to act as a flameholder, has been mentioned by Sverdrup personnel as a potential concern. The occurrence of this does seem possible, as it is known that fuel-rich pockets of gas could exist immediately downstream of the combustors. Using the present hardware, this situation is unavoidable, but it should be stressed that the Astron probe is no more likely to show this catalytic effect than any bare-wire platinum thermocouple. New techniques used to eliminate this phenomena when using conventional thermocouples should be investigated, as these methods could most likely benefit the Astron probe as well. Evidence of catalytic action, such as sudden rises or drops in temperature at the thermocouple junction, have not been observed.

3.4.9 Summary of Probe Errors

Eight potential sources of nonideal probe behavior have been investigated. Their effects have been quantified in engineering terms when possible. The results of this investigation are summarized as Table 3-3. In most cases we can either measure the nonideal behavior or identify this effect as being too small to quantify experimentally. The last column of the table indicates whether our calculated gas temperature will overpredict or underpredict the true gas temperature based on our assumption of ideal behavior.

3.5 ERROR ANALYSIS

During the design phase of a program, tradeoffs must be made between the desire to obtain "ideal" probe performance and the need to come up with a probe design that can be fabricated. Properly performing this task requires an understanding of how nonideal behavior translates into uncertainty in the calculated true gas temperature. Examples of nonideal behavior were exadined in the previous section. Other measurement uncertainties that were not covered include errors in the thermocouple junction temperature measurement and the calculation to the temperature derivatives.

The goal of our Phase II design study was to determine a method of obtaining acceptable instrument accuracy in a durable

and easily fabricated design. A study using partial derivatives to determine calculated gas temperature sensitivity to uncertainties in other parameters is ideal for this type of study, and this method is presented in Section 3.4.1. The Air Force has established a standard method for estimating measurement errors, and the accuracy of the Astron probe will be discussed in accordance with the proper Air Force terminology in Section 3.5.2.

3.5.1 Partial-Derivative Error Analysis

To evaluate errors, a partial derivative expansion of all unknowns in Equation 3-32 was performed. This equation solves explicitly for gas temperature and is repeated here for convenience.

$$T_g = (T_1 \dot{T}_{h2} - T_2 \dot{T}_{h1}) / (\dot{T}_{h2} - \dot{T}_{h1}) \qquad (3-32)$$

To simplify the resulting equations, the combination $(\dot{T}_c - \dot{T}_r)$ is presented as $\dot{T}_h$ except where $\dot{T}_c$ or $\dot{T}_r$ must be broken out separately in the partial derivative expansion. The derivatives with respect to the six measurements required to calculate T_g are shown in Equations 3-41 through 3-46.

Table 3-3. Sources of Nonideal Probe Behavior

Error Source	Magnitude	Bias
Non-Constant Heat Transfer Coefficient	Measurable	Overpredict T_g
Isothermal Probe	Negligible	Underpredict T_g
Change in Conduction Environment	Measurable	Overpredict T_g
Change in Radiation Environment	Unknown	Overpredict T_g
Static vs. Stagnation Temperatures	Measurable	Underpredict T_g
Stagnant Gas Conduction	Measurable	Underpredict T_g
Flow Control Time Lag	Negligible	Unknown
Catalytic Effects	Unknown	Overpredict T_g

$$\left|\frac{\partial T_g}{\partial T_1}\right| = \frac{\dot{T}_{h2}}{\dot{T}_{h2} - \dot{T}_{h1}} \qquad (3\text{-}41)$$

$$\left|\frac{\partial T_g}{\partial T_2}\right| = \frac{\dot{T}_{h1}}{\dot{T}_{h2} - \dot{T}_{h1}} \qquad (3\text{-}42)$$

$$\left|\frac{\partial T_g}{\partial \dot{T}_{1c}}\right| = \frac{\dot{T}_{h2}(T_1 - T_2)}{(\dot{T}_{h2} - \dot{T}_{h1})^2} \qquad (3\text{-}43)$$

$$\left|\frac{\partial T_g}{\partial \dot{T}_{1r}}\right| = \frac{\dot{T}_{h2}(T_1 - T_2)}{(\dot{T}_{h2} - \dot{T}_{h1})^2} \qquad (3\text{-}44)$$

$$\left|\frac{\partial T_g}{\partial \dot{T}_{2c}}\right| = \frac{\dot{T}_{h1}(T_1 - T_2)}{(\dot{T}_{h2} - \dot{T}_{h1})^2} \qquad (3\text{-}45)$$

$$\left|\frac{\partial T_g}{\partial \dot{T}_{2r}}\right| = \frac{\dot{T}_{h1}(T_1 - T_2)}{(\dot{T}_{h2} - \dot{T}_{h1})^2} \qquad (3\text{-}46)$$

The maximum error associated with a calculation of T_g is:

$$\Delta T_{g(max)} = \left|\frac{\partial T_g}{\partial T_1}\right|\Delta T_1 + \left|\frac{\partial T_g}{\partial T_2}\right|\Delta T_2 + \left|\frac{\partial T_g}{\partial \dot{T}_{1c}}\right|\Delta \dot{T}_{1c}$$
$$+ \left|\frac{\partial T_g}{\partial T_{1r}}\right|\Delta \dot{T}_{1r} + \left|\frac{\partial T_g}{\partial T_{2c}}\right|\Delta \dot{T}_{2c} + \left|\frac{\partial T_g}{\partial T_{2r}}\right|\Delta \dot{T}_{2r} \qquad (3\text{-}47)$$

If measurement errors for all variables are random, which is a more reasonable assumption, the estimate of the error associated with the value of T_g is:

Data on this page shall be subject to the restriction appearing on page ii of this document.

$$\Delta T_{g(RMS)} = \left\{ \left(\frac{\partial T_g}{\partial T_1} \Delta T_1 \right)^2 + \left(\frac{\partial T_g}{\partial T_2} \Delta T_2 \right)^2 + \left(\frac{\partial T_g}{\partial T_{1c}} \Delta \dot{T}_{1c} \right)^2 \right.$$

$$\left. + \left(\frac{\partial T_g}{\partial T_{1r}} \Delta \dot{T}_{1r} \right)^2 + \left(\frac{\partial T_g}{\partial T_{2c}} \Delta \dot{T}_{2c} \right)^2 + \left(\frac{\partial T_g}{\partial T_{2r}} \Delta \dot{T}_{2r} \right)^2 \right\}^{1/2} \qquad (3-48)$$

Evaluation of $\Delta T_{g(RMS)}$ requires that we assign values to all variables in Equation 3-48. These values should represent as accurately as possible the nominal operating conditions of the probe. The deltas (relative errors of variables) should also be assigned based on our best estimate of measurement uncertainties. This will be done using the baseline gas properties and probe dimensions used throughout Section 2 and Section 3. The probe dimensions used in the earlier examples closely approximate the dimensions of the actual Phase II probe. We will have to assume values of T_c and T_r to evaluate derivatives, but this will be based on experience gained from experiments. We will assume that for a gas temperature of 2800°F, T_c will be 2750°F and T_r will be 2650°F. These are reasonable asymptotes for probe operation based on use in a strongly contributing radiation environment.

A value for the thermocouple time constant was calculated to be approximately 0.3 sec in Section 2.1. Again, experimental results have validated this calculation to be nearly correct. The maximum value of the derivative $\dot{T}_c$ will occur at the temperature T_r, and this maximum value will occur at the instant that flow is drawn past the probe by opening the actuated gas valve. The magnitude of the derivative $\dot{T}_c$ at that instant is calculated to be 500°F/s by using the following equation:

$$\dot{T}_{c(max)} = (T_g - T_r)/\tau \qquad (3-49)$$

In a similar manner it was found both analytically and experimentally that $\dot{T}_{r(max)}$ was typically about one-third to one-fourth the magnitude of $\dot{T}_{c(max)}$. The value or $\dot{T}_r$ we will use for this analysis will be 125°F/s.

Suppose that we evaluate Equation 3-48 at probe temperatures of 2660°F and 2740°F. These values are chosen instead of the two asymptote temperatures because at T_c and T_r 2 of the 4 derivative terms are zero. This would be a simpler and possibly less convincing case to analyze. Rough estimates of $\dot{T}_c$ and $\dot{T}_r$ are the following:

At T_p = 2660°F; $\dot{T}_c$ = 443°F/sec and $\dot{T}_r$ = -33°F/sec.

At T_p = 2740°F; $\dot{T}_c$ = 8°F/sec and $\dot{T}_r$ = -67°F/sec.

These numbers may appear to be arbitrary, but the values of the temperatures and the derivatives are all consistent with the

Data on this page shall be subject to the restriction appearing on page ii of this document.

maximum derivative values previously defined. T_c varies from 500°F/s at 2650°F to 0°F/s at 2750°F. Likewise, T_r varies from 0°F/s to 125°F/s over the range of temperatures between T_c and T_r.

Values are now assigned to the uncertainties in our measurements of probe temperatures and derivatives. We are assuming that the probe temperature can be known to an accuracy of 0.2 percent of the temperature. This is based on a calibration accuracy of 0.1 percent for calibration-grade noble metal thermocouples, and on signal conditioning uncertainties and possible environmental contamination that would double this uncertainty to 0.2 percent. The uncertainty in the combined mode temperature derivative is assumed to be 5 percent of the maximum value, while the radiation derivative uncertainty is assumed to be much greater at 20 percent. The greater uncertainty in T_r is attributed to several potential error sources discussed in Section 3.4, namely changes in the convection and radiation environments and the possibility of conduction to the stagnant gas in the zero-flow condition. The uncertainty values are summarized below:

$$\Delta T_1 = 0.002 \ (2640°F) = 5.32°F$$

$$\Delta T_2 = 0.002 \ (2740°F) = 5.48°F$$

$$\Delta \dot{T}_c = 0.05 \ (500°F/s) = 25.0°F/s$$

$$\Delta \dot{T}_r = 0.20 \ (125°F/s) = 25.0°F/s$$

Performing the calculation of Equation 3-48 (where the partial derivative terms are defined by Equations 3-41 through 3-46 and the uncertainties in T_1, T_2, $\dot{T}_c$ and $\dot{T}_r$ are those presented above) results in:

$$\Delta T_{g(RMS)} = 10.8°F = 0.39 \text{ percent} \qquad (3-50)$$

The RMS analysis is based on the assumption that all measured values are unrelated. In fact, we are using one thermocouple for all measurements. To see how this affects error, first study how an offset error in temperature measurement propagates through the calculation of T_{gas}.

Assume that T_1 and T_2 are both offset from their correct values by 5°F.

$$T_g = \frac{(T_1 + 5°F)\dot{T}_{h2} - (T_2 + 5°F)\dot{T}_{h1}}{\dot{T}_{h2} - \dot{T}_{h1}} \qquad (3-51)$$

3-30

$$T_g = \frac{T_1 \cdot \dot{T}_{h2} - T_2 \cdot \dot{T}_{h1}}{\dot{T}_{h2} - \dot{T}_{h1}} + 5°F \qquad (3-52)$$

So, a 5°F offset in the measurement of temperature at the junction results in the same 5°F error in calculated temperature. A better estimate of the RMS error would add a term to the RMS equation that accounted for only the offset error. This error would be the same 0.2-percent error associated with T_1 and T_2. T_1 and T_2 error values would then be zero and $0.002(T_2 - T_1)$ respectively in Equation 3-32. So in effect the T_1 term would disappear (except in the offset error), and the T_2 term would be referenced to T_1.

Based on this analysis, we are led to believe that an accurate calculation of T_1 and T_2 will allow rather substantial errors in the derivatives while still providing a calculation of T_{gas} that is accurate to within 0.5 percent. Further error reduction could be achieved by actively controlling the shield temperature to drive the temperature difference of T_c and T_r to zero. At this point $T_{gas}=T_c=T_r$ and the uncertainty associated with this measurement would be on the order of 0.2 to 0.3 percent.

3.5.2 Air Force Error-Analysis Methodology

A handbook detailing uncertainty analysis in gas turbine engine measurements[8] was created by the Air Force in 1973. The need for this handbook was obvious to its creators. Comparisons of data between different Air Force and private engine test facilities were difficult, if not impossible, due to the large number of uncertainty analysis techniques in use. The purpose of this handbook was not to present the "best" analysis method, but rather to present a consistent method that could be applied to all facilities. Errors associated with temperature measurements in gas turbines can be discussed in common terminology using this method.

Portions of this methodology are more appropriate to a production instrument. Admittedly, the probe described in this report is still in a developmental stage. As an example, the importance of the calibration hierarchy errors discussed in Section 5.4.1 of the referenced report is understood. However, for the purposes of our probe development effort, calibration curves specified by the manufacturer were acceptable. Also we are not advanced enough in our development to discuss statistical run-to-run or calibration-to-calibration indices.

Techniques from this handbook that are appropriate in a probe development program are the distinctions made between bias and precision errors and the distinction made between different sources of bias. Acting in the suction mode, the Astron probe

has a high precision. Over the course of a several-hour test, or over the course of several tests over several days, the temperature measured by our probe (when acting as a conventional aspirated probe) would probably change by no more than 5°F under constant engine conditions. However, this precision is obtained at the cost of a large unknown bias, the radiation error. Most likely the sign of this error is known, but the magnitude of the error can only be guessed. As discussed in Section 2.1, other potential sources of bias can be shown to be small.

This large bias can be accounted for and corrected using the technique described in this Final Report. A technique is demonstrated that allows one to quantify this previously unknown bias term. The remaining measurement uncertainty when using this technique would be an unknown bias on the order of +15°F where the magnitude and sign are both unknown. It is anticipated that due to the calculations required to eliminate the radiation bias, some precision will be lost in the process. This has been shown to be the case in practice, where test results have a large amount of scatter in the calculated gas temperature. Given the current state of development, it is probably accurate to claim that the sign of the radiation bias is accurately calculated by the Astron technique, but that the magnitude of the bias cannot be demonstrated with sufficient precision to be useful.

3.6 SIGNAL PROCESSING

Due to the important role that data analysis must play in order for the Astron measurement technique to be successful, it is instructive to briefly discuss these requirements. Steady-state voltages generated by the thermocouple in the probe will provide no more information concerning the true gas temperature than would be provided by a conventional shielded thermocouple junction. A necessary requirement of the Astron technique is that temperature derivatives with respect to time be accurately determined between the asymptotes T_r and T_c.

Early in the program it was determined that probe temperature would be measured as a function of time, and that derivatives would be calculated using the digitized data. The option was to include an analog differentiating circuit on the signal conditioning board and to record the temperature derivative as a separate channel. One obvious shortcoming of the analog technique was that first-derivative discontinuities exist in the probe waveform at T_r and T_c that are an important part of normal operation. Another problem is that analog differentiators are typically difficult to implement, although the same can be said for digital differentiation. In general, differentiation of data is a difficult process that highlights the presence of noise.

A data sampling rate of 50 Hz was used for the probe for all tests. The probe response time of 0.3 sec during temperature rises from T_r to T_c and the approximate response time of 1.2 sec

during decays resulted in a large number of sample points being available to model the response curves. During early tests data was collected for 1-min tests (approximately six rise and decay cycles), and then the digitized data was analyzed after the test. Several different types of reduction techniques were employed, with the differences being mainly due to differences in calculating the derivatives. Using the method of least squares, first- and second-order curve fits based on exponential functions were used, along with quadratic polynomial functions of temperature as a function of time. In addition numerical differentiation was employed using several differencing techniques.

Several of these techniques were demonstrated using real-time hardware, although the results were unpredictable. An industrial controller based on the commonly used 8088 microprocessor was purchased to perform the required real-time computational work. This controller, although slow by today's standards, could easily perform the required calculations in near-real time. We were clearly not limited by hardware, but by our inability to accurately differentiate our signals in the presence of small to moderate amounts of noise.

SECTION 4 - TEST FACILITIES

A major portion of the Phase II program was devoted to the demonstration of the Astron probe under conditions intended to be representative of the rugged gas turbine combustor environment. The principal purposes of this testing were to demonstrate the feasibility of the proposed measurement concept, to gather valuable information on the implementation of the probe in terms of required controls and proper data-reduction algorithms, and to verify the structural integrity of the probe prior to insertion in a real engine.

Environmental conditions representative of a gas turbine combustor environment were presented in Table 3-1 of Section 3.2, and probe design requirements were introduced in Table 3-2 of the same section. The Astron furnace, associated instrumentation, and the data acquisition system (DAS) are described in Section 4.1. A comparison is made between the Astron furnace environment and expected combustor conditions. Section 4.2 describes the combustor rig at NASA-Lewis Research Center and discusses the differences between the Astron and NASA facilities. The discussion of vibrational loads tests performed at Astron as a demonstration of structural integrity, including test hardware and results, is presented in Section 6.

4.1 ASTRON FURNACE FACILITY

To provide a capability for onsite high-temperature probe testing, a furnace was fabricated and installed at Astron as part of the Phase II program. It would have been desirable to duplicate the operating conditions of a gas turbine exactly at Astron, but cost and safety constraints made this option unfeasible. As an example, we briefly considered the possibility of obtaining a small jet engine, but safety constraints primarily related to the rotating turbomachinery eliminated this possibility. Velocity and temperature were determined to be the primary flow variables to match, both from the standpoint of validating our measurement concept, and also demonstrating the durability of our materials. It was therefore determined that the Astron facility would duplicate at least these two parameters. Gas pressure effects are obviously important, but their effect is primarily seen in increased structural loading and higher heat transfer rates caused by higher gas density. The design of a facility to withstand operating pressures of 10 to 15 atm in a combustor size suiting our needs (approximately 24-inch diameter by 10-ft length) would have required a substantial amount of design time and would have significantly increased the cost of our facility. Due to safety and cost considerations, the decision to test at near-atmospheric pressure was made.

The Astron furnace was designed to operate at 3000°F, allowing us to observe the behavior of probe materials at high temperatures for extended periods of time. Probe vibrational loading effects are also important, and vibration due to vortex shedding is a likely failure mode particularly at elevated temperatures. By matching the combustor velocity in the Astron facility, survivability under vortex loading conditions was demonstrated to some extent. However, instrumenting the probes with strain gages at elevated temperatures was not feasible in the current program. It was determined, also due to cost and safety, that vibrational testing would be carried out under ambient laboratory conditions. Stress and strain levels would be measured and extrapolated analytically to high-temperature behavior.

The operating conditions of the Astron facility are presented as Table 4-1, and a comparison of temperature and velocity capabilities of the facility are compared with the targeted combustor conditions and with the NASA combustor rig in Figure 4-1. As can be seen, the targeted combustor temperature and velocity were fairly well matched at Astron. The radiation environment was also accurately matched. Kerosene was used as fuel due to the similarity in burn characteristics between kerosene and Jet A. This was done to provide an emitting flame capable of transmitting radiant energy to our probe. Radiant transfer to facility walls also approximately matched combustor conditions, with facility wall temperatures typically being in the 1800°F to 2400°F range. Pressure in the facility, as mentioned, is essentially atmospheric, with the only additional pressure being caused by drag losses through the furnace at high velocity.

Table 4-1. Astron Facility Conditions

Temperature	2000°F - 3000°F
Velocity	100 - 450 fps
Pressure	1 atm
Gas Composition	Air mixed with kerosene fuel
Test Duration	Up to 8 hours, (limited by fuel tank)

A photograph of the facility is shown as Figure 4-2. The burner is to the left, the large cylindrical section is the low velocity combustor, the square section is the high-velocity test section, and the vertical section is the exhaust stack. A schematic of the facility is provided as Figure A-3 in Appendix A.
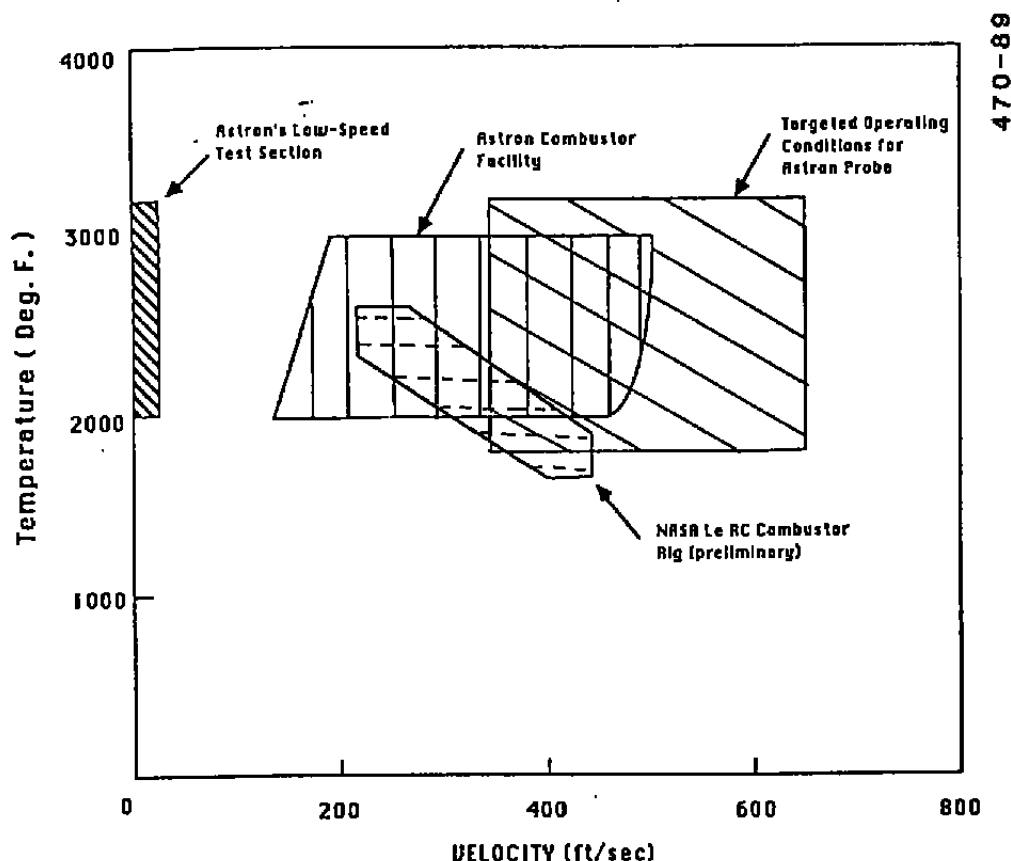
Figure 4-1. Comparison of Test Facilty Operating Conditions

Table 4-2 presents a description of all test instrumentation including location (refer to Figure A-3 for a schematic of locations), instrument accuracy, and response time. Thermocouple response times are presented as the characteristic time constant, the time required to achieve 63 percent of a step change in temperature. The other instrument response times are presented as settling times required to reach a specified accuracy. Data sampling rates are included as the last column of the table.

The DAS consisted of a microcomputer-based A/D plug-in board developed by Analog Devices. The board had 12-bit accuracy (1 part in 4096), capability of 16 simultaneous input channels, and data rates in excess of 20 kHz. Probe temperature and the position of the solenoid valve on the suction line were sampled at 50 Hz. All other input channels were sampled at 0.1 to 1 Hz, depending on test conditions. In early tests, the gas temperature was calculated at the conclusion of a test using the sampled probe temperature data and reduction algorithms programmed on the DAS microcomputer. From October 1988 to the completion of the program, data were recorded at 50 Hz by the A/D
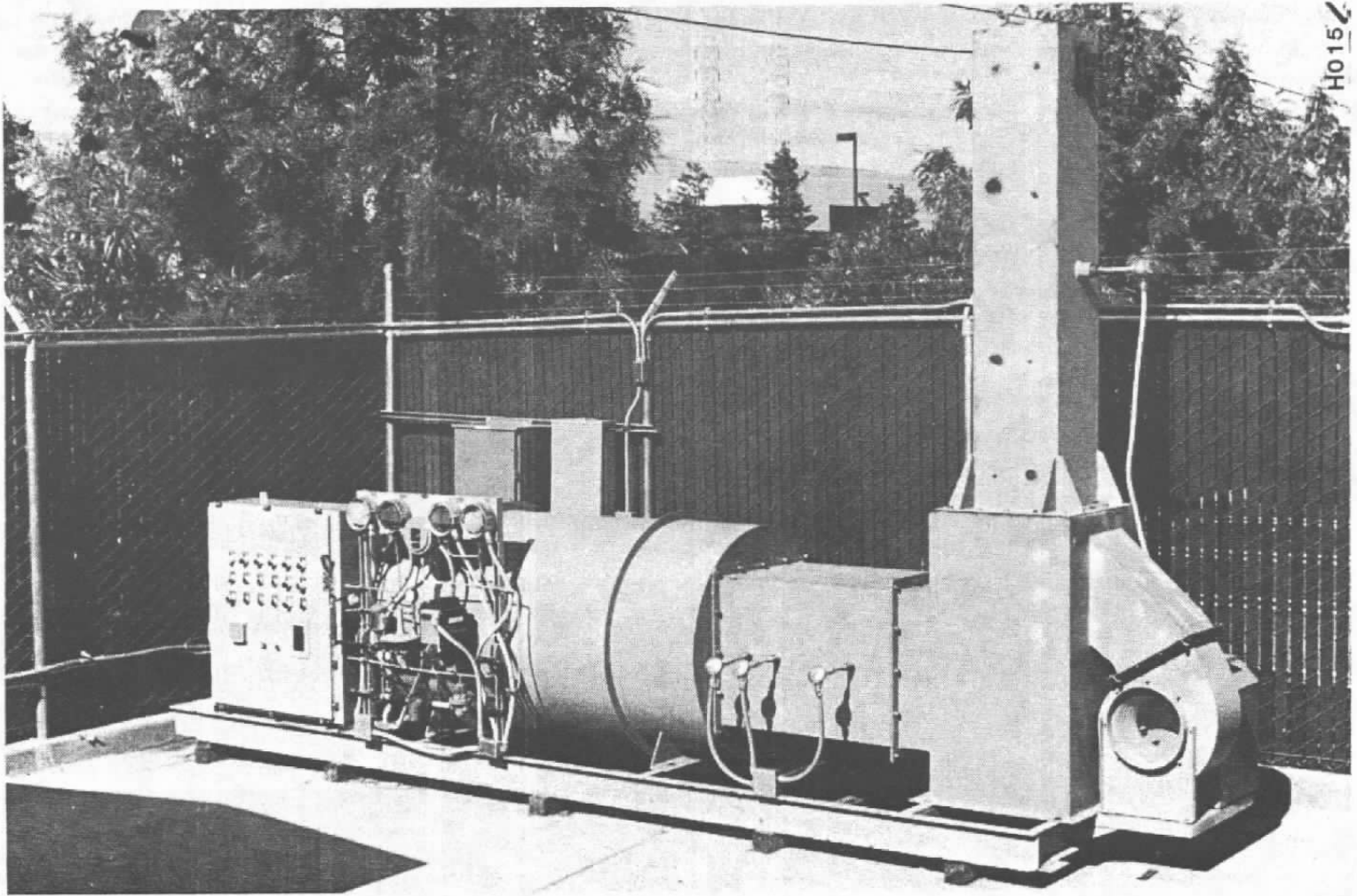
Figure 4-2. Astron High-Temperature Test Facility

Table 4-2. Astron Combustor Facility Instrumentation List

Instrument Description	Accuracy	Range	Time Response	Sampling Rate
Wall TC (3 places) Type R, Calibration Grade Wire	0.2% of reading	500°F- 2900°F	10 sec	0.1-1 Hz
Combustor TC Type R, Calibration Grade Wire	0.2% of reading	500°F- 2900°F	2 sec	0.1-1 Hz
Blower p	1% of FS	0-16 osi	<20 ms	0.1-1 Hz
Kerosene Flowrate	2% of FS	0-10 gph	0.1 sec	0.1-1 Hz
Furnace Skin Temperatures	0.5% of reading	32°F- 500°F	0.1 sec	0.1-1 Hz
Probe Body TC Type B	0.5% of reading	500°F- 3200°F	1 sec	0.1-1 Hz
Probe TC Type B	0.2% of reading	500°F- 3200°F	0.3 sec	50-100 Hz

board while the uMAC microcontroller simultaneously recorded the temperature trace and performed a real-time calculation of T_g. Communication to the DAS computer was provided by both a 0 to 10 volt analog signal and ASCII transmission of temperature data using RS-232 transmission protocol. A summary of data transmission options requested by AEDC personnel to provide a compatible interface with current data acquisition facilities is provided as Table 4-3. Performance specifications for the uMAC controller are provided as Table 4-4.

4.2 NASA-LEWIS RESEARCH CENTER COMBUSTOR FACILITY

One of the goals of the Phase II program was to demonstrate the Astron probe in an engine at an Air Force test facility. Based on discussions at the September 1987 design review at AEDC, it was apparent that an engine suitable for probe demonstration would not be available at AEDC during the August to December 1988 timeframe. Test facilities at Wright-Patterson AFB and NASA Lewis Research Center were investigated, and permission was received from NASA to test our probe in the Lewis Combustor Rig.

Table 4-3. Data Transmission Formats for Astron Probe

Serial Half-Duplex RS-232-C

    Word Format - two or more 8-bit bytes with parity and
    stop bit. Baud rate - 9600

16-Bit Parallel Interface

    Word Format - one or more 16-bit words. Protocol -
    output controlled by "freeze signal" from DAS. Freeze
    goes high when DAS ready for transmission. Probe
    shall output data within 1 ms and shall hold data
    stable for 10 ms. Freeze signal may go high up to 200
    times per second. All signal levels TTL.

Analog Output

    Output level - 0 to 10 volts
    Output current - 0 to 5 milliamps
    Signal "de-glitched" if generated by D/A converter

Table 4-4. Performance Specifications For uMAC Controller

Operating Temperature	0°F to 140°F
Storage Temperature	-10°F to 180°F
Communications	RS-232C, IEEE-488 4-20mA current
Processor	Intel 80188 (5 MHz)
Memory	256 kBytes
Program Battery Backup	6 months
A/D Resolution	12 bit

The NASA facility can operate at a peak gas temperature of about 2200°F at a gas velocity of 250 ft/s. While the Astron furnace operates at a higher temperature and velocity, there are several features of the NASA facility that more closely resemble the gas turbine combustor environment.

• The NASA facility uses an array of combustor cans mounted in an annular configuration inside of a 16-inch metal duct.

The annular geometry of the combustor matches a gas turbine geometry, but the center of the annulus in the Lewis facility is open. A schematic of the NASA facility is shown on page A-6.

- The combustor rig operates at a pressure of about 50 psia (3.5 atm). While low by modern Air Force standards, this value was significantly higher than the pressure in the Astron facility.

- The gas flow is contained in water-cooled metal walls. The walls were cooled to temperatures of several hundred degrees, which was expected to significantly increase radiation losses.

- The temperature probe was mounted only about 2 ft downstream from the combustors. A considerable amount of mixing between hot and cold gas was taking place in the vicinty of the probe, and this type of gas behavior can be expected in the engine environment also. In the Astron facility the gas was well mixed and the combustion reaction was complete before contact was made with the probe.

Scaled drawings of the temperature probe in the Astron and NASA Lewis test facilities are provided in Figure 4-3.

During testing the NASA Combustor Facility is operated remotely. NASA provided personnel to operate the facility and also provided the instrumentation necessary to record all facility temperatures, pressures, and mass flowrates. These values were recorded and presented to Astron at the end of testing to be used in our data analysis. Astron was responsible for recording our probe temperature, the temperature of the probe body (to verify safe body temperature of 1500°F), and the position of our solenoid valve. The real-time microcontroller was placed in a location approximately 5 ft from the probe and the hot-gas duct, while our data-acquisition computer was located in the control room 50 ft away. Communications with our controller were made by sending command sequences over the RS-232 line, and data from the controller were received in the same manner.

12 inch

472-89

3 inch Dia
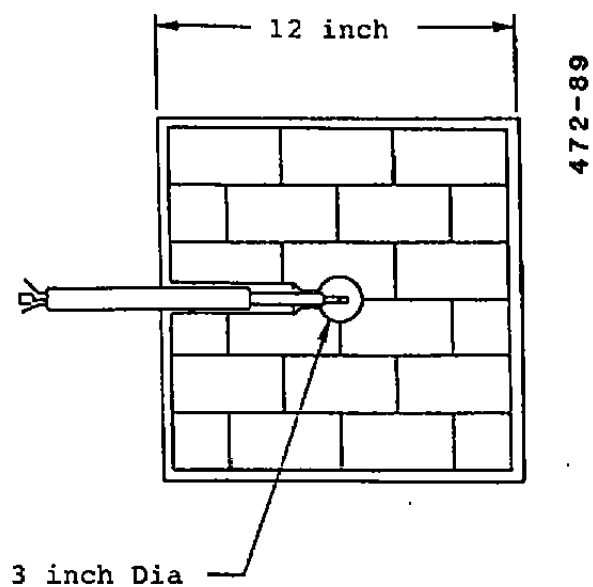
a.   Probe in Astron Furnace Facility

16 inch Dia

473-89
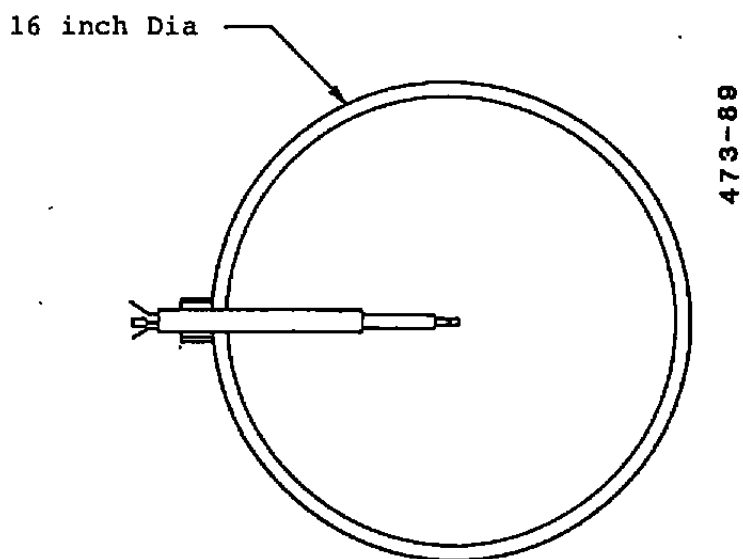
b.   Probe in NASA Lewis Combustor Rig

Figure 4-4.   Schematic of Probe in Combustor Facilities

SECTION 5 - TEST RESULTS

The results of all temperature measurement tests are presented in this section. Three test programs were carried out during Phase 2, and they are discussed in the order that they were conducted except where stated. The Inconel preliminary probe design tests are described in Section 5.1, and this is followed by a discussion of the real-time data analysis work in Section 5.2. Section 5.3 describes the high-temperature platinum probe tests performed at Astron, and Section 5.4 discusses the NASA Lewis tests.
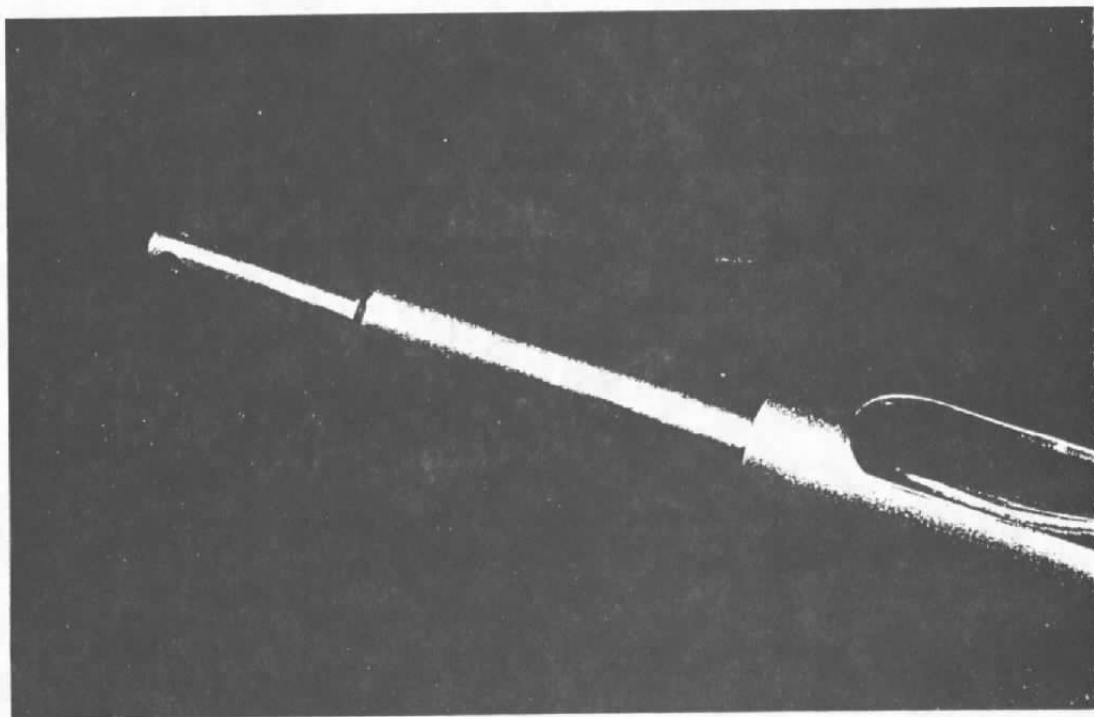
5.1 INCONEL PROBE CONCEPT VALIDATION TESTS

As discussed in Section 3, it was determined early in this program that probe survivability goals in the gas turbine combustor environment could best be met by using a probe body fabricated from platinum or a platinum-rhodium alloy. However, there are several problems associated with the use of platinum, especially in the early stages of a probe development program. These problems include high cost, fabrication difficulties, and long material lead times. Because of these difficulties, and due to our need to validate our basic design in an expedient manner, the decision was made to fabricate two probes from Inconel and stainless steel. The delivery time on these probes allowed us to gain confidence in our basic hardware design prior to committing to fabrication of our platinum probes.

Since the purpose of the Inconel probes was to validate our hardware design, the probes were fabricated to specifications that are nearly identical to those shown in Section 3 and Appendix A. The Inconel body could survive at gas temperatures up to about 2400°F, and the thermocouple used was a Type B, platinum-rhodium junction, with an operating range of up to 3000°F to 3200°F. By using the same type thermocouple as was planned for use in the high-temperature probes, we could use our signal conditioning electronics for both the low-temperature and high-temperature probes.

Two Inconel probes were fabricated by ARi Industries, Inc., and delivered to Astron in May of 1988. Photographs of the probes are shown as Figures 5-1a and 5-1b. The slotted main body visible in Figure 5-1a would serve a purpose in an actual jet engine application, so in keeping with our plan of validating as closely as possible the final probe in all phases of design and shakedown, the slotted body was included in the Inconel probe design. In actual gas turbine application, the "hot" end of the probe, as shown in Figure 5-1b, will be directly exposed to combustion gases and must survive the 3000°F design temperature. However, a large portion of the probe body will not be in direct

Data on this page shall be subject to the restriction appearing on page ii of this document.
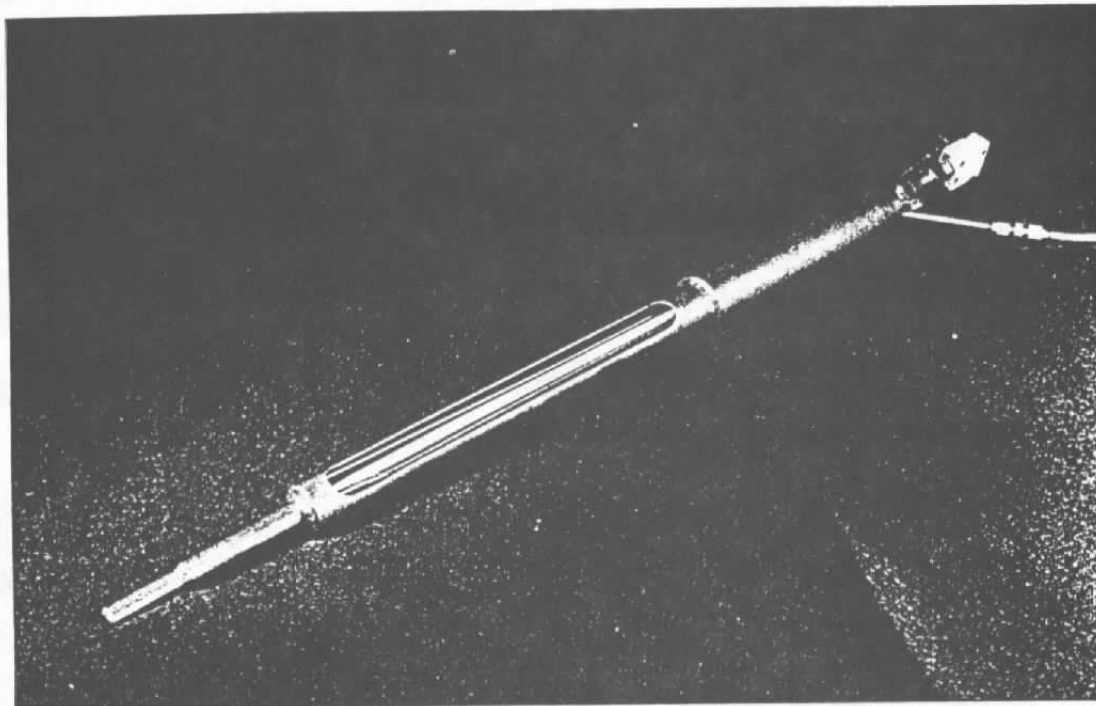
a. Slotted Probe Body

b. Closeup of Probe Tip

Figure 5-1. Inconel Temperature Probe

5-2

contact with these hot gases, but will instead be subjected to the bypass airstream passing through the engine between the annular combustor and the external engine walls. The purpose of the slotted body is to minimize blockage of the bypass air, cool the probe base to a temperature consistent with the use of Inconel (instead of platinum), reduce the cross-sectional area of the conduction path between the combustor and the cool end of the probe, and provide a rigid support structure. This concept has been demonstrated in earlier probe designs, and is not specific to the design and operation of the Astron probe. (Due to the need to air cool the platinum probe body, the high-temperature probes were not slotted.)

After a cursory visual inspection of all welds and solder joints, the probes were installed in the Astron furnace and heated to approximately 1700°F. Exterior joints and fittings were checked for possible leaks, and proper operation of the two Type B thermocouple junctions was verified. Following this test, the probe was removed from the furnace and inspected for visual damage. No damage was found, indicating that the probe design was structurally sound under the conditions of the Astron furnace.

The results of a 10-min test of the Inconel probe are shown in Figures 5-2 through 5-4. In Figure 5-2, the temperature trace of the probe over the duration of the test is presented. The test was run at essentially steady-state conditions, but the gas temperature was rising at approximately 5°F per minute. This level of temperature ramp rate should be acceptably slow to allow proper operation of the probe. As seen in Figure 5-2, the probe was operated in the radiation-equilibrium mode over most of the test. Approximately 80 sec into the test, the probe was run through the suction and stagnation sequence once. At 240 sec, the probe was run through a 1-min sequence of five cycles, and at 400 sec the probe was run through a 100-sec sequence of eight cycles.

The results of these tests can be best observed by expanding the time and temperature scales as is done for three representative temperature pulses in Figure 5-3. The pulses do behave in a manner similar to that proposed by the theory of Section 3. More importantly, the signal-to-noise ratio of the thermocouple signal was about 200:1 (8°F out of about 1600°F), indicating that our thermocouple design and signal conditioning were adequate. Unfortunately, calculation of the gas temperature will require an analysis of the pulse train generated by cycling the air flow past the thermocouple. The amplitude of this pulse train is 80°F in the test shown in Figure 5-3.

While the temperature difference between T_c and T_r will vary significantly with operating conditions, it is reasonable to expect that an 80°F temperature difference is a good "nominal" value. Assuming that our signal amplitude is the amplitude of

Data on this page shall be subject to the restriction appearing on page ii of this document.
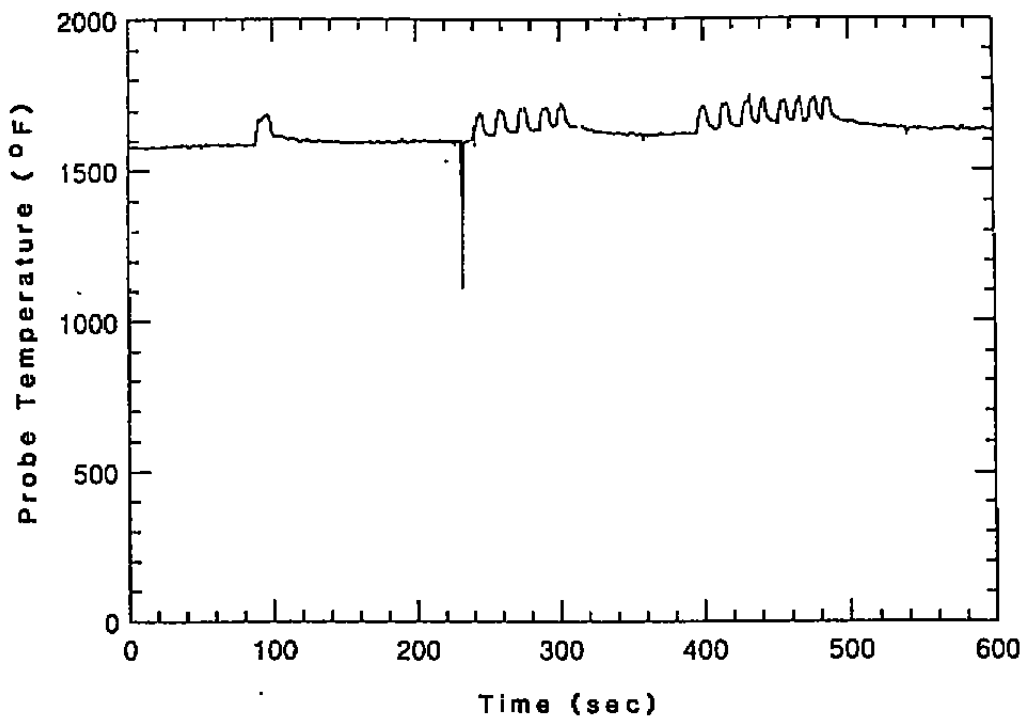
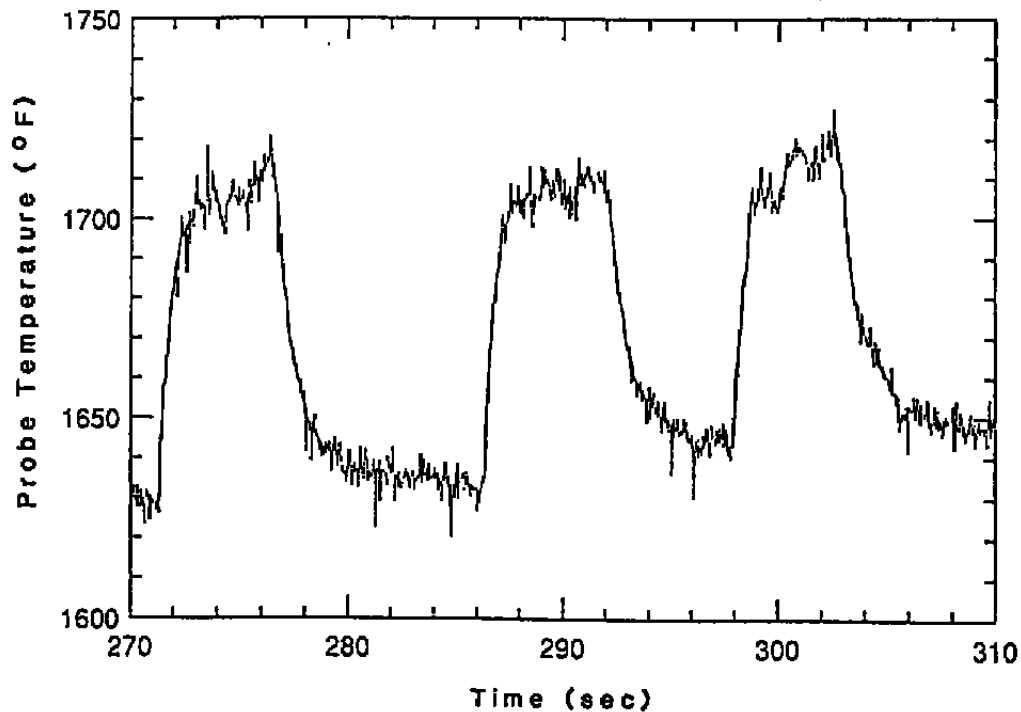Figure 5-2. Probe Temperature Trace From Typical Test

Figure 5-3. Expanded View of Three Temperature Perturbations

the pulse train and that the noise level is still 8°F, our actual signal-to-noise ratio could be quoted as 10:1 -(80°F divided by 8°F). This important distinction between the two interpretations of signal amplitude leads to a significant difference in the stated noise level in our signal. At the time of the Inconel probe tests, it was felt that our signal noise level was acceptably low to allow calculation of gas temperatures.

Signal traces were also analyzed for isothermal probe response. Due to the presence of radiation, the probe rise and decay segments cannot be expected to follow true exponential response curves. However, due to the nature of thermocouple measurements (i.e., lumped thermal mass), the response to a step change in signal will almost always resemble, at least approximately, an exponential. The first temperature rise and decay from Figure 5-3 were plotted in logarithmic form in Figures 5-4a and 5-4b. A straight line was fit to the data, and it can be seen that the straight line does fit the data well over a large portion of the transient. Information from the straight-line fits in Figures 5-4a and 5-4b provided the information necessary to calculate the actual gas temperature.

This gas temperature calculation was performed for the three rise and decay pulses from Figure 5-3. The straight lines fit to the data were made by viewing the response curves and hand fitting. The temperatures calculated for the three pulses are shown in Figure 5-5 as point-temperature values above the rise portion of each pulse. Since the gas temperature was approximately 1700°F and the furnace walls were only heated to about 1000°F during this test, it was anticipated that the true gas temperature would be higher than the measured temperature. As indicated in Figure 5-5, this was indeed the case. The uncorrected probe temperature in the combined heat transfer mode was about 1710°F, while the calculated true gas temperature was 15°F to 20°F higher. The three calculated temperatures varied between themselves by about 8°F, and the maximum variation from the average of the three was only 4°F. These results, although preliminary, did indicate that fabrication of the platinum probes should proceed.

During June through October of 1988, many additional tests of the Inconel probes took place with the intention of testing to higher gas temperatures and demonstrating data reduction algorithms. An example of this work is presented along with a discussion of data reduction algorithms from an Inconel probe test from June 1988.

A plot of temperature versus time for a 60-sec probe trace is presented as Figure 5-6. For roughly the first 10 sec of the test the probe was in thermal equilibrium in the nonsuction, or radiation, mode. The wall temperature in the vicinity of the probe was also measured during this test and was found to be roughly 1500°F, which is considerably lower than the 2000°F

Data on this page shall be subject to the restriction appearing on page ii of this document.
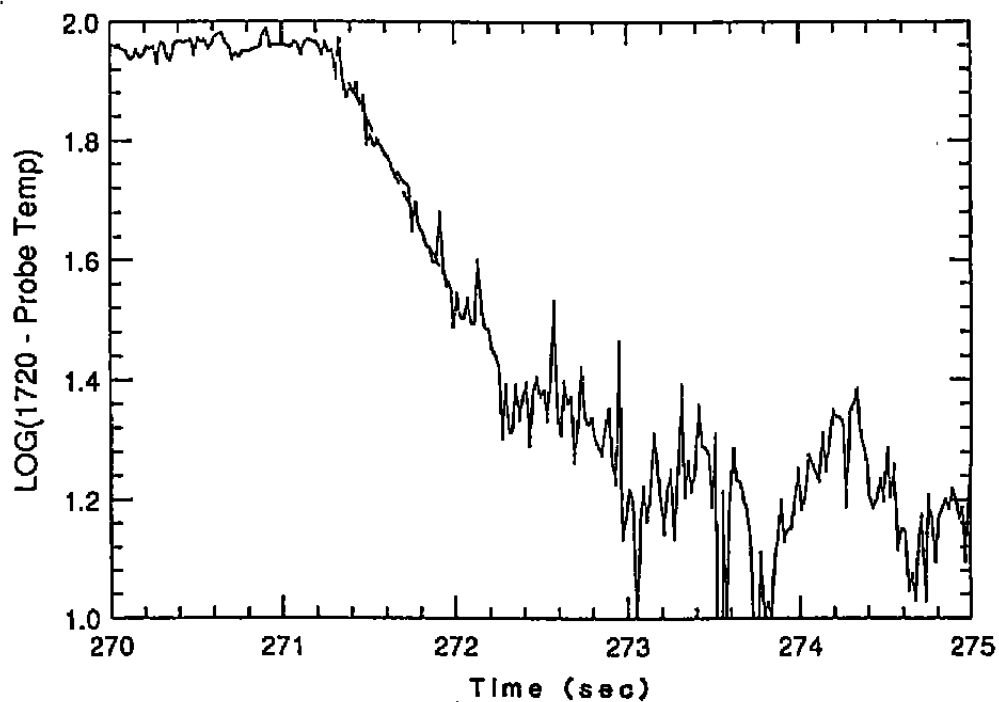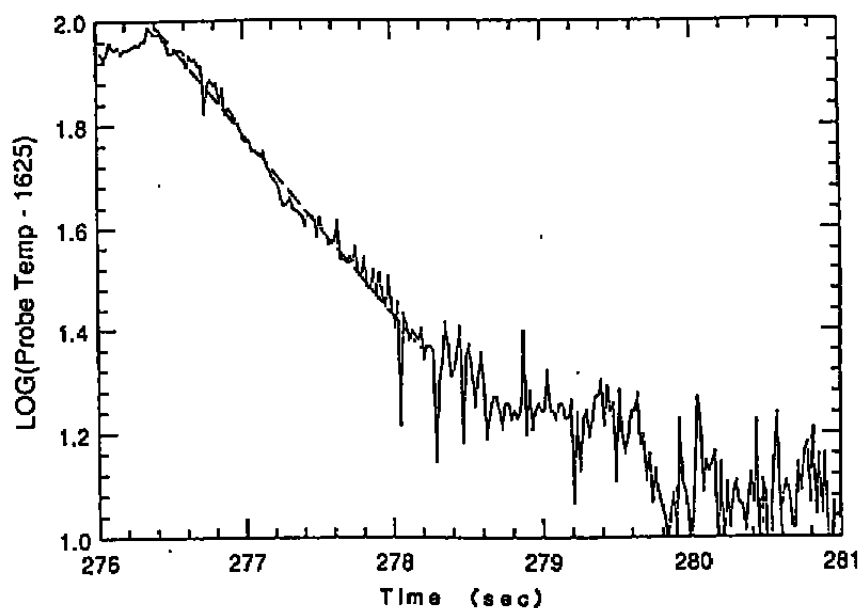
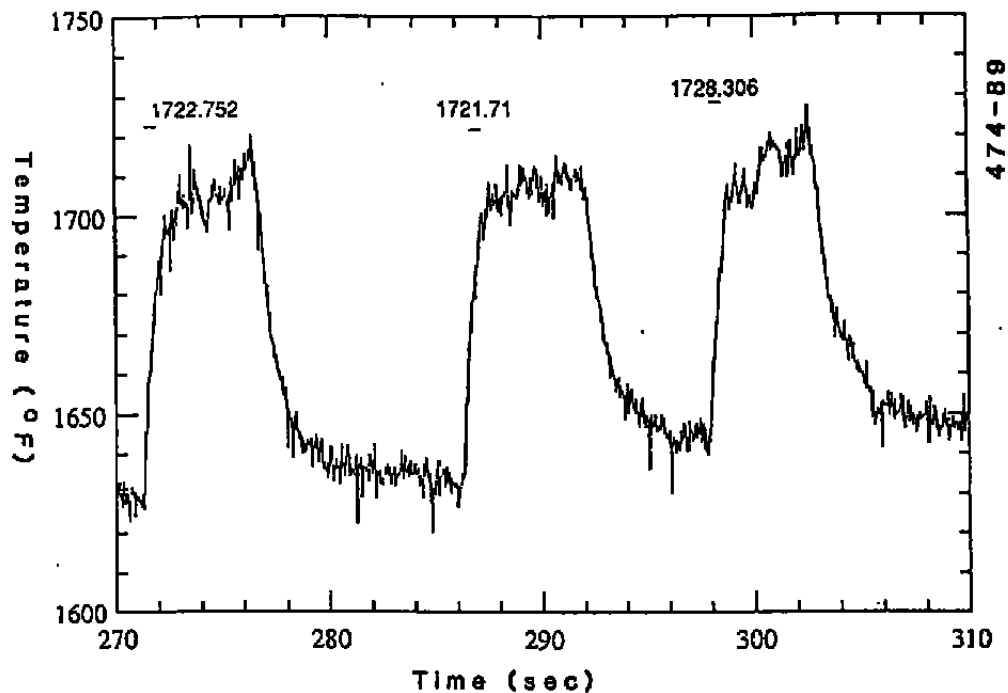a. Temperature Rise

b. Temperature Decay

Figure 5-4. Logarithmic Curve-Fits of Data
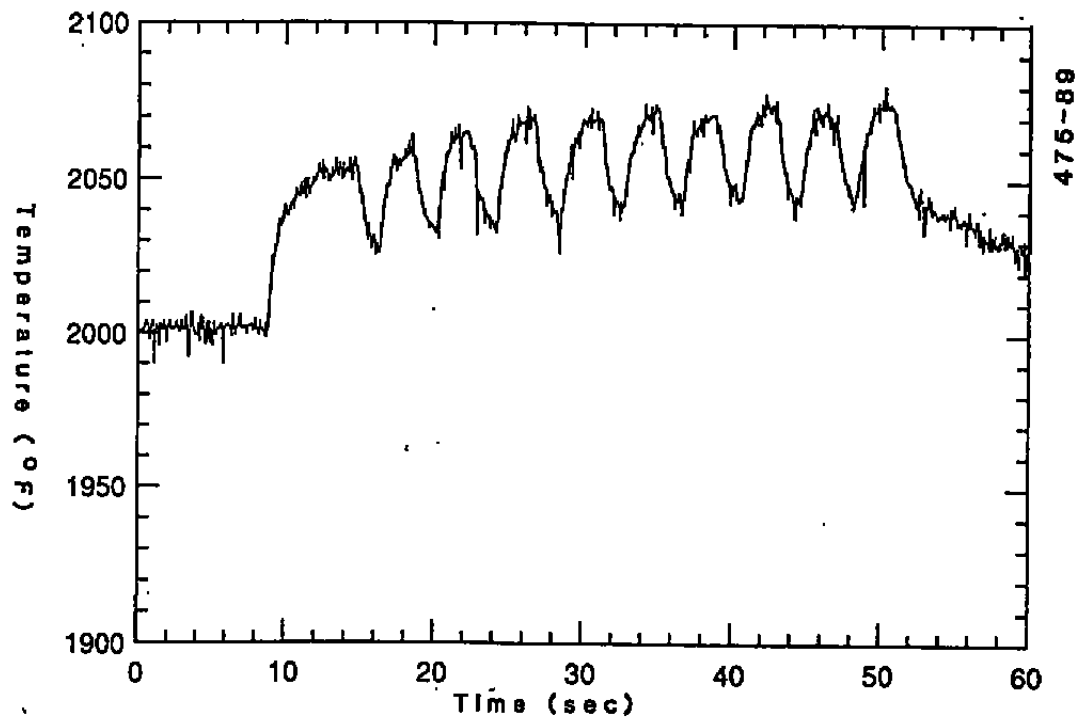
Figure 5-5. Calculated Gas Temperature Using Inconel Probe

Figure 5-6. Temperature Probe Data From Test 102

Data on this page shall be subject to the restriction appearing on
page ii of this document.

junction temperature. This high equilibrium radiation temperature, relative to the wall temperature, is indicative of the effectiveness of the radiation shield. However, it should be expected that the radiation losses would still cause a significant error in the temperature measurement. At 10 sec into the test, the suction valve was opened and flow was drawn past the thermocouple at roughly 150 ft/s. The result of this can be seen as the first temperature rise of Figure 5-6. As expected, the temperature rose sharply and approached the combined heat transfer equilibrium value, T_c. At this time, roughly 12 sec into the test, the probe was cycled at 2.5-sec intervals to obtain the desired temperature pulse train.

There is roughly the same amount of noise in this signal as seen in the earlier test, and it was felt that this was representative of data that should be able to be successfully analyzed. Attempts were made to fit different mathematical functions to the curves. The purpose of the curve fitting, rather than numerically differentiating the curves, was to allow the calculation of acceptably smooth temperature derivatives. Since the first derivative of the probe temperature with respect to time is discontinuous at each point where the suction valve is cycled on or off, it is desirable to fit curves piecewise to the data. This method was employed and separate curves were fit to each temperature rise and decay.

In our first attempt at reducing the data, quadratic functions of temperature with respect to time were fit. First derivatives of these functions can be easily calculated, and in general computational requirements are small. This analysis was performed on the temperature data after the tests, but with the intention of performing the same calculation in real time at some later date. Because of this, careful attention was paid to computational requirements.

As previously discussed, the response behavior of the probes does approximately resemble an exponential, so a second-order exponential function was also fit to some of the data. It was intended that an exponential curve could fit the data more accurately at the expense of increased computation time. Results of exponential curve fits of a temperature rise and temperature decay are shown in Figure 5-7. The graphical technique of presenting temperature derivatives as a function of temperature, as shown in Figure 3-6b of Section 3, is repeated in Figure 5-8 using data from Test 102. The nearly straight $\dot{T}_c - \dot{T}_r$ line as a function of probe temperature is indicative of good data and good curve fits. Although $\dot{T}_c$ and $\dot{T}_r$ by themselves cannot be expected to be straight lines, the sum of the two functions must be a straight line based on assumptions of ideal probe behavior.

The gas temperature extrapolated from these curves was 2103°F based on asymptote values of T_r = 2042°F and T_c = 2072°F. As there was no standard to compare our calculated temperature
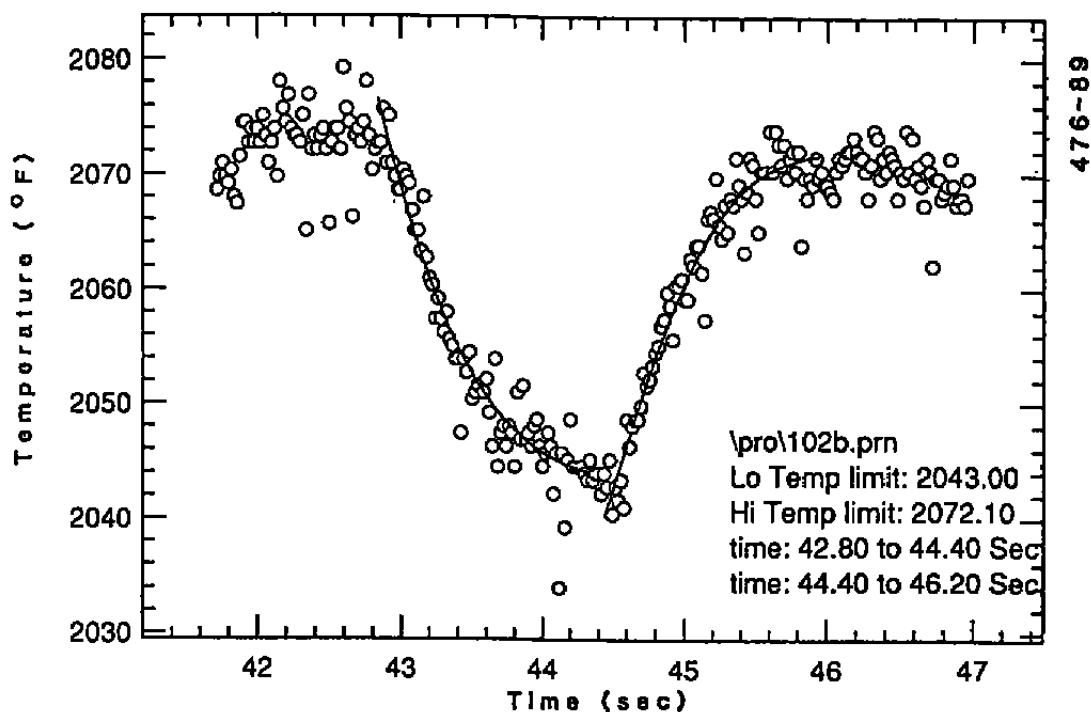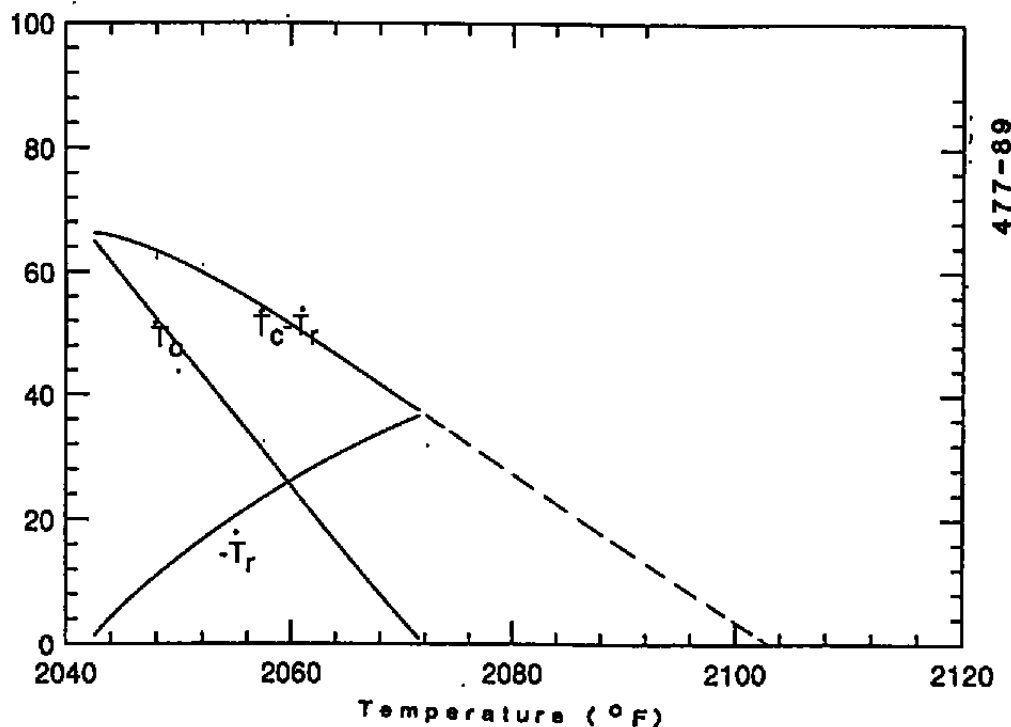
5-8

Figure 5-7 Exponential Curve-Fits to Data From Test 102

Figure 5-8. Solution for T_g in Temperature Derivative vs. Temperature Coordinates

with, it was assumed to be correct. At this stage of the program we were more concerned with determining if curves could be fit to data or if numerical differentiation would provide better answers. While the data just presented may seem to indicate that analysis was easily performed, this was an example of a good fit of data. Much. of the other data collected was not so easily analyzed. Since data were all analyzed after the completion of a test, there was a considerable amount of user interaction in the data- reduction process. The large amount of data generated led us to observe that fits such as those shown in Figure 5-8 were the exception rather than the rule, and the development of reduction algorithms continued.

Another example of data from the Inconel tests is presented from Test 101. In this test, the burner in the furnace was shut down and the gas temperature decreased rapidly. Due to the mass of the furnace walls, the gas temperature decreased at a more rapid rate than the furnace walls. At a point where the gas temperature was nearly equal to the wall temperature a test was run, with the results shown as Figure 5-9. Since the furnace was off, the flame radiation source is eliminated. In addition, the wall temperature is nearly equal to the gas temperature, so the effects of radiation on the probe temperature are nearly zero. There should be little or no difference in the junction temperature during the cycling of the suction valve, and this was in fact what was observed. Approximate locations of the first four cycling points are indicated by arrows in this figure. Under these conditions, where T_r is nearly equal to T_c, the true gas temperature is being measured by the probe.
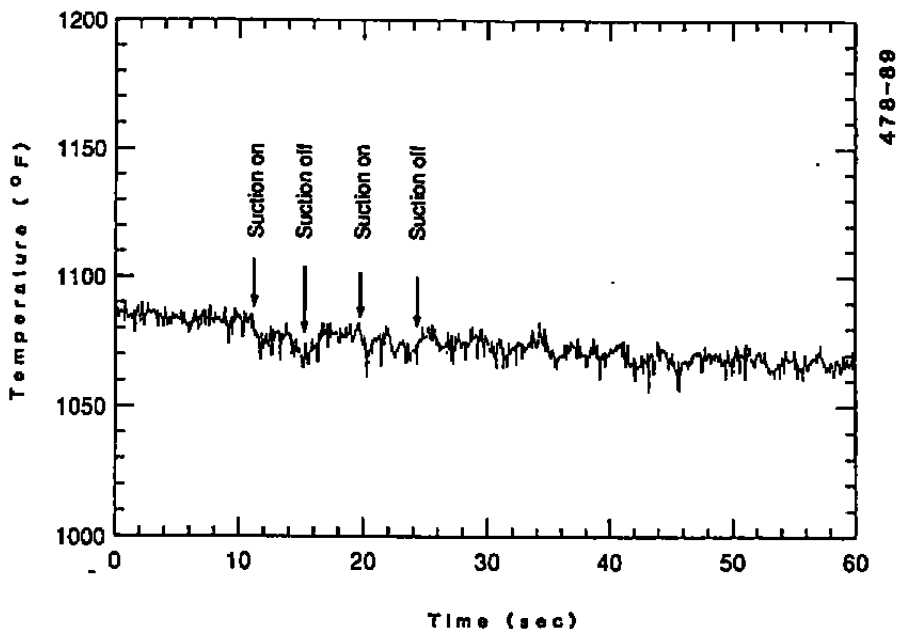
Figure 5-9. Data From Test With T_p Equal to T_g

Data on this page shall be subject to the restriction appearing on page ii of this document.

5.2 REAL-TIME DATA ANALYSIS

One of the purposes of the tests of the Inconel probes was to provide data to be used in demonstrating real-time control of the Astron probe. It was intended that control algorithms be developed and demonstrated using the Inconel probes, so that this task would be completed, or at least partially completed, by the time that the platinum probes were delivered.

After collecting a substantial amount of data using the Inconel probes, as discussed in Section 5.1, our efforts were directed to the development of control algorithms. The technique favored for data reduction was to fit first-order exponential curves to the individual rise and decay segments of a probe signal. This requires a knowledge of the high and low asymptotes of the rise and decay curves (T_r and T_c). Determination of these two temperatures is an integral part of our data reduction technique, and it is important that these measurements be very accurate. This was made evident in posttest analysis of tests in which our real-time controller was operating.

In the particular case studied, the high-temperature asymptote used by the controller agreed with the calculated asymptote in our posttest analysis. However, the low-temperature asymptote disagreed with our analysis by about 20°F. Using our capability to recalculate a run after the completion of a test, the data from this run were reprocessed using asymptotes that more clearly approximated what we observed to be the correct values. Figure 5-10 shows the poor curve fits that resulted from the erroneous low-temperature asymptote. The calculated true gas temperature are scattered and do not fit on the scale of the figure. Figure 5-11 illustrates the improvement in the calculated gas temperature that results when a more reasonable low-temperature asymptote of 1890°F is used. This new asymptote was chosen by visually examining the plots and picking a low asymptote by hand. The improvement in the prediction of the gas temperature, at least from the standpoint of repeatability, is clear.

While Figure 5-11 represents a better fit of the exponential curve to the data, it appears from a close examination of the data that the low-temperature asymptote should be chosen to have a slightly higher value. Figure 5-12 shows what happens to the calculated gas temperature when the asymptote is increased to 1900°F. The fits of the temperature decays appear to have improved, but a new problem surfaces. The calculated true gas temperature now varies by about 25°F over the course of eight calculations. This is an unacceptable amount of scatter, indicating a lack of precision in our measurements.

While these plots show results from tests using the Inconel probes, they are instructive to use in the discussion of data reduction over the course of the Phase II program. During
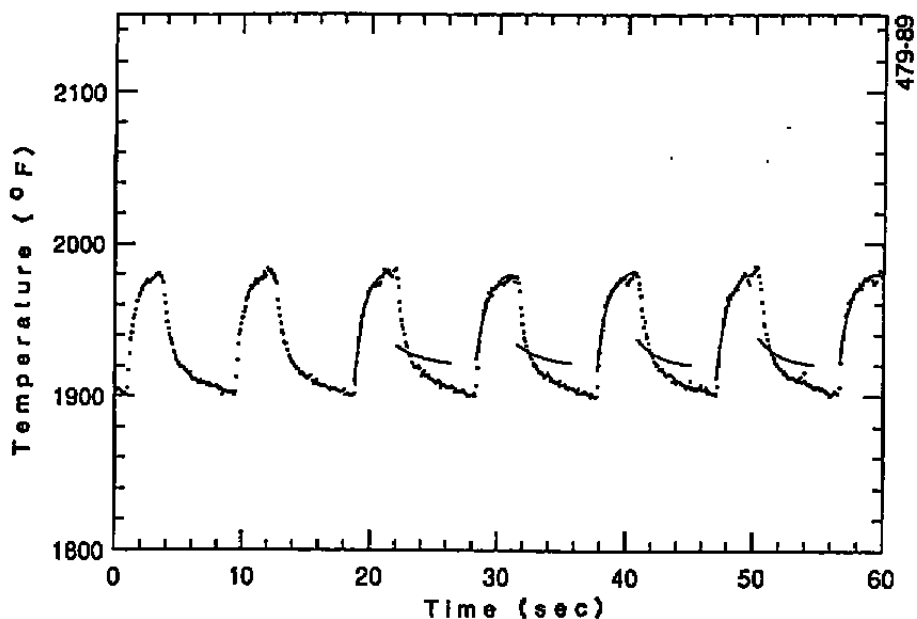
Figure 5-10. Curve-Fit of Data Based on Controller Defined Asymptotes
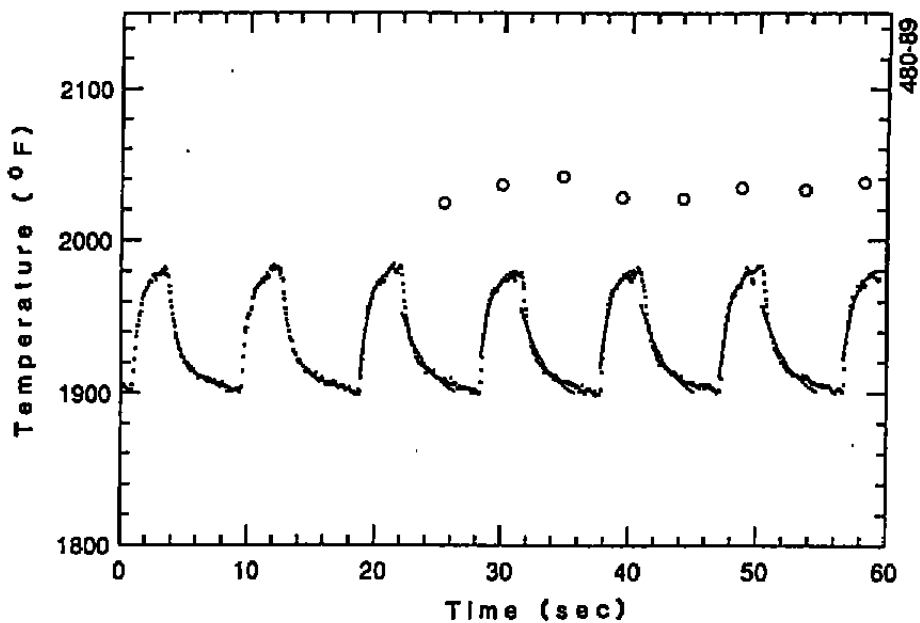
Figure 5-11. Improved Curve-Fits Resulting From Better Choice of Low Asymptote

5-12
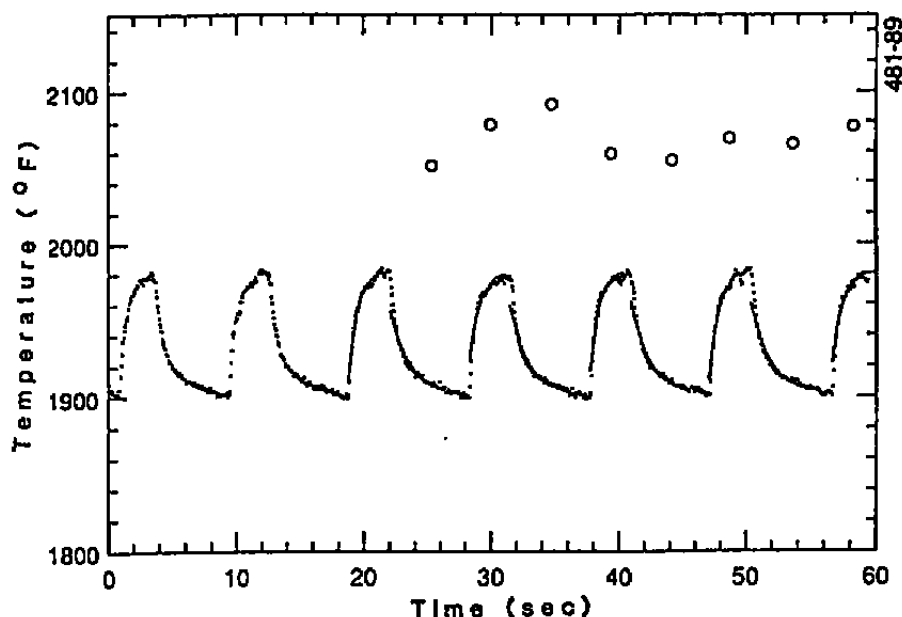
Figure 5-12. Increased Scatter Due to Small Variation in T_r

posttest analysis it was usually apparent when curve fits were closely following the data. This was clear either because the fitted curves were observed in plots to follow the data, or because the calculated gas temperature was consistent with a reasonable gas temperature and with other temperature calculations from the same pulse train. While the approach of curve-fitting data to allow differentiation of an analytic function has not been a complete success, the other option considered, direct numerical differentiation of digitized data, has also been demonstrated to be difficult.

5.3 PLATINUM PROBE TESTS

Based on the results discussed in Section 5.1, temperature probes with platinum bodies were ordered from ARi Industries. These probes were nearly identical in appearance to the Inconel probes. Drawings of the probe are shown in Appendix. A, and photographs of a platinum probe are shown in Figures 3-7a through 3-7d in Section 3.2. The platinum probes were delivered in November 1988, and the first tests using those probes were conducted in early December. The purposes of these tests were to further refine our data-reduction techniques, and to demonstrate probe survivability at temperatures up to 3000°F.

A summary of tests run in December and February is shown as Figure 5-13. As seen in this figure, we did reach a peak gas

5-13

temperature of 3000°F, and ran a substantial number of tests above 2500°F. Tests at high wall temperatures and low gas temperatures were more difficult to run than had been anticipated due to higher than expected conduction losses through the facility walls.

Comparisons of data from four tests run on 20 December 1988 are presented. Data from these runs are summarized in Table 5-1. Plots of the temperature traces are presented as Figures 5-14a through 5-14d. First, a comparison is made between tests with distinctly different radiation environments. Using the difference between gas temperature (as measured by our probe in suction mode) and wall temperature as the means of defining the magnitude of radiation effects, the tests chosen for comparison were at the high and low extremes. In Test 18 the gas temperature was 140°F higher than in Test 26, but the wall temperature was 150°F lower. As expected, the effect of the cool furnace walls is to increase radiation losses and hence to increase the difference between T_r and T_c. This phenomena is observed. The span of the temperature perturbation signal is 32°F in Test 18 and 20°F in Test 26. Further quantification of this observed behavior is difficult due to the presence of the furnace flame as an additional radiation source.

Table 5-1.   Comparison of Platinum Probe Test Conditions

Test	T_c(°F)	T_{wall}(°F)	T_c-T_r(°F)	$T_{combstr}$(°F)	T_{calc}(°F)
18	2765	1892	32	2639	2770
24	2627	2034	20	2500	2636
25*	2590	2048	22	2505	2592
26	2625	2046	20	2495	2638
NOTE: Probe rotated 90° (see text).					

A different comparison was made between Test 24 and Test 25. These tests were run sequentially in an attempt to test the probe in two different flow orientations under the same conditions. In Test 24 the probe was positioned in its normal orientation with the shield entrance facing upstream, while in Test 25 the probe was rotated 90 degrees so that the shield entrance was facing a facility wall. In the normal orientation it is assumed that gas coming in contact with the thermocouple junction has not been in contact with the probe body. Such contact would introduce an error in our measurement. In the rotated position, some gas will probably contact the probe body prior to interacting with the thermocouple, but due to the high velocity of the suction flow this error should be small. The purpose of Test 25 was to
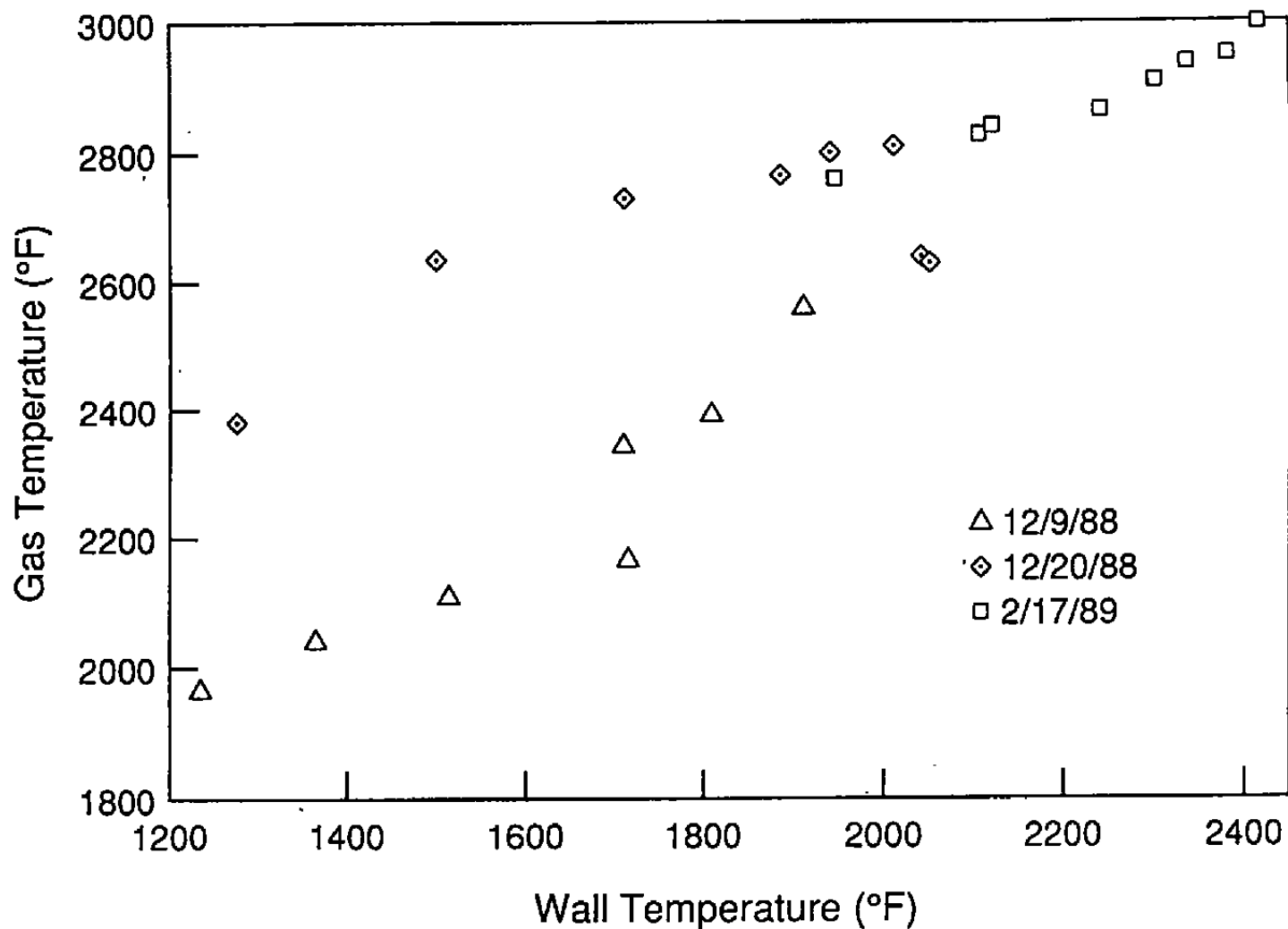
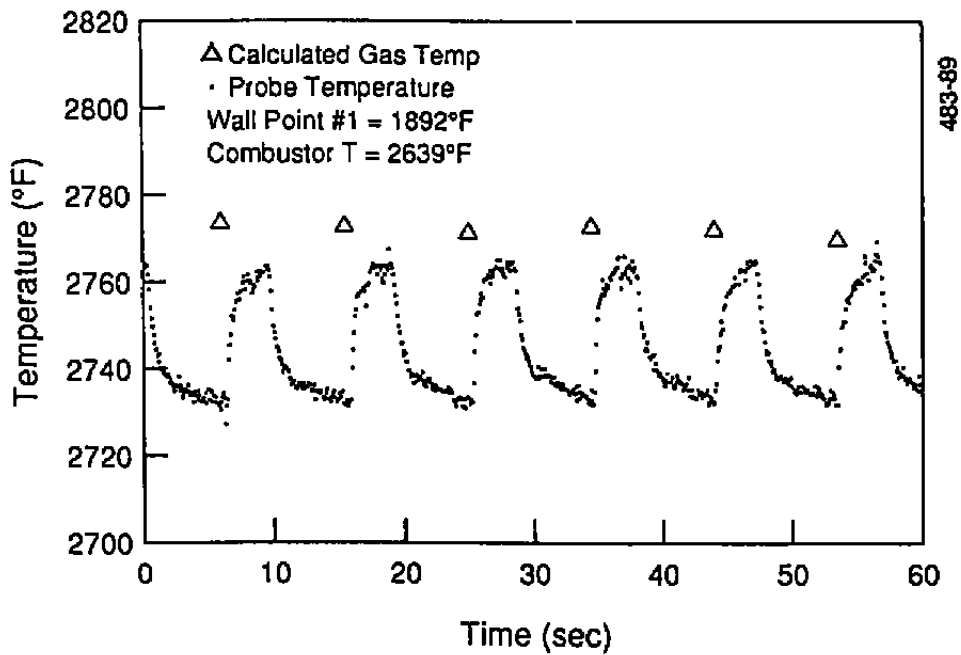Figure 5-13.   Comparison of Platinum Probe Test Conditions

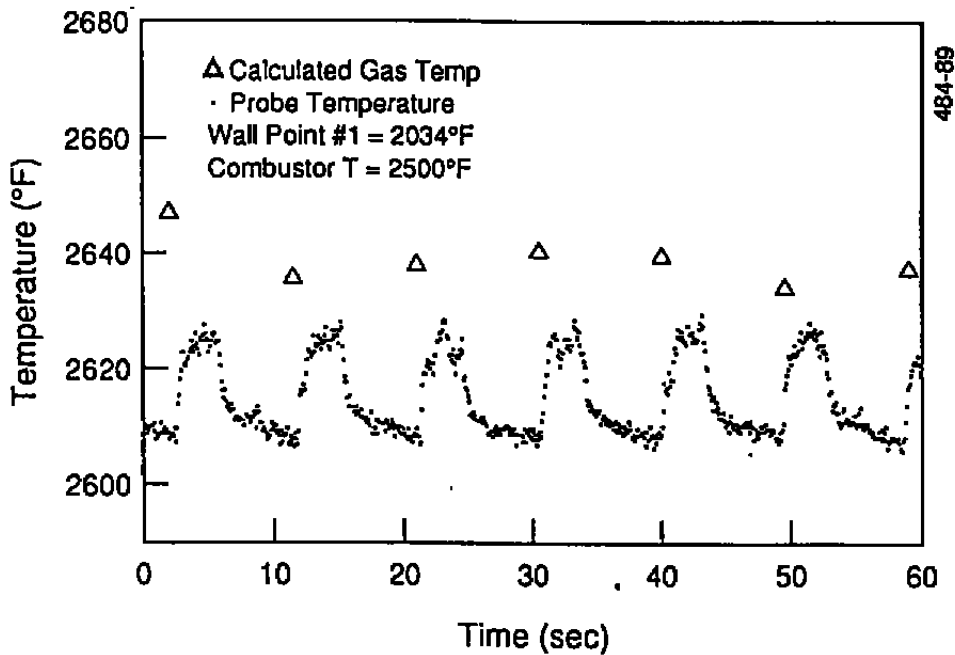Figure 5-14a.   Platinum Probe Data From Test 18

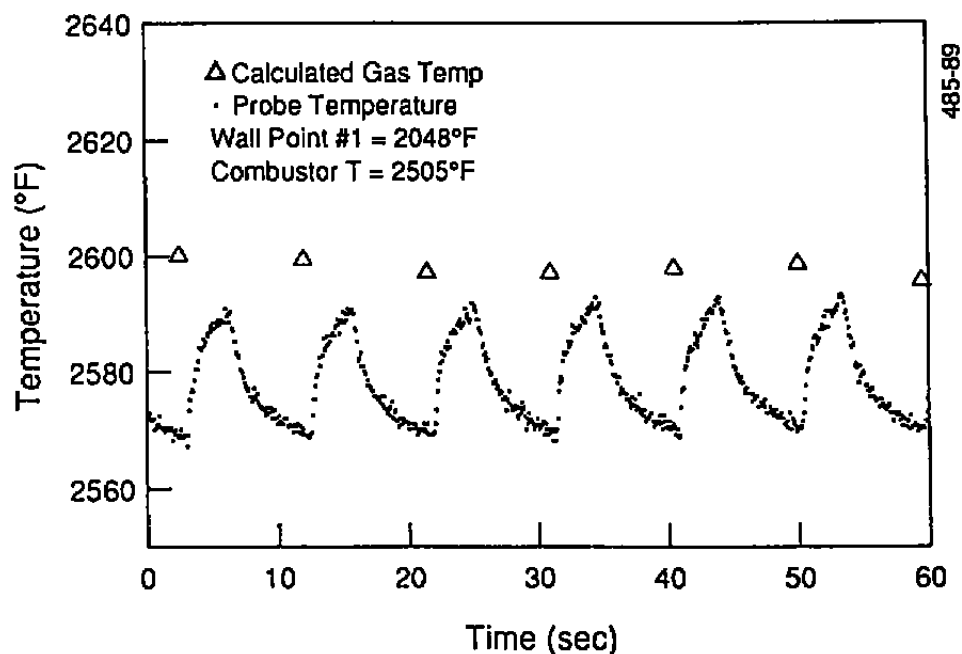Figure 5-14b.   Platinum Probe Data From Test 24

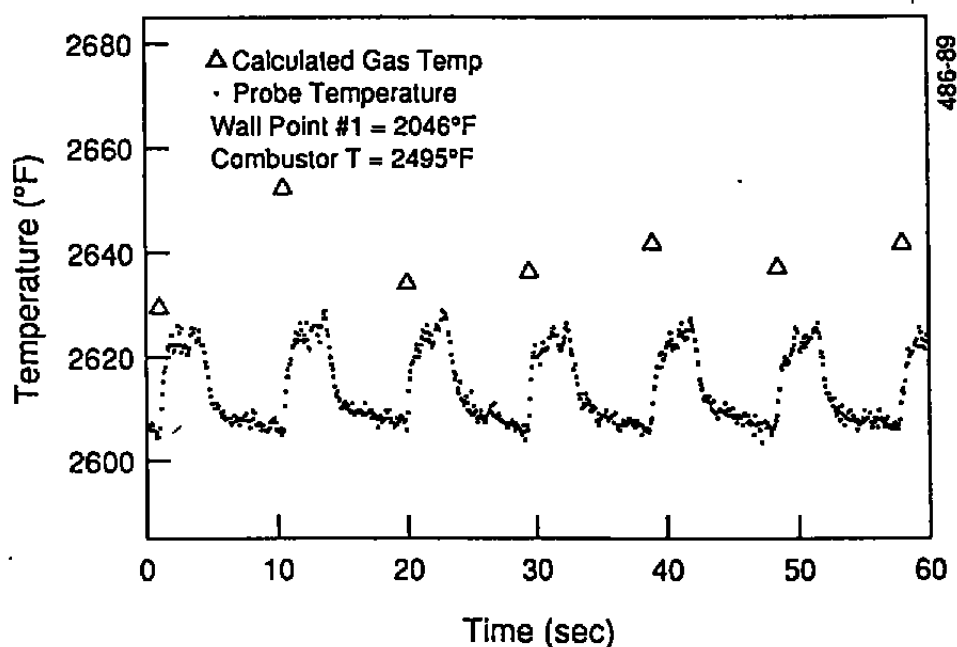Figure 5-14c. Platinum Probe Data From Test 25

Figure 5-14d. Platinum Probe Data From Test 26

see if a cleaner (improved signal-to-noise ratio) signal would result if the flame radiation was isolated from the thermocouple by the probe shield, and if this cleaner signal would justify operating in this mode.

As seen in Figure 5-14c, noise in the temperature signal is significantly reduced when the probe is rotated. As expected, both temperature asymptotes are lower due to the decreased radiant exchange with the flame. Unfortunately, the temperatures predicted using our reduction algorithm are not consistent with each other as they should be. This is probably due to inaccuracy in our data-reduction method, but could be due, at least in part, to the gas contact with the probe body.

After completing Test 25, the probe was rotated back to its normal orientation and another test was run. Test 26 should compare well with Test 24, and this is the case. Even the calculated gas temperature is consistent, indicating that our controller was correctly tracking asymptotes. While the similarity between these test results was expected, several important points should be made. In rotating the probe 90 degrees and then returning it to the original position, it is likely that the orientation in Test 26 is slightly different from Test 24 in terms of both insertion depth and probe angle. Also our controller tracked a 35°F swing in the asymptote values and returned to the correct value. While agreement between the two tests is inconclusive, a disagreement would have alerted us to a strong sensitivity to changes in probe placement.

5.4 NASA LEWIS RESEARCH CENTER COMBUSTOR RIG TESTS

Based on the results of the high-temperature tests at Astron, the control algorithm chosen for the NASA demonstration was the following:

- The probe solenoid valve was cycled to provide high and low asymptote temperatures (T_r and T_c).

- High-speed data scans of 50 points at approximately 1 kHz were performed at the initiation of both the temperature rise and temperature decay.

- Straight lines were fit to these points to determine the derivatives $\dot{T}_r$ and $\dot{T}_c$.

- Equation 3-22 from Section 3 was solved for T_g.

Although this algorithm is considered to be less accurate than the general equation 3-32, our demonstrated inability to accurately fit the rise and decay temperature traces dictated our use of Equation 3-22. Testing was performed over a 3-day period, with the first day being used for setup, the second day for a

full day of testing, and the third day for cleaning up the combustor facility and presenting test results to NASA personnel.

Our test plan called for running approximately ten 70-sec tests in a manner identical to the procedure demonstrated at Astron. After running several tests and attempting to analyze data in which the temperature rise and decay were not discernable, the facility was shut down to allow examination of our probe for possible damage. The suction line solenoid valve was checked for proper operation, the probe was removed from the test duct for a visual inspection, and a thermocouple calibrator was used to check our signal conditioning electronics. Having observed no damage to any of our equipment, it was determined that the noise observed in our temperature signal was most likely due to real temperature fluctuations in the gas flow.

An amplifier with an adjustable low-pass cutoff frequency was borrowed from NASA to attempt to further filter our data. Unfortunately, the frequency of the temperature fluctuations observed in the flow were too close in frequency to our probe perturbation signal. We could not selectively filter the flow disturbances. However, due to the apparent randomness of the flow oscillations, and the periodic nature of our probe trace, NASA personnel suggested the use of ensemble averaging to improve our signal-to-noise ratio. Although we could not demonstrate this technique at NASA, we increased the duration of two of our tests from 70 sec to 300 sec to provide a large number of probe cycles for averaging.

The results from the two 300-sec tests provided the only useful probe data collected at NASA. The results from these tests are shown in their final averaged form in Figures 5-15a and 5-15b. Data collected by NASA personnel defining facility conditions are presented with the Astron probe results. The array of gas temperature measurements in the duct was made using unshielded thermocouples. In all cases these temperatures were below the temperature measured by our probe, as would be expected. The calculated temperatures based on Equation 3-22 are determined in graphical form on the temperature-time traces of the ensemble average data for both 300-sec tests.

As an example of the amount of random noise in the NASA data, the temperature history for a single probe trace is presented as Figure 5-16a. Successive averaging of 5 and 10 traces is provided as Figures 5-16b and 5-16c. AEDC has stated that in a typical steady-state test, engine conditions are held constant for 2 minutes. Using the present hardware, this would allow the averaging of 10 to 20 probe periods.

Important results of the NASA Lewis test program include:

• We are much more aware of potential signal-to-noise problems due to flow randomness. We had previously been concerned mostly with eliminating electrical noise.

5-19

• We were introduced to the concept of ensemble averaging and have now demonstrated that this technique is beneficial in the noisy environment.

• We demonstrated probe structural integrity under conditions in which the fluid density was significantly higher than in previous tests, and with the probe supported at the midpoint of a 16-inch-diameter duct.

1416.

1530.

1624.

1809.   Astron probe
        location

2045.

1355. 1493. 1596. 1760.   •   1788. 1589. 1501. 1408.

2037.

1886.

1724.

1635.

1496.

Main Airflow	lb/s	15.153
Bypass Airflow	lb/s	4.538
Total Airflow	lb/s	19.691
J-58 Fuel-Air Ratio		0.0252
J-58 Exit Press (psia)		50.49

$T_g = 2123°F$

487-89

Temp (F)

Time (S)
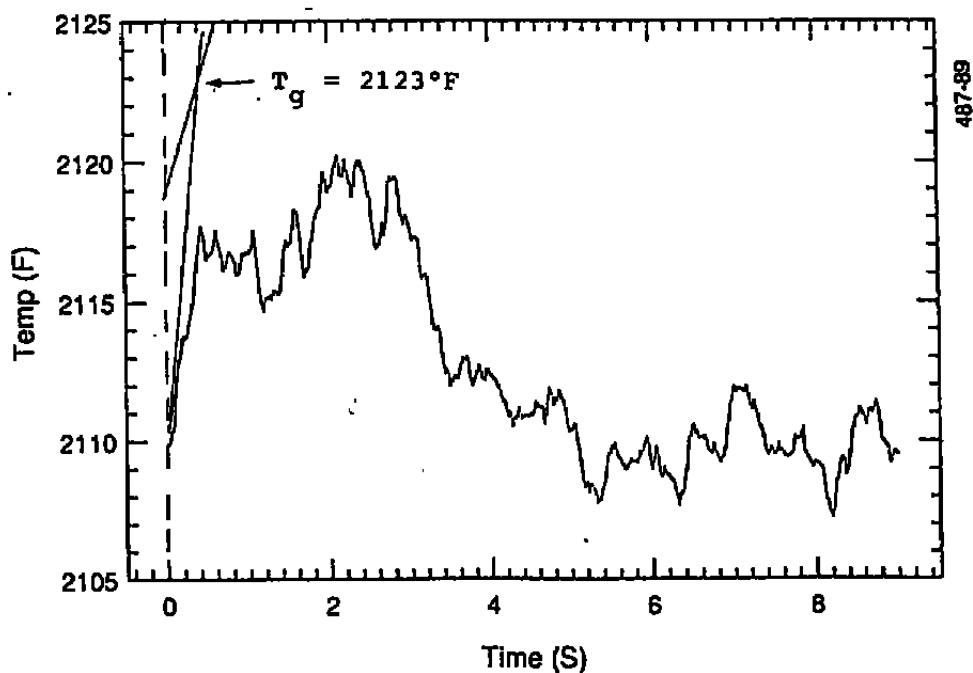
Figure 5-15a. Results of NASA Lewis Test 7

5-21

1441.

1558.

1658.

1853.   Astron probe
                         location
2110.

1366. 1508. 1613. 1777.   •   1882. 1666. 1570. 1470.

2078.

1905.

1738.

1646.

1507.

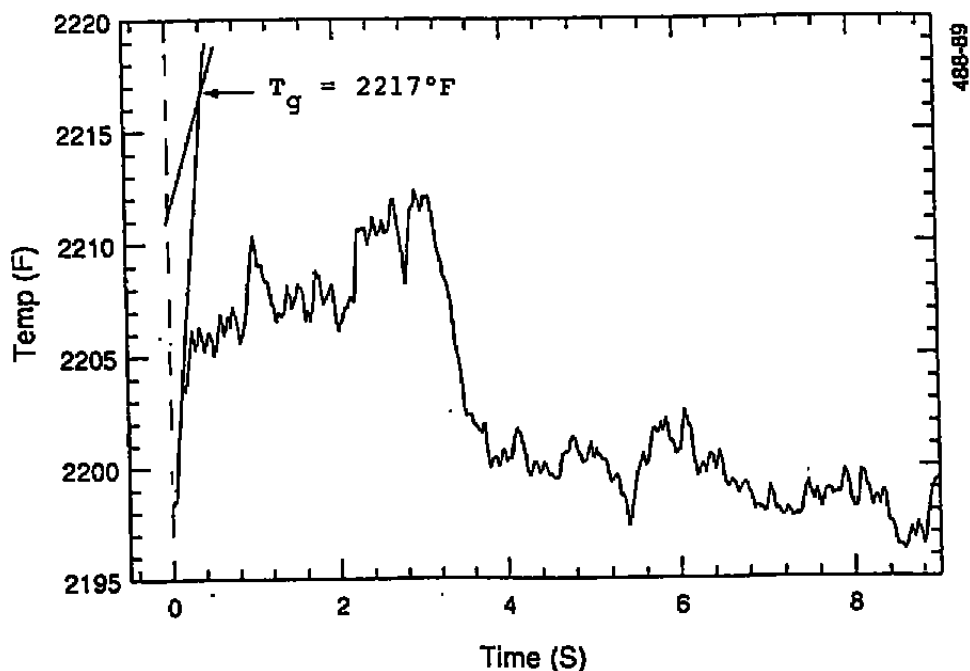|		
Main Airflow	lb/s	15.043
Bypass Airflow	lb/s	4.525
Total Airflow	lb/s	19.567
J-58 Fuel-Air Ratio		0.0265
J-58 Exit Press (psia)		50.22

T_g = 2217°F

488-89

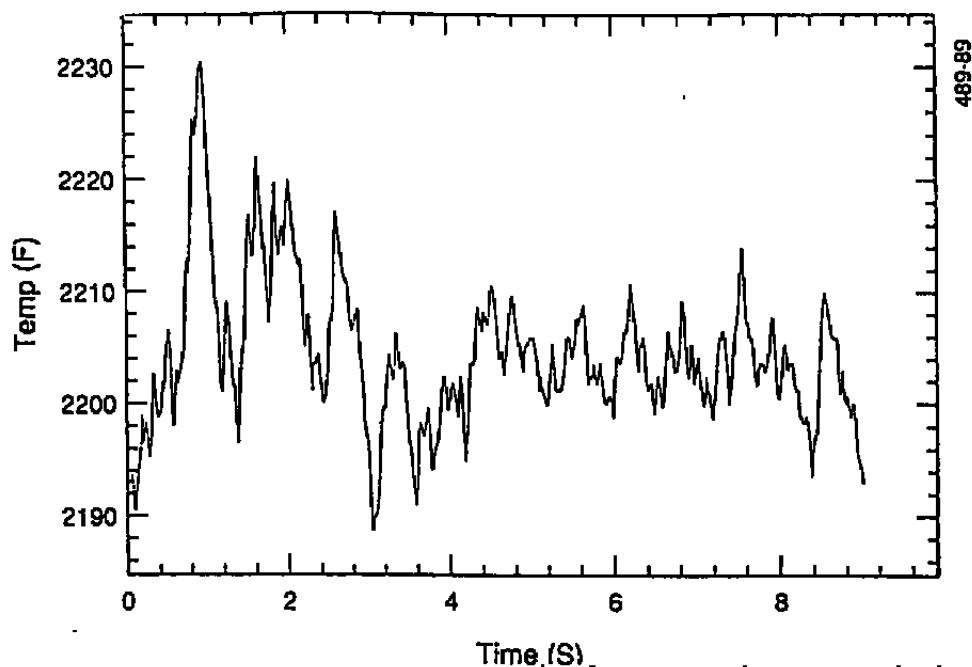Figure 5-15b. Results of NASA Lewis Test 9

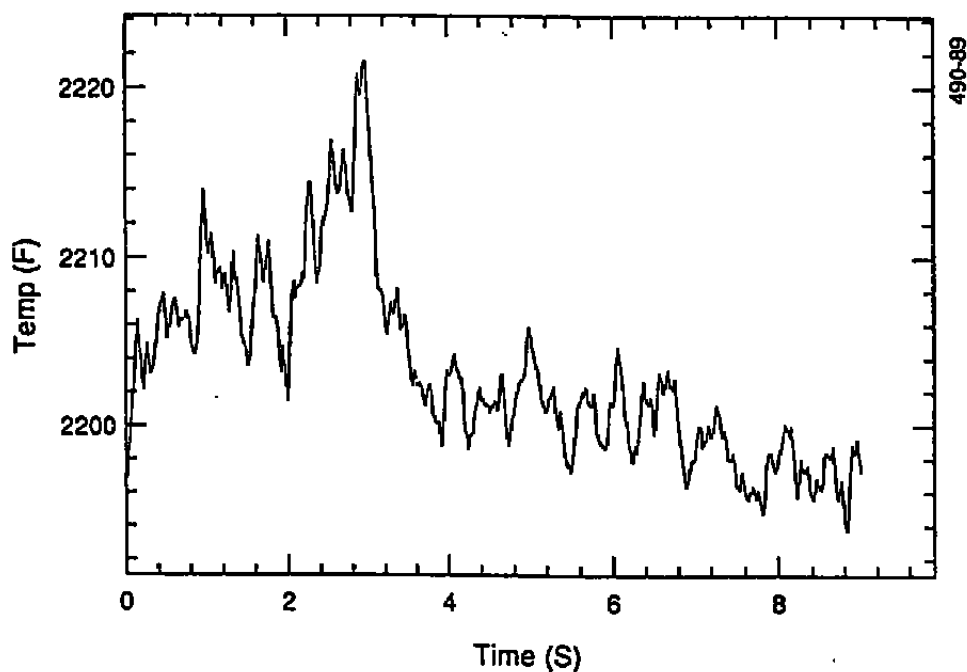Figure 5-16a. Single Probe Trace from Test 9

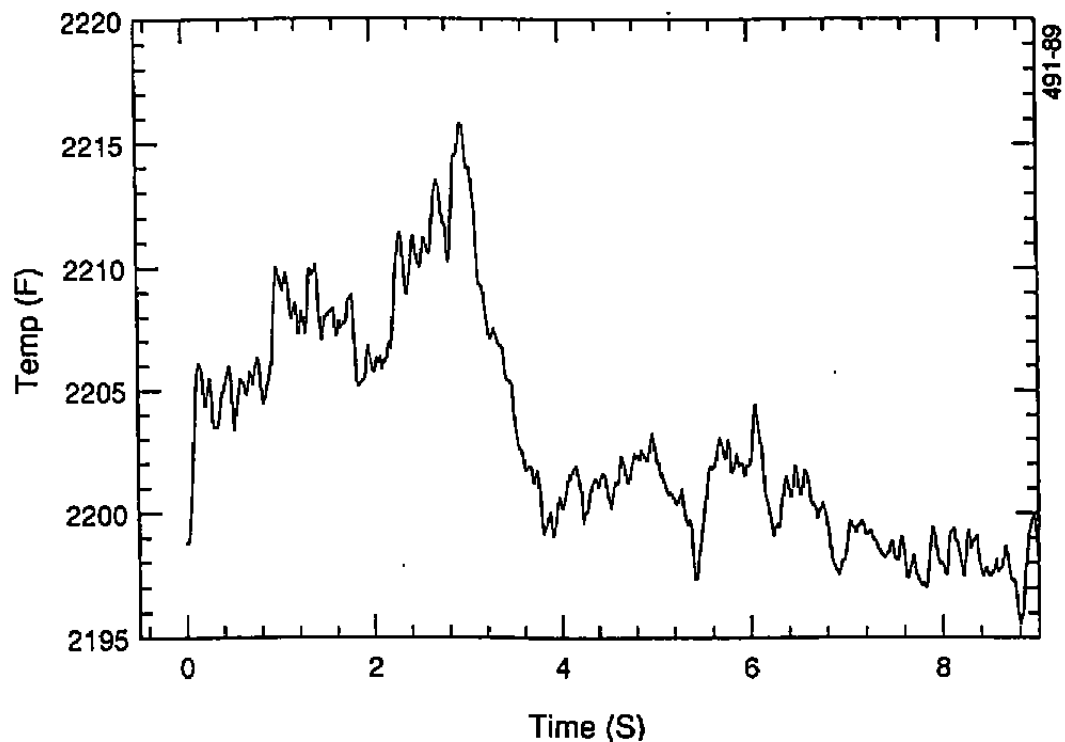Figure 5-16b. Ensemble Average of 5 Data Periods

Figure 5-16c.   Ensemble Average of 10 Data Periods

SECTION 6 - STRUCTURAL INTEGRITY TESTS

Structural integrity is an important concern in the design of a combustor exit probe. Survivability is difficult due to the severe environment, but more importantly, the consequences of a failure in the section of the engine between the combustor and the turbine blades will most likely be catastrophic. With this in mind, structural integrity must be demonstrated prior to the installation of a probe in an operating engine. As the current goal of our design effort was to furnish an instrument to be used in an engine test rig rather than in flight, the survivability requirements are defined in terms of hours rather than hundreds of hours. The probe is specified to be operable for at least 4 hours, and to be structurally sound for at least 20 hours.

6.1 ANALYSIS

Potential failure modes for the platinum probe designed for use at Astron and at NASA Lewis were analyzed during the Astron test program and prior to installation of the probe in the NASA combustor. Available data indicated that our probes would not fail due to the high temperature, although temperatures in the 3000°F range will reduce the tensile strength of our probe alloys substantially. As a rough rule, a maximum design stress on the order of several thousand psi should be safe at 3000°F.

Although this number is low compared to ambient temperature values, our probe as designed can easily withstand bending stress due to drag. Failure of the probe would most likely be caused by fatigue brought on by vortex shedding or some other oscillatory fluid motion, or by engine vibration coinciding with the resonant frequency of the probe. An analysis of the probe to determine the first two vibrational modes was performed. Modeling the probe as a uniformly loaded cantilever, the following equation was used[9]:

$$f_n = (K/2\pi) \cdot (EI/wl^4)^{1/2} \qquad (6-1)$$

K is equal to 3.52 for the first vibrational mode and 22.0 for the second mode. The three platinum tubes making up the "hot" end of the Astron probe were assumed to be concentric, resulting in the following. The natural frequency of the first mode of the probe was found to be 200 Hz, and the second mode frequency was calculated as 1260 Hz. The vortex shedding frequency of a 0.5-inch-diameter cylinder was calculated to vary from 500 to 1900 Hz in a hot gas environment in the velocity range of 100 to 400 ft/s. We calculated that a vibrational loading problem would potentially occur in the Lewis facility at a velocity of 250 fps, but only by exciting the second mode.

Tests in the Lewis facility at a velocity of approximately 275 ft/s resulted in no observable damage to the probe.

6.2 TEST HARDWARE

Structural integrity tests were performed at Astron to subject the probe to stresses and vibrational loadings anticipated to be similar to those encountered in a gas turbine. Based on communications with AEDC personnel[10], nominal test conditions were defined. These conditions are presented as Table 6-1.

Table 6-1. Vibrational Loading Test Conditions

Load	10g max
Frequency range	20-200 Hz
Max Displacement	0.003 to 0.005 inch (double amplitude)

An electromechanical shaker was used to excite our probe. Three different attachment methods were employed, consisting of:

- End loading the cantilever-mounted probe to provide large tip displacements and high stresses

- Excitation of the probe near the cantilever mount in an attempt to cause resonance

- Axially loading of the probe, allowing it to slide freely in the axial direction.

The end-loading and axial-loading test setups are shown as Figures 6-1a and 6-1b. The probe was instrumented at locations of probable maximum stress as indicated in Figure 6-2. Two types of excitation were attempted, a random frequency excitation and a frequency sweep of 20 to 200 Hz. Both types of excitation were used in the end loading and axial loading tests. Tests with loading near the cantilever base used only the swept-frequency excitation signal. Results are presented in the following section.

6.3 RESULTS

Results from the tip-loading tests are provided as Figures 6-3a through 6-3c. As seen from the accelerometer trace, a peak loading of 15g was achieved at a frequency of approximately 150 Hz. Peak stress values of 7.5 kpsi and 15.8 kpsi were measured at the first and second strain gage locations. Approximately ten
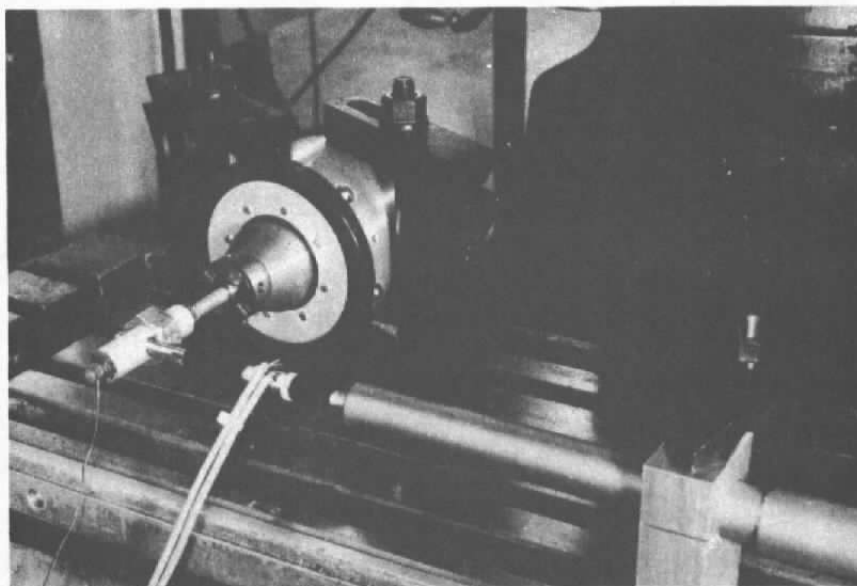
a.   End Loading Tests
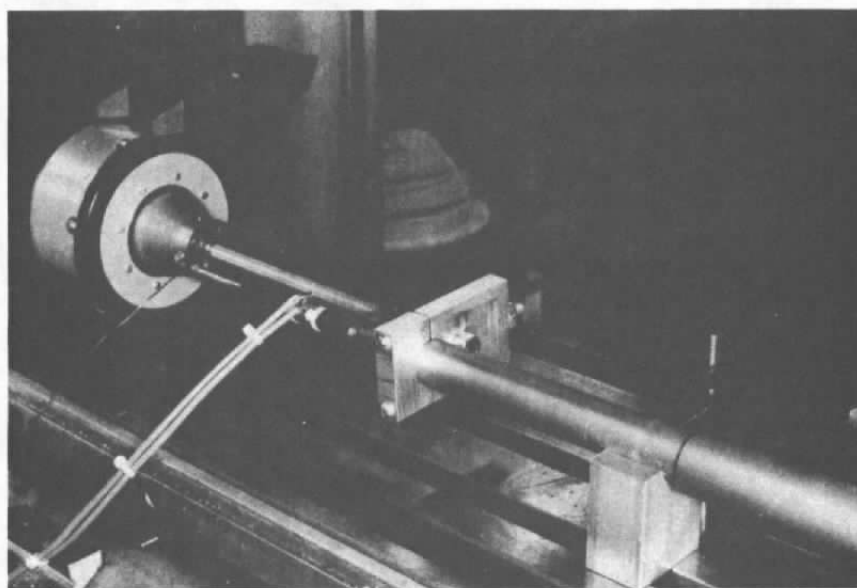
b.   Axially Loading Tests

Figure 6-1.   Vibrational Loading Test Setups

492-89

Strain Gage Location 1

Strain Gage Location 2
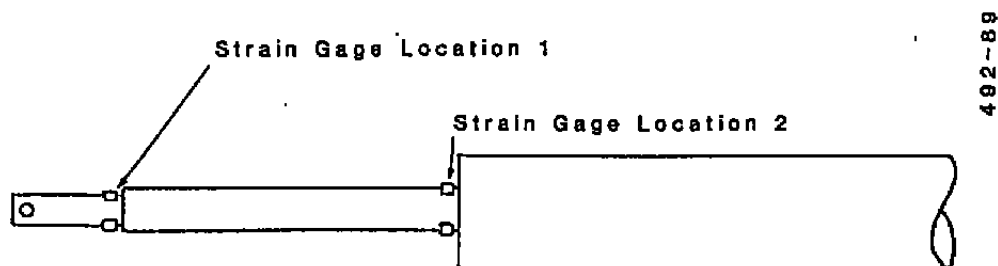
Figure 6-2.   Schematic of Strain Gage Locations

of these 8-sec tests were run with no visible damage to the
probe. Based on the observed g-loads and excitation frequencies,
the displacement of the probe tip exceeded 0.010 inch (double
amplitude). Resonance in this mode would be difficult to observe
due to the position of the excitation source.

In the midpoint loading tests it was intended that by using
a swept-frequency forcing function we could observe the presence
of resonant frequencies in the 20-Hz to 200-Hz range. No strong
amplitude peaks as a function of frequency were observed. Peak
measured strain values were in the 5 kpsi to 7 kpsi range.

Instrumentation in the axial loading tests consisted only of
the accelerometer. Structural failure of tubing and welds was
not a concern, and the only suspected failure mode was that the
ceramic insulator would break loose from its cemented position in
the platinum shield. The probe was subjected to a maximum load
of 8g for about five 8-sec tests. No damage to the probe was
observed.

The vibration tests were performed over a several-day period
(including setup) due to time and budget constraints. The data
we have collected is believed to be good, and we did subject the
probe to substantial loads with no observable consequences.
Detailed frequency analysis was beyond the scope of the current
effort, but the data is available for further review. As will be
discussed in Section 7, questions of structural integrity should
not be the primary concern at this time.
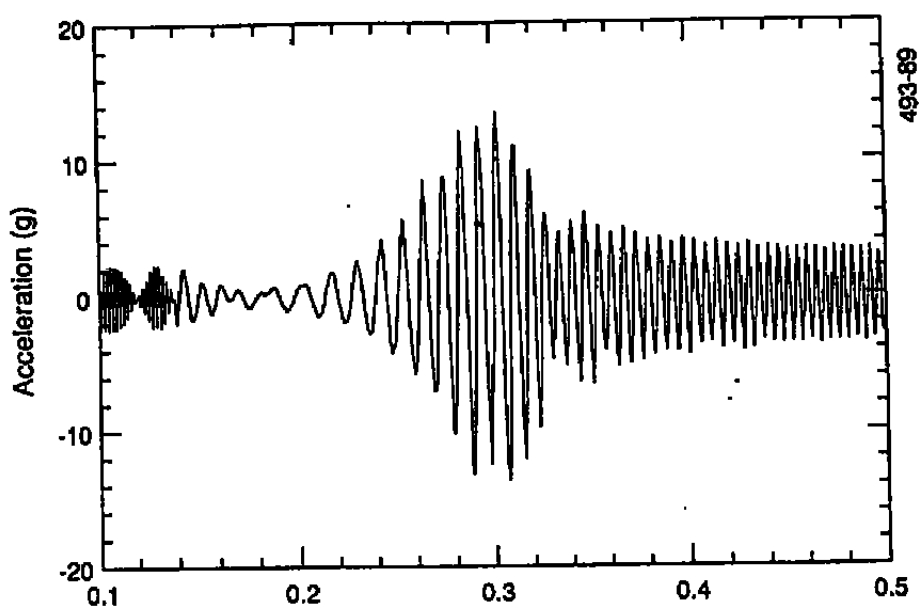
a. Accelerometer
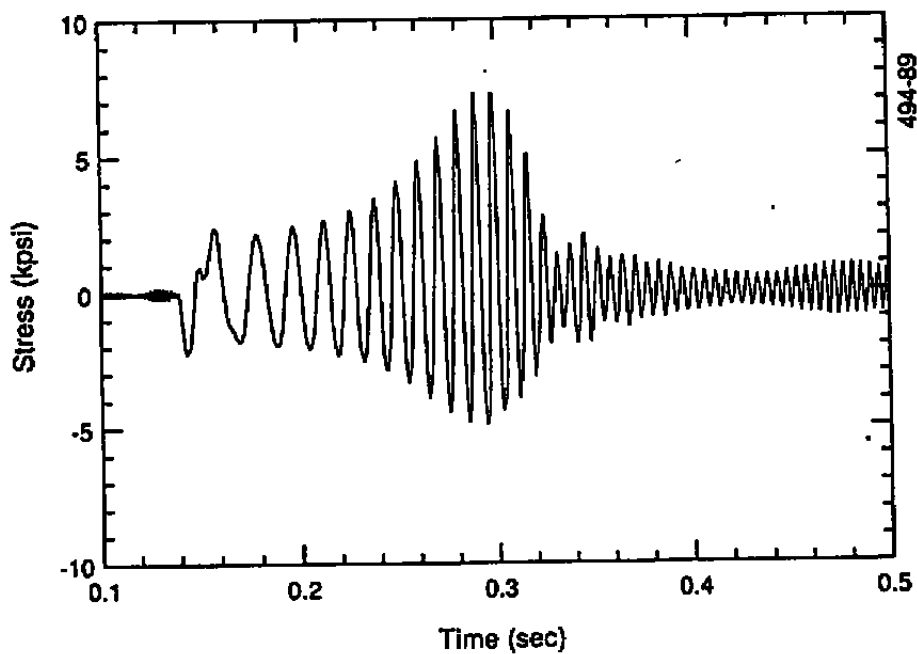
b. Stress at Location 1

Figure 6-3. Results From Tip Loading Tests
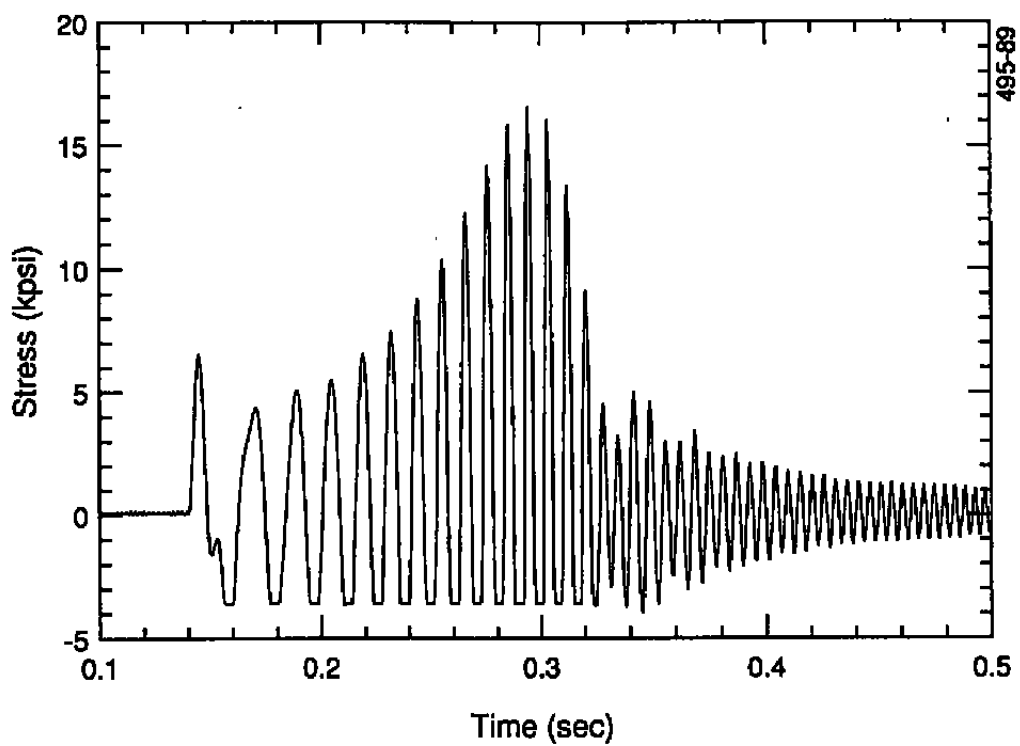
c. Stress at Location 2

Figure 6-3. Results From Tip Loading Tests

SECTION 7 - CONCLUSIONS AND RECOMMENDATIONS

This program had ambitious objectives of demonstrating a new temperature measurement technique, designing and fabricating an instrument capable of surviving in the combustor exit environment, and incorporating high-speed data analysis algorithms into a real-time temperature measurement system, all within a 2 year timeframe. Although we have not achieved all of our objectives, considerable progress has been made. A review of accomplishments in Phase II as well as a description of problems encountered during the performance of this program are discussed in Section 7.1. Recommendations concerning the future of this probe development program are presented in Section 7.2.

7.1 CURRENT STATUS

Probe operation has been demonstrated over a wide range of operating conditions both at Astron and at NASA Lewis Research Center. Flow conditions around the probe were altered by periodically drawing hot gas past the probe thermocouple through a suction line and then stagnating the flow by means of actuating a solenoid valve on a vacuum line. The probe behaved as predicted, and reasonable data traces were obtained. The signal-to-noise ratio of the perturbation signal appears to be acceptable if data smoothing techniques are employed.

Probe signals recorded in the Astron furnace facility were significantly cleaner than the data traces collected from the NASA Lewis Combustor Rig. Although the Astron facility was not designed with particular emphasis on obtaining well-mixed flow, this in fact was accomplished. While these well-behaved gas temperatures that exist in the Astron facility are beneficial from a probe development standpoint, the probe must be capable of operating in an environment similar to that encountered in the NASA facility. Further testing of the probe in a "noisy" environment will be required to demonstrate probe potential in a gas turbine.

During the NASA Lewis tests, individual data traces were completely obscured by high-frequency temperature fluctuations in the gas stream. However, by ensemble-averaging the individual probe traces, which in theory should be identical, it was possible to extract a useful signal. The time required to obtain a suitable number of samples was on the order of 2 to 5 min. The theoretical operation of this probe is ideally suited to the ensemble-averaging technique just described, and this type of data smoothing will probably be required in the gas turbine environment.

The probe that was demonstrated in this program is substantially more rugged than our original Phase II probe. The original probe required a moveable sapphire window in the flow stream, while the current design has no moving parts at the high temperature end of the probe. A brief series of vibrational loading tests have further demonstrated the ruggedness of this design, but further tests are recommended due to uncertainties in structural properties at high temperatures.

Our selection of a platinum-rhodium alloy as the probe body has proven to be a good choice. Although this adds substantially to the cost of the probe, reliability in an oxygen-rich environment is virtually certain. The platinum alloys are known to deteriorate in a fuel-rich environment so further tests are required. However, this probe is intended for laboratory use, rather than as flight instrumentation, so a structural design life of 24 hours was specified. If a longer probe life is required, protective coatings must be investigated.

The primary problem encountered in this program has been the difficulty in numerically differentiating our digitized data. This is a common problem, but one that we had hoped to circumvent. It is doubtful that an analog differentiating circuit alone could solve our problems, but possibly some combination of analog and digital filtering would allow us to obtain more useful values of the temperature derivatives. Several types of data smoothing were employed, including curve-fitting to quadratic and exponential equations and conventional numerical smoothing, all with limited success.

We had considerable trouble reducing our data after the completion of tests due to the differentiation problem just described. Until suitable posttest algorithms are demonstrated, further promotion of this technique for real-time use is not justified. On a positive note however, even posttest capability to cancel radiation errors in the laboratory environment would be useful and should be pursued.

7.2 RECOMMENDATIONS

A large body of experimental data has been collected, and further analysis of this existing data would be beneficial prior to proceeding with further tests. This data should be analyzed to determine the accuracy of some of our "ideal probe" assumptions of Section 3 and to validate the current design. Further analysis may indicate that design improvements are required. This existing data can also be used to demonstrate new data analysis algorithms suitable for either posttest use or in a real-time mode.

If the analysis of the existing data yields promising results, the following actions should be pursued:

• Air Force personnel and contractors should help define a suitable qualification test for this probe. At the present time no method of adequately demonstrating the accuracy of our probe exists. Input from the potential end users concerning a believable means of demonstrating accuracy would be extremely valuable.

• If additional tests are performed, the probe body should be instrumented to provide information such as the shield temperature, the temperature of the ceramic insulator (to calculate conduction losses), suction flow velocity, and pressure inside of the shield (to check on the level of velocity fluctuations during the stagnation mode). Probe delivery delays in Phase II did not allow sufficient time to incorporate this additional instrumentation, but the present probes could be modified if desired.

• Additional probe design changes that should be investigated include the use of butt-welded thermocouples to improve isothermal junction performance, and the evaluation of a lower cut-off frequency on the analog signal conditioning board.

REFERENCES

1. Doebelin, O. Ernest, "Measurement Systems Application and Design," McGraw-Hill, Inc., New York, 1966 (Revised Edition, 1975).

2. Vonada, Capt. J.A., USAF, "A Thermal Investigation of the AFAPL-TR-52 Turbine Engine Heat Transfer Test Facility," 1978, Tech Report AFAPL-TR-77-52.

3. Wormser, A.F., and R.A. Pfuntner, "Pulse Technique Extends Range of Chromel-Alumel to 7000°F, Instr. Control Systems, p.101, May 1964.

4. Will, Herbert A., "Computer Program for Pulsed Thermocouples with Corrections for Radiation Effects," NASA Technical Paper 1895, 1981.

5. Menshikov, V.I., "Measurement of Gas-Flow Temperatures by Two Thermocouples," Institute of Geochemistry, Vol.31, No.5, pp. 794-799, November 1976.

6. Astron Research and Engineering, "Gas Turbine Combustor Exit Temperature Measurement," Phase I FY85 SBIR Final Report, Contract No. F40600-85-C0007, April 1986.

7. Gebhart, B., "Heat Transfer", McGraw-Hill, New York, p.80, 1961. (Second Edition 1971).

8. Abernethy, Dr. R.B. et al, and J.W. Thompson, Jr., "Handbook, Uncertainty in Gas Turbine Measurements."

9. Roark, Raymond J., and Warren C. Young, "Formulas for Stress and Strain," Fifth Edition, McGraw-Hill, Inc., New York, 1975.

10. Memo from AEDC/PKP dated 18 Apr 1988.

APPENDIX A

FABRICATION DRAWINGS

A-2

.000
DATUM

2.00

6.00

14.25

20.25

21.00

SUCTION
MAIN T.C.
COOLING AIR
JUNCTION T.C.

1.00 O.D. X .030 WALL
INCONEL TUBE

COOLING AIR VENTS
.25 DIA (4X)

PLATINUM TIP
ASSEMBLY REF P.2

.438 O.D. X .030 WALL
PLATINUM TUBE

1.25 O.D. X 1.00 I.D. TUBE

ASTRON RESEARCH AND ENGINEERING

AIR COOLED PROBE

C | REV A | 7109-095

SHT 1/2 | SHEET 1 - 2

APPLICATION

NOTES:
⚠️1 SMOOTH WELD SURFACE TO FLAT

⚠️2 BEND IN .438 O.D. TUBE TO MINIMIZE GAP
BEFORE WELDING

INCONEL COUPLE

.188 O.D. X .025 WALL PLATINUM TUBE

.188 O.D. X .025 WALL
INCONEL TUBE

INCONEL JUNCTION

2.00 REF

.25

COOLING AIR
SUCTION

MAIN THERMOCOUPLE

JUNCTION THERMOCOUPLE

SAUEREISEN CEMENT

.156 REF.

.125 DIA ALUMINA
2 HOLES @ .031 DIA ON .052 CNTRS.

.25

.150 DIA THRU NEAR WALL

.03

.156

.033 DIA THRU FAR
WALL 3X ON .040 CNTRS

SECTION B-B
SCALE: 4X

VIEW A-A
SCALE: 4X

ASTRON

AIR COOLED PROBE

C | REV A | 7101-095

SCALE 2X | SHEET 1 OF 2

A-4

DIFFERENTIAL PRESSURE GAGE

1½ NPTF (4X)

OIL PUMP

PILOT LIGHT

FLAME SENSOR

COMBUSTION BLOWER

BURNER

COMBUSTION CHAMBER

3 DIA TEST SECTION

DILUTION FAN

EXHAUST STACK

ELECTRIC CONTROL

LIMIT SWITCHES & OIL CONTROL

OIL FLOW METER

¾ NPTF (3X)

PLAN VIEW

ITEM	T.C. TYPE	T.C. NO	DESCRIPTION
17	K	10	UNDERSIDE SKIN TEMP
16	K	9	UNDERSIDE SKIN TEMP
15	K	8	BURNER TEMP
14	K	5	STACK GAS TEMP
13	K	7	PIPE FTG. TEMP
12	K	8	PIPE FTG TEMP
11	K	11	PIPE FTG TEMP
10	R	6	PROBE
9	R	5	PROBE
8	K	4	PIPE FTG. TEMP.
7	R	4	COMBUSTION CHAMBER TEMP
6	K	3	PIPE FTG TEMP
5	R	3	TEST SECT INNER WALL TEMP
4	K	2	PIPE FTG TEMP
3	R	2	TEST SECT INNER WALL TEMP
2	K	1	PIPE FTG TEMP
1	R	1	TEST SECT INNER WALL TEMP

ASTRON

HIGH TEMP PROBE TEST
FACILITY INSTRUMENTATION

D | 7109-070

TC

\+

\-

500
.01%

500
.01%

13 V

.1µF

5

11

10

4

1K 1%

OUT

1 8

2 7

.1µF

.1µF

.1µF

.1µF

1µF

1µF

-1.5V

400K
.01%

.047 µF
poly

+13V

OUT

IN

9V   9V

220µF
16V

28K
1%

ADJ

LM2931CT

28K
1%

GND

on/off

1.5 V

-1.5 V

		UNLESS OTHERWISE SPECIFIED DIMENSIONS ARE IN INCHES TOLERANCES ARE:	CONTRACT NO. 7109.		**ASTRON** RESEARCH AND ENGINEERING	
		FRACTIONS DECIMALS ANGLES ± .XX ± ± .XXX ±	APPROVALS	DATE	2028 Old Middlefield Way • Mountain View, CA 94043 • (415) 962 8165	
			DRAWN JDS	10/4/89	Circuit Schematic - TC	
		MATERIAL	CHECKED JDS	10/4/89	Signal Conditioning	
					SIZE C	CODE IDENT NO.	DRAWING NO. 7109-100
		FINISH				
NEXT ASSY	USED ON				SCALE		SHEET OF
APPLICATION		DO NOT SCALE DRAWING				

3   2   1

Notes:
1) Test Section is 16 in. Diam. duct with water cooled outer shell.

2) J-58 located approx. 2 ft. upstream of Test Section.

Air Flow Control

Gas Preheat
J-41

Air Inlet

Inlet Blower

Exhaust to Atmosphere

Back-Pressure Control Valves (2)

Exhaust to Atmosphere

Jet A
J-58

Test Section

Cooling Water

A-6

	REVISIONS		
LTR	DESCRIPTION	DATE	APPROVED

UNLESS OTHERWISE SPECIFIED DIMENSIONS ARE IN INCHES TOLERANCES ARE:
FRACTIONS DECIMALS ANGLES
.XX ±   ±
.XXX ±
MATERIAL
FINISH

CONTRACT NO. 7109.

APPROVALS	DATE
DRAWN JDS	10/4/99
CHECKED JDS	10/4/99

ASTRON RESEARCH AND ENGINEERING
2028 Old Middlefield Way • Mountain View, CA 94043 • (415) 962 8165

NASA Lewis — Combustor Rig Facility Schematic

SIZE	CODE IDENT NO.	DRAWING NO.
B		7109-101

SCALE   SHEET   OF

NEXT ASSY   USED ON
APPLICATION   DO NOT SCALE DRAWING